RS
#7 2631
6-29-04

# IN THE UNITED STATES PATENT AND TRADEMARK OFFICE

| | |
|---|---|
| In re patent application of<br>Sofiène Affes *et al* | CASE NO. AP660761US |
| Serial No:     09/742,421 | Group Art Unit:        2631 |
| Filed:          December 22, 2000 | Examiner:      Tesfaldet Bocure |
| For:    Interference Suppression in CDMA Systems | |

Commissioner of Patents and Trademarks
United States Patent & Trademark Office
P.O. Box 1450
Alexandria, VA 22313-1450
U.S.A.

Sir:

To substantiate applicant's claim to priority, I enclose a certified copy of Canadian patent application No. 2,318,658 filed September 12, 2000.

Respectfully submitted,

Thomas Adams
Reg. No. 31078

Date:   June 16, 2004

Adams Patent & Trademark Agency
Box 11100, Station H
Ottawa, Ontario
K2H 7T8

Tel:    (613) 254 9111
Fax:   (613) 254 9222

AP660761\us'cert copy.po

*Bureau canadien des brevets*

Certification

*Canadian Patent Office*

Certification

La présente atteste que les documents ci-joints, dont la liste figure ci-dessous, sont des copies authentiques des documents déposés au Bureau des brevets.

This is to certify that the documents attached thereto and identified below are true copies of the documents on file in the Patent Office.

Specification and Drawings, as originally filed, with Application for Patent Serial No: **2,318,658**, on September 12, 2000, by **SOFIENE AFFES, HENRIK HANSEN AND PAUL MERMELSTEIN**, for "Interference Suppression in CDMA Systems".

Agent certificateur/Certifying Officer

June 14, 2004

Date

Canadä

(CIPO 68)
04-09-02

OPIC CIPO

110

# ABSTRACT OF THE DISCLOSURE

A receiver of the present invention addresses the need for improved interference
5  suppression rates without the number of transmissions by the power control system being
increased, and, to this end, provides a receiver for a CDMA communications system
which employs interference subspace rejection to obtain a substantially unity response
for a propagation channel via which a corresponding user's signal was received and a
substantially null response to interference components from selected signals of other user
10  stations.  The receiver may be used in a base station or in a user/mobile station.

1

## INTERFERENCE SUPPRESSION IN CDMA SYSTEMS
## DESCRIPTION

TECHNICAL FIELD:

The invention relates to Code-Division Multiple Access (CDMA) communications
5  systems, which may be terrestrial or satellite systems, and in particular to interference
suppression in CDMA communications systems.


BACKGROUND ART:

Code-Division Multiple Access communications systems are well known. For a
10  general discussion of such systems, the reader is directed to a paper entitled "Multiuser
Detection for CDMA Systems" by Duel-Hallen, Holtzman and Zvonar, *IEEE Personal
Communications*, pp. 46-58, April 1995.

In CDMA systems, the signals from different users all use the same bandwidth,
so each user's signal constitutes noise or interference for the other users. On the uplink
15  (transmissions from the mobiles) the interference is mainly that from other transmitting
mobiles. Power control attempts to maintain the received powers at values that balance
the interference observed by the various mobiles, but, in many cases, cannot deal
satisfactorily with excessive interference. Where mobiles with different transmission
rates are supported within the same cells, the high-rate mobiles manifest strong
20  interference to the low-rate mobiles. On the downlink (transmission towards the
mobiles) transmissions from base-stations of other cells as well as strong interference
from the same base-station to other mobiles may result in strong interference to the
intended signal. Downlink power control may be imprecise or absent altogether. In all
these so called near-far problem cases, the transmission quality can be improved, or the
25  transmitted power reduced, by reducing the interference. In turn, for the same
transmission quality, the number of calls supported within the cell may be increased,
resulting in improved spectrum utilization.

Power control is presently used to minimize the near-far problem, but with
limited success. It requires a large number of power control updates, typically 800 times
30  per second, to reduce the power mismatch between the lower-rate and higher-rate users.
It is desirable to reduce the number of communications involved in such power control
systems, since they constitute overhead and reduce overall transmission efficiencies.
Nevertheless, it is expected that future CDMA applications will require even tighter

power control with twice the number of updates, yet the near-far problem will not be completely eliminated. It is preferable to improve the interference suppression without increasing the number of transmissions by the power control system.

Multiuser detectors achieve interference suppression to provide potential benefits
5  to CDMA systems such as improvement in capacity and reduced precision requirements for power control. However, none of these detectors is cost-effective to build with significant enough performance advantage over present day systems. For example, the complexity of the optimal maximum likelihood sequence detector (MLSD) is exponential in the number of interfering signals to be cancelled, which makes its implementation
10 excessively complex. Alternative suboptimal detectors fall into two groups: linear and subtractive. The linear detectors include decorrelators, as disclosed by K.S. Schneider, "Optimum detection of code division multiplexed signals", *IEEE Trans. on Aerospace and Electronic Systems*, vol. 15, pp. 181-185, January 1979 and R. Kohno, M. Hatori, and H. Imai, "Cancellation techniques of co-channel interference in asynchronous spread
15 spectrum multiple access systems", *Electronics and Communications in Japan*, vol. 66-A, no. 5, pp. 20-29, 1983. A disadvantage of such decorrelators is that they cause noise enhancement.

Z. Xie, R.T. Short, and C.K. Rushforth, "A family of suboptimum detectors for coherent multiuser communications", *IEEE Journal on Selected Areas in*
20 *Communications*, vol. 8, no. 4, pp. 683-690, May 1990, disclosed the minimum mean square error linear (MMSE) detector, but such detectors are sensitive to channel and power estimation errors. In both cases, the processing burden still appears to present implementation difficulties.

Subtractive interference cancellation detectors take the form of successive
25 interference cancellers (SIC), as disclosed by R. Kohno *et al.*, "Combination of an adaptive array antenna and a canceller of interference for direct-sequence spread-spectrum multiple-access system", *IEEE Journal on Selected Areas in Communications*, vol. 8, no. 4, pp. 675-682, May 1990, and parallel interference cancellers (PIC) as disclosed by M.K. Varanasi and B. Aazhang, "Multistage detection
30 in asynchronous code-division multiple-access communications", *IEEE Trans. on Communications*, vol. 38, no. 4, pp. 509-519, April 1990, and R. Kohno *et al.*, "Combination of an adaptive array antenna and a canceller of interference for direct-sequence spread-spectrum multiple-access system", *IEEE Journal on Selected*

3

*Areas in Communications*, vol. 8, no. 4, pp. 675-682, May 1990. Both SIC detectors and PIC detectors require multi-stage processing and the interference cancellation achieved is limited by the amount of delay or complexity tolerated. These detectors are also very sensitive to channel, power and data estimation errors.

5        One particular subtractive technique was disclosed by Shimon Moshavi in a paper entitled "Multi-User Detection for DS-CDMA Communications", *IEEE Communications Magazine*, pp. 124-136, October 1996. Figure 5 of Moshavi's paper shows a subtractive interference cancellation (SIC) scheme in which the signal for a particular user is extracted in the usual way using a matched filter and then spread again using the same

10      spreading code for that particular user, *i.e.*, the spreading code used to encode the signal at the remote transmitter. The spread-again signal then is subtracted from the signal received from the antenna and the resulting signal is applied to the next user's despreader. This process is repeated for each successive despreader. Moshavi discloses a parallel version that uses similar principles.

15      A disadvantage of this approach is its sensitivity to the data and power estimates, *i.e.*, their accuracy and the sign of the data. A wrong decision will result in the interference component being added rather than subtracted, which will have totally the wrong effect.

        For more information about these techniques, the reader is directed to a paper by

20 P. Patel and J. Holtzman entitled "Analysis of a Simple Successive Interference Cancellation Scheme in a DS/CDMA System", *IEEE Journal on Selected Areas in Communications*, Vol. 12, No. 5, pp. 796-807, June 1994.

        In a paper entitled "A New Receiver Structure for Asynchronous CDMA: STAR - The Spatio-Temporal Array-Receiver", *IEEE Transaction on Selected Areas in*

25 *Communications*, Vol. 16, No. 8, October 1998, S. Affes and P. Mermelstein (two of the present inventors), disclosed a technique for improving reception despite near/far effects and multi-user interference. In contrast to known systems in which the spread-again signal is supplied to the input of the despreader of the channel to be corrected, Affes' and Mermelstein's proposed system treated all of the users' signals together and

30 processed them as a combined noise signal. If the components of the received signal from the different users were uncorrelated and all had equal power, or substantially equal power, this process would be optimal. In practice, however, there will be significant differences between the power levels at which the different users' signals are received

4

at the base station antenna. The same applies to the downlink. For example, a data user may generate much more power than a voice user simply because of the more dense information content of the data signal. Also, imperfect power control will result in power differences, *i.e.*, channel variations may result in received powers different from

5 their intended values, despite the best effort of the power-control process to equalize them.

DISCLOSURE OF INVENTION:

The present invention addresses the need for improved interference suppression

10 without the number of transmissions by the power control system being increased, and, to this end, provides a receiver for a CDMA communications system which employs interference subspace rejection to obtain a substantially unity response for a propagation channel via which a corresponding user's signal was received and a substantially null response to interference components from selected signals of other user stations.

15 According to one aspect of the invention, there is provided a receiver suitable for either a base station or a user station of a CDMA communications system comprising at least one base station (11) and a plurality of user stations ($10^1$...$10^U$) each communicating with said at least one base station via a corresponding one of a plurality of channels, said base station and each user station having a transmitter and a said receiver, the receiver

20 receiving a signal comprising components corresponding to signals from the different transmitters of the base station and/or user stations. The receiver comprises processing means (18) for deriving an observation matrix from the received signal, the receiver comprising a plurality of receiver modules (21) each comprising means (19) for deriving from the observation matrix one or both of a corresponding observation vector and post-

25 correlation observation vector and a beamformer for processing one or other of the observation vector and the post-correlation observation vector to provide estimates of symbols transmitted by a corresponding user station, and means (42,43) for providing at least one constraint matrix representing interference subspace of components of the received signal corresponding to selected ones of the user signals of the plurality of

30 receiver modules, at least one ($21^d$) of said plurality of receiver modules having means ($28^d$) responsive to at least the post-correlation observation vector for deriving an estimate of the channel parameters for the channel between the receiver and the corresponding transmitter, and a beamformer ($47^d$) for processing one or other of the

5

observation vector and the post-correlation observation vector to produce estimates of the symbols transmitted by said transmitter, the beamformer having means for adjusting coefficients of the beamformer in dependence upon the constraint matrix and the channel estimate so as to tune the beamformer to provide a substantially unity response for that

5  portion of the received signal from the corresponding transmitter and a substantially null response to that portion of the received signal corresponding to predetermined ones of other user signals and/or base station signals also received by the receiver.

According to the present invention, there is provided a receiver for either a base station (or a mobile station) of a CDMA communications system in which a plurality of

10  user stations $(10^1...10^U)$ each having an antenna array comprising one or more antennas communicate with a base station (11) having an antenna array (12) comprising one or more reception antennas $(12^1...12^M)$, each of the user stations having spreading means $(13^1...13^U)$ for using a spreading code $(c^1(t)...c^U(t))$ unique to that station to spread a corresponding one of a plurality of user signals $(b^1_n...b^U_n)$ and means for transmitting

15  the spread user signals to the base station antenna array (12) via a propagation channel $(14^1...14^U)$ unique to that user station,

the receiver comprising preprocessing means (18) and a plurality of receiver modules $(21^1...21^U)$ having their respective inputs connected in common to an output of the preprocessing means (18) and each corresponding to a respective one of the user

20  stations,

the preprocessing means (18) being arranged to receive from the antenna array an antenna array signal vector $(X(t))$ comprising a plurality of spread data vectors $(X^1(t) ... X^U(t))$ corresponding to the signals from the different user stations received by the reception antenna array and having means for filtering, sampling and

25  buffering the antenna array signal vector $(X(t))$ to produce a succession of observation matrices $(Y_n)$, and supplying the observation matrices $(Y_n)$ to each of the receiver modules $(21^1...21^U)$;

each of the receiver modules $(21^1...21^U)$ comprising a despreader $(19^u)$, a channel identification means $(28^u)$, a beamformer $(27^u)$ and output means $(29^u,30^u)$,

30  the despreader $(19^u)$ being arranged to despread each observation matrix using the spreading code of the corresponding user to form a post-correlation observation vector $(Z^u_n)$ and the channel identification means $(28^u)$ being arranged to derive from the post-correlation observation vector a set of estimated channel parameters $(\hat{H}^u_n)$ for the

6

channel whereby the signal from the corresponding user station reached the antenna array,

the beamformer ($27''$) having means (51) for weighting each of the elements of each observation vector in turn using weighting coefficients ($\underline{W}_n^u$), tuning means (50)
5 for adjusting the weighting coefficients ($\underline{W}_n^u$) in dependence upon at least said estimated channel parameters, and means (52) for combining the weighted elements to produce a respective symbol of a corresponding one of a plurality of output signals ($\hat{b}_n^1...\hat{b}_n^U$) corresponding to the plurality of user signals ($b_n^1...b_n^U$) , respectively,

the receiver further comprising constraints-set generation means (42) responsive
10 to a set of channel parameter estimates and either or both of an actual value of the symbol from at least one of the beamformers and at least one hypothetical symbol value for deriving a constraints-set, and

constraint matrix generation means (43) responsive to said constraints-set for forming at least one constraint matrix and corresponding inverse matrix;
15 the respective tuning means of at least some of the beamformers being responsive to said at least one constraint matrix to adjust the weighting coefficients ($\underline{W}_n^d$) of their respective beamformers such that, in successive symbol periods, the coefficients of each of said at least some of the beamformers are adjusted so as to tune a substantially unity response for that portion of the antenna array signal vector corresponding to the user
20 signal from the corresponding user station and a substantially null response to that portion of the antenna array signal vector corresponding to the user signals received from those user stations corresponding to the receiver modules which contribute a constraint waveform to the constraint matrix generation means;

the output means of each receiver module being responsive to the output of the
25 corresponding beamformer for providing estimates of the symbols of the corresponding user signal.

Embodiments of the invention may employ one of several alternative modes of implementing interference subspace rejection (ISR), *i.e.* characterizing the interference and building the constraint matrix. In a first embodiment, using a first mode
30 conveniently designated ISR-TR, each receiver module in the first group generates its re-spread signal taking into account the amplitude and sign of the symbol and the channel characteristics. The re-spread signals from all of the receiver modules of the first group

are summed to produce a total realization which is supplied to all of the receiver modules in the second group.

Where each receiver module of the second set uses decision feedback, it further comprises delay means for delaying each frame/block of the observation vector before 5 its application to the beamformer.

Whereas, in ISR-TR embodiments, just one null constraint is dedicated to the sum, in a second embodiment, which uses a second mode conveniently designated ISR-R, estimated realisations of all the interferers are used, and a null constraint is dedicated to each interference vector. In this second embodiment, in each receiver 10 module of the first set, the symbols spread by the spreader comprise estimated realisations of the symbols of the output signal. Also, the constraint waveforms are not summed before forming the constraint matrix. Thus, the receiver module estimates separately the contribution to the interference from each unwanted (interfering) user and cancels it by a dedicated null-constraint in the multi-source spatio-temporal beamformer. 15 In most cases, estimation of the interference requires estimates of the past, present and future data symbols transmitted from the interferers, in which case the receiver requires a maximum delay of one symbol and one processing cycle for the lower-rate or low-power users and, at most a single null constraint per interferer.

In a third embodiment of the invention which uses a third mode conveniently 20 designated ISR-D, *i.e.* the observation vector/matrix is decomposed over sub-channels/fingers of propagation path and the beamformer nulls interference in each of the sub-channels, one at a time. In most cases, the maximum number of constraints per interferer is equal to the number of sub-channels, *i.e.* the number of antenna elements $M$ multipled by the number of paths $P$.

25 In a fourth embodiment using a fourth mode conveniently designated ISR-H because it implements null-responses in beamforming over all possible realisations of the interference, without any delay, each receiver module of the first group further comprises means for supplying to the spreader possible values of the instant symbols of the output signal and the spreader supplies a corresponding plurality of re-spread signals 30 to each of the receiver modules of the second group. In each receiver module of the second group, the despreader despreads the plurality of re-spread signals and supplies corresponding despread vectors to the beamformer. This embodiment suppresses any

sensitivity to data estimation errors and, in most cases, requires a maximum of 3 null constraints per interferer.

In a fifth embodiment using a fifth mode conveniently designated ISR-RH because it uses the past and present interference symbol estimates, in each receiver module of the

5 first group, the spreader spreads the symbols of the output signal itself and, in each receiver module of the second group, the beamformer then implements null-responses over reduced possibilities/hypotheses of the interference realization. Conveniently, application of the output of the first despreader to the beamformer will take into account the time required for estimation of the interferer's symbol. In most cases, the

10 beamformer will provide a maximum of 2 null constraints per interferer.

In any of the foregoing embodiments of the invention, the channel identification unit may generate the set of channel parameter estimates in dependence upon the extracted despread data vectors and the user signal component estimate.

For each of the above-identified modes, the receiver modules may employ either

15 of two procedures. On the one hand, the receiver module may apply the post-correlation observation vector to the channel identification unit but supply the observation matrix itself directly to the beamformer, i.e. without despreading it. The constraint matrix then would be supplied to the beamformer without despreading.

Alternatively, each receiver module could supply the post-correlation observation

20 vector to both the channel identification unit and the beamformer. In this case, the receiver module would also despread the constraint matrix before applying it to the beamformer.

Where the reception antenna comprises a plurality of antenna elements, the beamformer unit may comprise a spatio-temporal processor, such as a filter which has

25 coefficients tuned by the estimated interference signals.

The receiver modules may comprise a first set that are capable of contributing a constraint waveform to the constraint matrix and a second set that have a beamformer capable of using the constraint matrix to tune the specified null response and unity response. In preferred embodiments, at least some of the plurality of receiver modules

30 are members of both the first set and the second set, i.e. they each have means for contributing a constraint waveform and a beamformer capable of using the constraint matrix.

9

In practice, the receiver modules assigned to the stronger user signals will usually contribute a constraint waveform and the beamformer units of the receiver modules assigned to other user signals will be capable of using it.

The receiver module may comprise an MRC beamformer and an ISR beamformer 5 and be adapted to operate in multi-stage, i.e., for each symbol period of frame, it will carry out a plurality of iterations. In the first iteration, the constraints set generator will receive the "past" and "future" estimates from the MRC beamformer and the "past" symbol estimate, i.e., from the previous frame, and process them to produce a new symbol estimate for the first iteration. In subsequent iterations of the current symbol 10 period or frame, the constraints-set generator will use the "future" estimate from the MRC beamformer, the previous estimate from the ISR beamformer and the symbol estimate generated in the previous iteration. The cycle will repeat until the total number of iterations have been performed, whereupon the output from the receiver module is the desired estimated symbol for the current frame which then is used in the similar 15 iterations of the next frame.

The ISR receiver module comprising both an MRC beamformer and an ISR beamformer may comprise means $\{101Q^d\}$ for extracting from the ISR beamformer $(47Q^d)$ an interference-reduced observation vector and reshaping the latter to produce an interference-reduced observation matrix for despreading by the despreader. The channel 20 identification unit then uses the despread interference-reduced observation vector to form interference-reduced channel estimates and supplies them to the residual MRC beamformer for use in adapting the coefficients thereof.

The ISR beamformer may process blocks or frames of the observation vector that are extended by concatenating a current set of data with one or more previous frames or 25 blocks of data.

The different receiver modules may use different sizes of frame.

In order to receive signals from a user transmitting multicode signals, the ISR receiver module may comprise a plurality of ISR beamformers and despreaders, each for operating upon a corresponding one of the multiple codes. The channel identification 30 unit then will produce a channel parameter estimate common to all of the multicodes, spread that channel estimate with each of the different multicodes and supply the resulting plurality of spread channel estimates to respective ones of the plurality of ISR beamformers.

10

The multicode ISR receiver module may have a despreader ($19^{d,\delta}$) which uses a compound code comprising each of the multicodes weighted by the corresponding symbol estimate from a respective one of a corresponding plurality of decision-rule units. The despreader will uses the compound code to despread the observation matrix and supply

5 the corresponding compound post-correlation observation vector to the channel identification unit. The channel identification unit will use that vector to produce the channel estimate and spread it using the different ones of the multicodes to produce the spread channel estimates.

The ISR receiver module may comprise a despreader $19S^{d,1}$, ..., $19S^{d,F_d}$ using

10 a plurality of codes which comprise segments of a main code specified for that user. Each segment corresponds to a symbol, and to a symbol duration in a large block of data, the number of segments being determined by the data rate, i.e., number of symbols within a block, of that user. Each receiver module may have a different number of segments assigned thereto according to the data rate of the corresponding user.

15 Embodiments of the invention may be adapted for use in a user/mobile station capable of receiving user-bound signals transmitted by a plurality of base stations each to a corresponding plurality of users, the receiver then comprising a selection of receiver modules each corresponding to a different base station and configured to extract a preselected number of said user-bound signals. Where the particular user/mobile station

20 is included in the preselected number, the receiver module may comprise a similar structure to the above-mentioned multicode receiver, the plurality of despreaders being adapted to despread the observation matrix using respective ones of a set of codes determined as follows: (1) a pre-selected number $NB$ of base stations from which the mobile receives signals and which have been selected for cancellation - represented by

25 index $v'$ which ranges from 1 to $NB$; (2) a preselected number (1 to $NI$) of interferers per base station preselected for cancellation; (3) the data rates of the selected interferers.

Where the signal destined for the particular user/mobile station is not one of the preselected number of signals from the corresponding base station, the receiver may

30 further comprise an ISR receiver module which has means for updating the ISR beamformer coefficients using the channel estimates from at least some of the receiver modules that have generated such channel estimates for the preselected signals for the same base station.

11

Where the rates of the different users are not known to the instant mobile station, the codes may comprise a fixed number of segments $N_m$ which is predetermined as a maximum data rate to be received. Any slower rates will effectively be oversampled for processing at the higher rate.

5      The complexity of the multicode embodiments may be reduced by reducing the number of codes that are used by the despreaders. In particular, the bank of despreaders may use a set of codes that represent summation of the codes of the different $NI$ interferers, to form a compound code which reduces the total number of codes being used in the despreaders.

10      According to another aspect of the invention, there is provided a STAR receiver comprising an MRC beamformer which operates upon an observation vector which has not been despread.

Of course, that does not preclude having all channels feed their interference components to all other channels.

15      The foregoing and other objects, features, aspects and advantages of the present invention will become more apparent from the following detailed description, in conjunction with the accompanying drawings, of preferred embodiments of the invention.


BRIEF DESCRIPTION OF THE DRAWINGS:

20      Figure 1 is a schematic diagram illustrating a portion of a CDMA communications system comprising a plurality of user stations, typically mobile, and a base station having a reception antenna comprising an array of antenna elements, and illustrating multipath communication between one of the user stations and the array of antennas;

25      Figure 2 is a simplified schematic diagram representing a model of the part of the system illustrated in Figure 1;

Figure 3 is a detail block diagram of a spreader portion of one of the user stations;

Figures 4(a) and 4(b) illustrate the relationship between channel characteristics, 30 power control and signal power;

Figure 5 is a simplified block schematic diagram of a base station receiver according to the prior art;

Figure 6 is a detail block diagram of a preprocessing unit of the receiver;

12

Figure 7 is a detail block diagram of a despreader of the receiver;

Figure 8 illustrates several sets of users in a CDMA system ranked according to data rate;

Figure 9 is a detail block diagram showing several modules of a receiver embodying the present invention, including one having a beamformer operating on data that has not been despread;

Figure 10 is a detail schematic diagram showing a common matrix generator and one of a plurality of beamformers coupled in common thereto;

Figure 11 is a block diagram corresponding to Figure 9 but including a module having a beamformer operating upon data which has first been despread;

Figure 12 is a schematic diagram of a user-specific matrix generator and an associated beamformer of one of the receiver modules of Figure 11;

Figure 13 is a detail block schematic diagram of a receiver using total realisation of the interference to be cancelled (ISR-TR) and without despreading of the data processed by the beamformer;

Figure 14 illustrates a respreader of one of the receiver modules of Figure 13;

Figure 15 is a detail block schematic diagram of a receiver using individual realisations of the interference (ISR-R) and without despreading of the data processed by the beamformer;

Figure 16 is a simplified block diagram of a receiver which decomposes each realisation of the interference over diversity paths (ISR-D) and without despreading of the data processed by the beamformer;

Figure 17 is a simplified schematic block diagram of a receiver employing interference subspace rejection based upon hypothetical values of the symbols (ISR-H) and without despreading of the data processed by the beamformer;

Figure 18 illustrates all possible triplets for the hypothetical values;

Figure 19 illustrates bit sequences for generating the hypothetical values;

Figure 20 is a simplified schematic block diagram of a receiver employing interference subspace rejection based upon both hypothetical values of the symbols and realisations (ISR-RH) and without despreading of the data processed by the beamformer;

Figure 21 is a simplified schematic block diagram of a receiver similar to the ISR-TR receiver shown in Figure 13 but in which the beamformer operates upon the data that has first been despread;

Figure 22 is a simplified schematic block diagram of a receiver similar to the ISR-R receiver shown in Figure 15 but in which the beamformer operates upon data that has first been despread;

Figure 23 is a simplified schematic block diagram of a receiver similar to the

5   ISR-D receiver shown in Figure 16 but in which the beamformer operates upon data that has first been despread;

Figure 24 is a simplified schematic block diagram of a receiver similar to the ISR-H receiver shown in Figure 18 but in which the beamformer operates upon data that has first been despread;

10   Figure 25 illustrates bit sequences generated in the receiver of Figure 24;

Figure 26 is a simplified schematic block diagram of a receiver similar to the ISR-RH receiver shown in Figure 20 but in which the beamformer operates upon data that has first been despread;

Figure 27 illustrates an alternative STAR module which may be used in the

15   receiver of Figure 5 or in place of some of the receiver modules in the receivers of Figures 13-17, 20-24 and 26;

Figure 28 illustrates a receiver module which both contributes to the constraint matrix and uses the constraint matrix to cancel interference (JOINT-ISR);

Figure 29 illustrates a mulit-stage ISR receiver module;

20   Figure 30 illustrates successive implementaton of ISR;

Figure 31 illustrates a receiver module which uses ISR to enhance channel identification;

Figure 32 illustrates extension of the frame size to reduce noise enhancement and facilitate asynchronous operation and processing of high data rates;

25   Figure 33 illustrates implementation of ISR with mixed spreading factors;

Figure 34 illustrates an uplink ISR receiver module for a user employing multicode signals;

Figure 35 illustrates a modification of the receiver module of Figure 34;

Figure 36 illustrates how multirate can be modelled as multicode;

30   Figure 37 illustrates frame size determination for multirate signals;

Figure 38 illustrates grouping of multirate signals to correspond to a specific user's symbol rate;

Figure 39 illustrates an "uplink" multirate ISR receiver module for a base station;

14

Figure 40 illustrates one of a plurality of "downlink" multirate receiver modules for a user station operating as a "virtual base station";

Figure 41 illustrates a "downlink" multirate receiver module of the user station of Figure 41 for extracting signals for that user station;

5      Figure 42 illustrates a multicode alternative to the receiver module of Figure 40; and

Figure 43 illustrates a second alternative to the receiver module of figure 40.

10

BEST MODE(S) FOR CARRYING OUT THE INVENTION:

In the following description, identical or similar items in the different Figures have the same reference numerals, in some cases with a suffix.

The description refers to several published articles. For convenience, the articles 15 are cited in full in a numbered list at the end of the description and cited by that number in the description itself. The contents of these articles are incorporated herein by reference and the reader is directed to them for reference.

Figures 1 and 2 illustrate the uplink of a typical asynchronous cellular CDMA system wherein a plurality of mobile stations $10^1 ... 10^U$ communicate with a base-station 20 11 equipped with a receiving antenna comprising an array of several antenna elements $12^1 ... 12^M$. For clarity of depiction, and to facilitate the following detailed description, Figures 1 and 2 illustrate only five of a large number (U) of mobile stations and corresponding propagation channels of the typical CDMA system, one for each of a corresponding plurality of users. It will be appreciated that the mobile stations $10^1 ... 10^U$ 25 will each comprise other circuitry for processing the user input signals, but, for clarity of depiction, only the spreaders are shown in Figure 2. The other circuitry will be known to those skilled in the art and need not be described here. Referring to Figure 2, the mobile stations $10^1 ... 10^U$ comprise spreaders $13^1 ... 13^U$, respectively, which spread a plurality of digital signals $b_n^1 ... b_n^U$ of a corresponding plurality of users, respectively, 30 all to the same bandwidth, using spreading codes $c^1(t) ... c^U(t)$, respectively. The mobile stations $10^1 ... 10^U$ transmit the resulting user signals to the base station 11 via channels $14^1 ... 14^U$, respectively, using a suitable modulation scheme, such as differential binary phase shift keying (DBPSK). Each of the mobile stations $10^1 ... 10^U$ receives commands

15

from the base station 11 which monitors the total received power, *i.e.* the product of transmitted power and that user's code and attenuation for the associated channel and uses the information to apply power control to the corresponding signals to compensate for the attenuation of the channel. This is represented in Figure 2 by multipliers
5 $15^1...15^U$ which multiply the spread signals by adjustment factors $\psi^1(t)...\psi^U(t)$, respectively. The array of $M$ omni-directional antenna elements $12^1...12^M$ at the base station 11 each receive all of the spread signals in common. The channels $14^1...14^U$ have different response characteristics $H^1(t)...H^U(t)$, respectively, as illustrated in more detail in Figure 1, for only one of the channels, designated channel $14^u$. Hence, channel $14^u$
10 represents communication via as many as $P$ paths between the single antenna of the associated mobile station $10^U$ and each of the base station antenna elements $12^1...12^M$. The other channels are similarly multipath.

As before, it is presumed that the base station knows the spreading codes of all of the mobile stations with which it communicates. The mobile stations will have
15 similar configurations so only one will be described. Thus, the mobile station $10^u$ first differentially encodes its user's binary phase shift keyed (BPSK) bit sequence at the rate $1/T$, where $T$ is the bit duration, using circuitry (not shown) that is well-known to persons skilled in this art. As illustrated in Figure 3, its spreader $13^u$ then spreads the resulting differential binary phase shift keyed (DBPSK) sequence $b_n^u$ (or $b^u(t)$ in the
20 continuous time domain as represented in Figure 3) by a periodic personal code sequence $c_l^u$ (or $c^u(t)$ in the continuous time domain) at a rate $1/T_c$, where $T_c$ is the chip pulse duration. The processing gain is given by $L=T/T_c$. For convenience, it is assumed that short codes are used, with the period of $c^u(t)$ equal to the bit duration $T$, though the system could employ long codes, as will be discussed later, with other applications and
25 assumptions. Over one period $T$, the spreading code can be written as:

$$c^u(t) = \sum_{l=0}^{L-1} c_l^u \phi(t - lT_c),\qquad(1)$$

where $c_l^u = \pm 1$ for $l = 0, ..., L - 1$, is a random sequence of length $L$ and $\phi(t)$ is the chip pulse as illustrated in Figure 3. Also, with a multipath fading environment with $P$
30 resolvable paths, the delay spread $\Delta\tau$ is small compared to the bit duration *(i.e. $\Delta\tau \ll T$)*.

As illustrated in Figures 4(a) and 4(b), following signal weighting by the poer control factor $\psi_{pc}^u(t)^2$, the spread signal is transmitted to the base station 11 via channel

16

$14^u$. Figure 4(a) shows the "real" situation where the channel characteristics comprise a normalized value $H^u(T)$ and a normalization factor $\psi_{ch}^u(T)$ which relates to the "amplitude" or attenuation of the channel, *i.e.* its square would be proportional to the power divided by the transmitted power. In Figure 4(a), power control is represented

5 by a multiplier $17^u$, and the subscript "$pc$". Figure 4(b) shows that, for convenience, the channel characteristics can be represented (theoretically) by the normalized value $H^u(t)$ and the normalization factor $\psi_{ch}^u(t)$ included in a single power factor $\psi^u(t)$ which is equal to $\psi_{pc}^u(t)\psi_{ch}^u(t)$. $\psi_{pc}^u(t)$ is the factor by which the transmitted signal is amplified or attenuated to compensate for channel power gain in $\psi_{ch}^u(t)$ and to maintain the received

10 power $(\psi^u(t))^2$ at the required level.

In such a CDMA system, the signal of each of the mobile stations $10^1...10^U$ constitutes interference for the signals of the other mobile stations. For various reasons, some of the mobile stations will generate more interference than others. The components of one of these "strongly interfering" user stations and its associated channel are

15 identified in Figures 1 and 2 by the index "i". The components of one of the other "low-power" user stations and its associated channel also are illustrated, and identified by the index "d". The significance of this grouping of "interfering" and "low-power" user stations will be explained later.

At the base station 11, the spread data vector signals $X^1(t)...X^U(t)$ from the base

20 station antenna elements $12^1...12^M$, respectively, are received simultaneously, as indicated by the adder 16 (Figure 2), and the resulting observation vector $X(t)$ is supplied to the receiver (see Figure 5). The sum of the spread data vectors (signals) $X^1(t)...X^U(t)$ will be subject to thermal noise. This is illustrated by the addition of a noise signal component $N_{th}(t)$ by adder 16. The noise signal $N_{th}(t)$ comprises a vector, elements of

25 which correspond to the noise received by the different antenna elements.

Figure 5 illustrates a spatio-temporal array receiver (STAR) for receiving the signal $X(t)$ at the base station 11. Such a receiver was described generally by two of the present inventors in reference [13]. The receiver comprises a preprocessing unit 18, a plurality of despreaders $19^1...19^U$, and a plurality of spatio-temporal receiver (STAR)

30 units $20^1...20^U$, each having its input connected to the output of a respective one of the despreaders $19^1...19^U$. Each of the STAR units $20^1...20^U$ and the associated one of the despreaders $19^1...19^U$ form part of a respective one of a plurality of receiver modules $21^1...21^U$. As shown in Figure 6, the preprocessing unit 18 comprises a matched filter

17

22, a sampler 23 and a buffer 24. Matched filter 22 convolves the antenna array signal vector $X(t)$, which is an $M \times 1$ vector, with a matched pulse $\phi(T_c - t)$ to produce the matched filtered signal vector $Y(t)$ which then is sampled by sampler 23 at the chip rate $1/T_c$, element by element. The sampler 23 supplies the resulting $M \times 1$ vectors $Y_{n,l}$, at

5  the chip rate, to buffer 24 which buffers them to produce an observation matrix $Y_n$ of dimension $M \times (2L-1)$. It should be noted that, although the present inventors' Canadian patent application No. 2,293,097 and United States Provisional application No. 60/171,604 had a duplicate of this preprocessing unit 18 in each of the despreaders $19^1...19^U$, it is preferable to avoid such duplication and use a single preprocessor 18 to

10  preprocess the received antenna array signal vector $X(t)$.

The despreaders $19^1...19^U$ each have the same structure, so only one will be described in detail with reference to Figure 7 which illustrates despreader $19^u$. Thus, despreader $19^u$ comprises a filter $25^u$ and a vector reshaper $26^u$. The observation matrix $Y_n$ is filtered by filter $21^u$ using the pseudo-random number sequence $c_{L-l}^u$ corresponding

15  to that used in the spreader $13^u$ of the transmitter, i.e. $c_l^u$, to produce the postcorrelation observation matrix $\underline{Z}_n^u$ for user $u$. Vector reshaper $26^u$ concatenates the $M \times L$ matrix $\underline{Z}_n^u$ to form a post-correlation observation vector $\underline{Z}_n^u$ of dimension $ML \times 1$. It should be noted that the vector reshaper $26^u$ need not be a distinct physical element but is depicted as such to represent a mathematical function. In practice, the function will

20  likely be determined merely by allocation of resources, such as memory.

Referring again to Figure 5, the post-correlation observation vectors $\underline{Z}_n^1...\underline{Z}_n^U$ from despreaders $19^1...19^U$ are processed by the STAR units $20^1...20^U$, respectively, to produce symbol estimates $\hat{b}_n^1...\hat{b}_n^U$ corresponding to the transmitted symbols $b_n^1...b_n^U$ (see Figure 2) and power estimates $(\psi_n^1)^2...(\psi_n^U)^2$ which are supplied

25  to subsequent stages (not shown) of the receiver for processing in known manner.

The STAR units $20^1...20^U$ each comprise the same elements, so the construction and operation of only one of them, STAR unit $20^u$, will now be described.

The STAR unit $20^u$ comprises a beamformer $27^u$, a channel identification unit $28^u$, a decision rule unit $29^u$ and a power estimation unit $30^u$. The channel identification unit

30  $28^u$ is connected to the input and output, respectively, of the beamformer $27^u$ to receive the post-correlation observation vector $\underline{Z}_n^u$ and the signal component estimate $\hat{s}_n^u$, respectively. The channel identification unit $28^u$ replicates, for each frame $M \times L$ the characteristics $H^u(t)$, in space and time, of the associated user's transmission

channel 14$^u$. More specifically, it uses the signals $\underline{Z}_n^u$ and $\hat{s}_n^u$ to derive a set of parameter estimates $\hat{\underline{H}}_n^u$, which it uses to update the weighting coefficients $\underline{W}_n^u$ of the beamformer 27$^u$ in succeeding symbol periods. The symbol period corresponds to the data frame of $M \times L$ elements.

5        The beamformer 27$^u$ comprises a spatio-temporal maximum ratio combining (MRC) filter which filters the space-time vector $\underline{Z}_n^u$ to produce the despread signal component estimate $\hat{s}_n^u$, which it supplies to both the decision rule unit 29$^u$ and the power estimation unit 30$^u$. The decision-rule unit 29$^u$ outputs a binary symbol $\hat{b}_n^u$ according to the sign of the signal component estimate $\hat{s}_n^u$. The binary

10  output signal constitutes the output of the decision rule unit 30$^u$ and is an estimate of the corresponding user signal $b_n^u$ spread by spreader 13$^u$ of the corresponding user station 10$^u$ (Figures 1 and 2).

        The signal component estimate $\hat{s}_n^u$ is processed in subsequent parts of the receiver. For example, it may be differentially decoded and, possibly, deinterleaved and

15  the data decoded--if the corresponding inverse operations were done before transmission.

        The power estimation unit 30$^u$ uses the raw signal component estimate $\hat{s}_n^u$ to derive an estimate $(\psi_n^u)^2$ of the power in that user's signal component $\hat{s}_n^u$ of the antenna array signal vector $X(t)$ and supplies the power estimate $(\psi_n^u)^2$ to the subsequent stages (not shown) of the receiver for derivation of power level adjustment signals in known

20  manner.

        The receiver shown in Figure 5 will perform satisfactorily if there are no strong interferers, *i.e.*, if it can be assumed that all users transmit with the same modulation and at the same rate, and that the base-station knows all the spreading codes of the terminals with which it is communicating. On that basis, operation of the receiver will be

25  described with reference to the user channel identified by index $u$.

        At time $t$, the antenna array signal vector $X(t)$ received by the elements 12$^1$...12$^M$ of the antenna array of the one particular cell shown in Figures 1 and 2 can be written as follows:

$$X(t) = \sum_{u=1}^{U} X^u(t) + N^{th}(t) \tag{2}$$

30

where $U$ is the total number of mobile stations whose signals are received at the base-station 11 from inside or outside the cell, $X^u(t)$ is the received signal vector from the mobile station 10$^u$, *i.e.*, of index $u$, and $N_{th}(t)$ is the thermal noise received at the $M$

antenna elements. The contribution $X^u(t)$ of the $u$-th mobile station $10^u$ to the observation vector $X(t)$ is given by:

$$
\begin{aligned}
X^u(t) &= \psi^u(t) H^u(t) \otimes c^u(t) b^u(t) \\
&= \psi^u(t) \sum_{p=1}^{P} G_p^u(t)\, \varepsilon_p^u(t)\, c^u(t - \tau_p^u(t))\, b^u(t - \tau_p^u(t))
\end{aligned}
\tag{2a}
$$

where $H^u(t)$ is the channel response vector of the channel $14^u$ between the $u$-th mobile station $10^u$ and the array of antenna elements and $\otimes$ denotes time-convolution. In the right-hand term of the above equation, the propagation time-delays $\tau_p^u(t) \in [0,T]$ along the $P$ paths, $p = 1, \cdots, P$, (see Figure 1), are chip-asynchronous, $G_p^u(t)$ are the propagation vectors and $\varepsilon_p^u(t)^2$ are the fractions along each path (i.e., $\sum_{p=1}^{P} \varepsilon_p^u(t)^2 = 1$) of the total power $\psi^u(t)^2$ received from the $u$-th mobile station $10^u$. The received power is affected by path-loss, Rayleigh fading and shadowing. It is assumed that $G_p^u(t)$, $\varepsilon_p^u(t)^2$ and $\psi^u(t)^2$ vary slowly and are constant over the bit duration $T$.

In the preprocessing unit 18 (see Figure 6), the antenna array signal vector $X(t)$ is filtered with the matched pulse to provide the matched-filtering signal vector $Y_n(t)$ for frame $n$ as follows:

$$
Y_n(t) = \frac{1}{T_c} \int_{D_\phi} X(aT/2 + nT + t + t')\, \phi(t')\, dt'
\tag{3}
$$

where $D_\phi$ denotes the temporal support of $\phi(t)$ and $a \in \{0,1\}$ stands for a possible time-shift by $T/2$ to avoid, if necessary, the frame edges lying in the middle of the delay spread (see reference [13]). For the sake of simplicity, it is assumed in the following that $a = 0$. Note that for a rectangular pulse $D_\phi$ is $[0,T_c]$. In practice, it is the temporal support of a truncated square-root raised- cosine.

It should be noted that the above description is baseband, without loss of generality. Both the carrier frequency modulation and demodulation steps can be embedded in the chip pulse-shaping and matched-filtering operations of Equations (1) and (3), respectively.

Thus, after sampling at the chip rate $1/T_c$ and framing over $2L - 1$ chip samples at the bit rate to form a frame, the preprocessing unit 18 derives the $M \times (2L -1)$ matched-filtering observation matrix:

$$
Y_n = \left[ Y_{n,0},\, Y_{n,1}, \cdots, Y_{n,2L-2} \right],
\tag{4}
$$

20

where $Y_{n,l} = Y_n(lT_c)$.

In the despreader $19^u$ (see Figure 7), the post-correlation vector for frame number $n$ for user number $u$ is obtained as:

5
$$Z_{n,l}^u = \frac{1}{L}\sum_{k=0}^{L-1} Y_{n,l+k}\ c_k^u. \tag{5}$$

Framing this vector over $L$ chip samples at the bit rate forms the post-correlation observation matrix:

$$Z_n^u = \left[Z_{n,0}^u, Z_{n,1}^u, ..., Z_{n,L-1}^u\right]. \tag{6}$$

10 The post-correlation data model (PCM) (see reference [13]) details the structure of this matrix as follows:

$$Z_n^u = H_n^u s_n^u + N_{PCM,n}^u, \tag{7}$$

where $Z_n^u$ is the spatio-temporal observation matrix, $H_n^u$ is the spatio-temporal propagation matrix, $s_n^u = b_n^u \psi_n^u$ is the signal component and $N_{PCM,n}^u$ is the spatio-

15 temporal noise matrix. Equation 7 provides an instantaneous mixture model at the bit rate where the signal subspace is one-dimensional in the $M \times L$ matrix space. For convenience, the vector reshaper $26^u$ of despreader $19^u$ transforms the matrices $Z_n^u$, $H_n^u$ and $N_{PCM,n}^u$ into $(M \times L)$-dimensional vectors $\underline{Z}_n^u$, $\underline{H}_n^u$ and $\underline{Z}_{PCM,n}^u$ respectively, by concatenating their columns into one

20 spatio-temporal column vector to yield the following narrowband form of the PCM model (see reference 13):

$$\underline{Z}_n^u = \underline{H}_n^u s_n^u + \underline{N}_{PCM,n}^u \tag{8}$$

To avoid the ambiguity due to a multiplicative factor between $\underline{H}_n^u$ and $s_n^u$, the norm of $\underline{H}_n^u$ is fixed to $\sqrt{M}$.

25 The PCM model significantly reduces inter-symbol interference. It represents an instantaneous mixture model of a narrowband source in a one-dimensional signal subspace and enables exploitation of low complexity narrowband processing methods after despreading. Processing after despreading exploits the processing gain to reduce the interference and to ease its cancellation in subsequent steps by facilitating estimation

30 of channel parameters.

As discussed in reference 13, the spatio-temporal array-receiver (STAR) can be used to detect each user separately at the base-station 11. In addition to exploiting the processing gain to reduce interference, the STAR allows accurate synchronization and

tracking of the multipath delays and components and shows inherent robustness to interference. The STAR also allows coherent combining of the data. This receiver is found to provide fast and accurate time-varying multipath acquisition and tracking. Moreover, it significantly improves call capacity by spatio-temporal maximum ratio

5   combining (MRC) in a coherent detection scheme implemented without a pilot signal. For the sake of clarity, the steps of STAR that are relevant to the implementation of the present invention will be reviewed briefly below, with reference to receiver module $21^u$ of Figure 5.

As shown in Figure 5, the despreader $19^u$ supplies the post-correlation observation

10  vector $\underline{Z}_n^u$, to both the channel identification unit $28^u$ and the MRC beamformer $27^u$ of STAR unit $20^u$. Using spatio-temporal matched filtering $(\underline{W}_n^u = \underline{\hat{H}}_n^u/M)$ (i.e. spatio-temporal maximum ratio combining, $\underline{W}_n^{uT}\underline{\hat{H}}_n^u = 1$), the STAR unit $20^u$ provides estimates of signal component $s_n^u$, its DBPSK bit sequence $b_n^u$ and its total received power $(\psi_n^u)^2$ as follows:

15

$$\hat{s}_n^u = Real\left\{\underline{W}_n^{uH}\underline{Z}_n^u\right\} = Real\left\{\frac{\hat{H}_n^{uH}\underline{Z}_n^u}{M}\right\},\tag{9}$$

$$\hat{b}_n^u = Sign\left\{\hat{s}_n^u\right\},\tag{10}$$

20

$$(\psi_n^u)^2 = (1 - \alpha)(\psi_{n-1}^u)^2 + \alpha \, |\hat{s}_n^u|^2,\tag{11}$$

where $\alpha$ is a smoothing factor. It should be noted that with ad hoc modifications, differential modulation and quasi-coherent differential decoding still apply with DMPSK.

25  Orthogonal modulation can even be detected coherently by STAR without a pilot (references [17] and [18]). Using the post-correlation observation vector $\underline{Z}_n^u$ and the new signal component estimate $\hat{s}_n^u$ from the beamformer $27^u$, the channel identification unit $28^u$ provides an estimate $\underline{\hat{H}}_n^u$ of the channel $14^u$ for user station $10^u$. The channel identification unit $28^u$ updates the channel parameter estimate $\hat{H}_n^u$ by means of a decision

30  feedback identification (DFI) scheme whereby the signal component estimate $\hat{s}_n^u$ is fed back as a reference signal in the following eigen-subspace tracking procedure:

$$\underline{\hat{H}}_{n+1}^u = \underline{\hat{H}}_n^u + \mu\left(\underline{Z}_n^u - \underline{\hat{H}}_n^u \hat{s}_n^u\right)\hat{s}_n^u,\tag{12}$$

22

where $\mu$ is an adaptation step-size. Alternatively, the product $\underline{\psi}_n^u \hat{b}_n^u$ could be fed back instead of the symbol component estimate $\hat{s}_n^u$. This DFI scheme allows a 3 dB coherent detection gain in noise reduction by recovering the channel phase offsets within a sign ambiguity without a pilot. Note that a reduced-power pilot can be used to avoid

5 differential coding and decoding (reference [21]). The procedure that further enhances the channel estimate $\underline{\hat{H}}_{n+1}^u$ to obtain $\underline{\hat{H}}_{n+1}^u$ from the knowledge of its spatio-temporal structure (i.e. manifold) allows a fast and accurate estimation of the multipath time-delays $\hat{\tau}_{1,n}^u,...,\hat{\tau}_{P,n}^u$ in both the acquisition and the tracking modes (both versions of this procedure can be found in reference [13]). This improved estimation accuracy

10 achieves robustness to channel estimation errors, and reduces sensitivity to timing errors, when STAR is used in multiuser operation.

For further information about STAR, the reader is directed to the articles by Affes and Mermelstein identified as references [13] and [17] to [21].

If, as was assumed in reference 13, the spatio-temporal noise vector $\underline{N}_{PCM,n}^u$ is

15 spatially uncorrelated, power control on the uplink is generally able to equalize the received signal powers. However, the assumption that noise is uncorrelated becomes untenable on the downlink due to path-loss and shadowing and when the power of particular users (e.g., "priority links", acquisition, higher-order modulations or higher data-rates in mixed-rate traffic) is increased intentionally. Within a particular cell, there

20 may be users having many different "strengths", perhaps because of different data rates. Figure 8 illustrates, as an example, a cell in which there are four different sets of users arranged hierarchically according to data rate. The first set I comprises users which have relatively high data rates, the second set M1 and third set M2 both comprise users which have intermediate data rates, and the fourth set D comprises users which have

25 relatively low data rates. In practice, the receivers of the high data rate users of set I will not need to cancel any "outset" interference from the users in sets M1, M2 and D, but their transmissions will contribute to interference for the receiver modules in those sets. Intermediate data rate users in sets M1 and M2 will need to cancel "outset" interference from the high data rate users of the set I but not from the users in set D.

30 They will themselves be contributors of "outset" interference to the users in set D. The receivers of users in set D must cancel "outset" interference from sets I, M1 and M2.

It is also possible for a receiver of a user within a particular set to cancel "inset" interference from one or more users within the same set; and itself be a contributor to

23

such "inset" interference. Embodiments of the invention applicable to these "outset" and "inset" situations will be described hereinafter. In the description, where a particular user's signal is treated as interference and cancelled, it will be deemed to be a "contributor" and, where a particular user's receiver module receives information to

5 enable it to cancel another user's interference, it will be deemed to be a "recipient". To simplify the description of the preferred embodiments described herein, it will be assumed that all users employ the same modulation at the same rate. For the purpose of developing the theory of operation, initially it will be assumed that, among the mobile stations in the cell, there will be a first set I of "strong" contributor users, one of which

10 is identified in Figures 1 and 2 by index "i", whose received signal powers are relatively high and hence likely to cause more interference, and a second set D of "low-power" recipient users, one of which is identified in Figures 1 and 2 by index "d", whose received signal powers are relatively low and whose reception may be degraded by interference from the signals from the strong users. In order to receive the low-power

15 users adequately, it usually is desirable to substantially eliminate the interference produced by the high-power users. For simplicity, most of the preferred embodiments of the invention will be described on the basis that the high-power users can be received adequately without interference suppression. It should be appreciated, however, that the "strong" user stations could interfere with each other, in which case one could also apply

20 to any interfering mobile the coloured noise model below and the near-far resistant solution proposed for the low-power user, as will be described later.

Assuming the presence of $NI$ interfering users assigned the indices $i = 1$ to $NI$, then the spatio-temporal observation vector of any interfering user $(u = i \in \{1,...,NI\})$ is given from Equation 8 by:

25

$$Z_n^i = H_n^i s_n^i + N_{PCM,n}^i \qquad (13)$$

where $N_{PCM,n}^i$ can still be assumed to be an uncorrelated white noise vector if the processing gain of this user is not very low. On the other hand, from the point of view of any low-power user $(u = d \notin \{1,...,NI\})$, the spatio-temporal observation vector is:

30

$$Z_n^d = H_n^d s_n^d + I_{PCM,n}^d + N_{PCM,n}^d = H_n^d s_n^d + \sum_{i=1}^{NI} I_{PCM,n}^{d,i} + N_{PCM,n}^d, \qquad (14)$$

24

where, in addition to the uncorrelated white noise vector $\underline{N}^d_{PCM,n}$, there is included a total interference vector $\underline{I}^d_{PCM,n}$ which sums a random coloured spatio-temporal interference vector from each interfering mobile denoted by $\underline{I}^{d,i}_{PCM,n}$ for $i = 1, ..., NI$. At frame number n, the realization of the vector $\underline{I}^{d,i}_{PCM,n}$ results from matched-pulse filtering, ship-

5 rate sampling, bit-rate framing, despreading with $c^d_i$, and matrix/vector reshaping of the received signal vector $X^i(t)$ from the $i$-th interfering mobile using Equations (3) to (6).

The receiver shown in Figure 5 would receive the signals from all of the user stations independently of each other. It should be noted that there is no cross-connection

10 between the receiver modules $21^1...21^U$, specifically between their STAR units $20^1...20^u...20^U$, for suppression of interference from the signals of mobile stations which constitute strong interferers. While the matched beamformer of Equation (9) is optimal in uncorrelated white noise, it is suboptimal when receiving the low-power users due to spatial correlation of the interference terms. To allow the accommodation of additional

15 users in the presence of much stronger interfering mobiles in the target cell, in embodiments of the present invention the receiver of Figure 5 is upgraded to obtain much stronger near-far resistance, specifically by adapting the beamformer of Equation 9 to reject the interference contributions from the interfering strong users.

In the general case, the total interference $\underline{I}^d_{PCM,n}$ experienced by a user $d$ in set

20 D is an unknown random vector which lies at any moment in an interference subspace spanned by a matrix, say $C^d_{PCM,n}$ (i.e., $\underline{I}^d_{PCM,n} \in Vec\{C^d_{PCM,n}\}$) with dimension depending on the number of interference parameters (i.e., power, data, multipath components and delays) assumed unknown or estimated a priori. As will become apparent from the following descriptions of preferred embodiments, in practice, the

25 matrix $C^d_{PCM,n}$, which will be referred to as the "constraint matrix", can be derived and estimated in different ways. To achieve near-far resistance, the beamformer must conform to the following theoretical constraints:

30
$$\begin{cases} \underline{W}^{d^H}_n \underline{H}^d_n = 1, \\ \underline{W}^{d^H}_n C^d_{PCM,n} = 0, \end{cases} \Rightarrow \begin{cases} \underline{W}^{d^H}_n \underline{H}^d_n = 1, \\ \underline{W}^{d^H}_n I^d_{PCM,n} = 0. \end{cases} \tag{15}$$

The first constraint provides a substantially distortionless response to the low-power user while the second instantaneously rejects the interference subspace and thereby

substantially cancels the total interference. This modification of the beamforming step of STAR will be referred to as interference subspace rejection (ISR).

With an estimate of the constraint matrix $\hat{C}^d_{PCM,n}$ available (as described later), the ISR combiner (i.e., the constrained spatio-temporal beamformer) $\underline{W}^d_n$ after
5    despreading is obtained by:

$$Q^d_{PCM,n} = \left( \hat{C}^{d^H}_{PCM,n} \hat{C}^d_{PCM,n} \right)^{-1}, \tag{16}$$

$$\Pi_{PCM,n} = I_{M \cdot L} - \hat{C}^d_{PCM,n} Q^d_{PCm,n} \hat{C}^{d^H}_{PCM,n}, \tag{17}$$
10

$$\underline{W}^d_n = \frac{\Pi^d_{PCM,n} \hat{\underline{H}}^d_n}{\hat{\underline{H}}^d_n \Pi^d_{PCM,n} \hat{\underline{H}}^d_n}, \tag{18}$$

where $I_{M \cdot L}$ denotes a $M * L \times M * L$ identity matrix. First, the projector $\Pi_{PCM,n}$ orthogonal to the constraint matrix $\hat{C}_{PCM,n}$ is formed. It should be noted from Equations
15   (16) and (17) that the inverse matrix $Q^d_{PCM,n}$ is not the direct inverse of constraint matrix $C^d_{PCM,n}$ but part of the pseudo-inverse of $C^d_{PCM,n}$. For convenience, however, it will be referred to as the inverse matrix hereafter. Second, the estimate of the low-power response vector $\hat{\underline{Y}}^d_n$ is projected and normalized.

Whereas, using the above constraints, the ISR beamformer may process the low-
20   power user's data vector after it has been despread, it is possible, and preferable, to process the data vector without first despreading it. In either case, however, the data vector will still be despread for use by the channel identification unit. Although it is computationally more advantageous to do so without despreading, embodiments of both alternatives will be described. First, however, the spread data model of Equation (2)
25   will be reformulated and developed and then used to derive various modes that implement ISR combining of the data, without despreading, suitable for different complementary situations.


### Data Model Without Despreading

30       The observation matrix $Y_n$ of Equation (4) which provides the post-correlation matrix $Z_n$ of Equation (7) by despreading and framing at the bit rate, can be expressed as:

$$Y_n = \sum_{u=1}^{U} Y^u_n + N^{pth}_n, \tag{19}$$

26

where each user $u$ contributes its user-observation matrix $Y_n^u$, obtained by Equations (3) and (4) with $X(t)$ replaced by $X^u(t)$ in Equation (3), and where the preprocessed thermal noise contributes:

$$N_n^{pth} = \left[ N^{pth}(nT), N^{pth}(nT + T_c), ..., N^{pth}(nT + (2L - 2)T_c) \right]. \qquad (20)$$

Using the fact that any bit-triplet $\left[ b_{n-1}^u, b_n^u, b_{n+1}^u \right]$ contributing to channel convolution (see Equation (2a) in $Y_n^u$ can be composed as:

$$\left[ b_{n-1}^u, b_n^u, b_{n+1}^u \right] = b_{n-1}^u [1, 0, 0] + b_n^u [0, 1, 0] + b_{n+1}^u [0, 0, 1], \qquad (21)$$

the sequence $b^u(t)$ can be locally approximated over the $n$-th block by means of the canonic generating sequences $g^1(t)$, $g^2(t)$ and $g^3(t)$ in Figure 22 as:

$$b^u(t) = b_n^u g^{l_{0,n}}(t) + b_{n-1}^u g^{l_{-1,n}}(t) + b_{n+1}^u g^{l_{+1,n}}(t), \qquad (22)$$

where the indices $l_{0,n}$, $l_{-1,n}$, $l_{+1,n} \in \{1, 2, 3\}$ are permuted at each block so that the corresponding canonic generating sequences locally coincide with [0, 1, 0], [1, 0, 0] and [0, 0, 1], respectively. Assuming slow time-variations of $\psi(t)$ and $H(t)$ compared to the symbol duration:

$$Y_n^u = s_n^u Y_{0,n}^u + s_{n-1}^u Y_{-1,n}^u + s_{n+1}^u Y_{+1,n}^u, \qquad (23)$$

where the canonic user-observation matrices $Y_{k,n}^u$ are obtained by Equations (3) and (4) with $X(t)$ in Equation (3) replaced, respectively for $k = -1, 0, +1$, by:

$$X_k^u(t) = H^u(t) \otimes g^{l_{k,n}}(t) c^u(t). \qquad (24)$$

Good approximations of $Y_{-1,n}$ and $Y_{+1,n}$ can be actually obtained at each iteration by $L$ simple backward/forward shifts of the columns of $Y_{0,n}^u$ with zero column inputs.

It should be noted that the canonic generating sequences allow more accurate reconstruction (e.g., overlap-add) of time-varying channels. Also, the resulting decomposition in Equation (23) holds for long PN codes.

It should be noted that this decomposition also holds for any complex-valued symbol-triplet $\left[ b_{n-1}^u, b_n^u, b_{n+1}^u \right]$. With *ad hoc* modifications, therefore, the ISR approach according to this invention applies to any complex modulation (*e.g.*, MPSK, MQAM, even analog). This new signal decomposition is used to derive the different implementations of ISR which will be described later.

With respect to the low-power user assigned the index $d$ and the $NI$ strong interfering mobiles assigned the indices $i = 1, ..., NI$, the observation vector obtained by reshaping the observation matrix, before despreading, can now be rewritten as:

$$\underline{Y}_n = \underline{Y}_{0,n}^d s_n^d + \underline{I}_{ISI,n}^d + \underline{I}_n + \underline{N}_n, \qquad (25)$$

where the first canonic observation vector $\underline{Y}^d_{0,n}$ appears as the "channel" vector of the low-power user $d$. The total interference vector before despreading:

$$\underline{I}_n = \sum_{i=1}^{NI} \underline{Y}^i_n = \sum_{i=1}^{NI} \left\{ s^i_n \underline{Y}^i_{0,n} + s^i_{n-1} \underline{Y}^i_{-1,n} + s^i_{n+1} \underline{Y}^i_{+1,n} \right\} = \sum_{i=1}^{NI} \left\{ s^i_n \underline{Y}^i_{0,n} + \underline{I}^i_{ISI,n} \right\}, \quad (26)$$

is the sum of the interfering signal vectors $\underline{Y}^i_n$ and:

$$\underline{I}^u_{ISI,n} = s^u_{n-1} \underline{Y}^u_{-1,n} + s^u_{n+1} \underline{Y}^u_{+1,n}, \quad (27)$$

is the intersymbol interference (ISI) vector of user $u$. In large processing gain situations, the self ISI vector $\underline{I}^d_{ISI,n}$ can be combined with the uncorrelated spatio-temporal noise vector $\underline{N}_n$, leading to the following data vector model before despreading:

$$\underline{Y}_n = \underline{Y}^d_{0,n} s^d_n + \underline{I}_n + \underline{N}_n. \quad (28)$$

Despreading the observation vector in the above equation with the spreading sequence of the low-power user $d$ provides the data vector model after despreading in Equaiton (14). It is possible to derive a finer decomposition of the date model to allow implementation of one or more of the ISR modes over diversities.

## *Finer Decomposition of the Data Model Over Diversities*

Thus, Equation (2a) can be further decomposed over the $N_f = MP$ diversity branches or fingers in such a way that the observation signal contribution $X^{u,f}(t)$ received by the $m$-th antenna along the $p$-th path for $f = (p - 1)M + m = 1,..., N_f$ can be separated as follows:

$$X^u(t) = \sum_{f=1}^{N_f} X^{u,f}(t). \quad (29)$$

The observation signal contribution from the $f$-th finger is defined as:

$$\begin{aligned} X^{u,f}(t) &= \psi^u(t) H^{u,f}(t) \otimes c^u(t) b^u(t) \\ &= \psi^u(t) G^{u,f}_p(t) \varepsilon^u_p(t) b^u(t - \tau^u_p(t)) c^u(t - \tau^u_p(t)), \end{aligned} \quad (30)$$

where the propagation vector from the $f$-th finger is:

$$G^{u,f}_p(t) = \gamma^u_f(t) \underline{R}_m. \quad (31)$$

28

In the above equation, the scalar $\gamma_f^u(t)$ is the channel coefficient over the $f$-th finger and $\underline{R}_m = [0,\ldots,0,1,0,\ldots,0]^T$ is a $M \times 1$ vector with null components except for the $m$-th one. With the above definitions, one can easily check the following decompositions of the channel and the propagation vectors:

$$H^u(t) = \sum_{f=1}^{N_f} H^{u,f}(t), \tag{32}$$

$$G_p^u(t) = \sum_{m=1}^{M} G_p^{u,(p-1)M+m}(t). \tag{33}$$

Accordingly, after preprocessing, the matched-filtering observation matrix can be decomposed as follows:

$$Y_n = \sum_{u=1}^{U} Y_n^u + N_n^{pth} = \sum_{u=1}^{U} \sum_{f=1}^{N_f} \psi_{n}^u \zeta_{f,n}^u Y_n^{u,f} + N_n^{pth}, \tag{34}$$

where each user $u$ contributes its user-observation matrices $Y_n^{u,f}$ from fingers $f = 1,\ldots,N_f$ obtained by Equations (3) and (4) with $X(t)$ replaced by $X^{u,f}(t)$ in Equation (3). Note that the complex channel coefficient $\gamma_f^u(nT) = \zeta_f^u(nT)\epsilon_p^u(nT)$ is separated from the matrix[1] $Y_n^{u,f}$ which contains a purely-delayed replica of the spread-data without attenuation or phase offset from finger $f$. This matrix, which is obtained by Equations (3) and (4) with $X(t)$ in Equation (3) replaced by:

$$X^{u,f}(t) = \underline{R}_m \delta(t - \tau_p(t)) \otimes b^u(t) c^u(t), \tag{35}$$

can be further decomposed over the canonic generating sequences as follows:

$$Y_n^{u,f} = b_n^u Y_{0,n}^{u,f} + b_{n-1}^u Y_{-1,n}^{u,f} + b_{n+1}^u Y_{+1,n}^{u,f}, \tag{36}$$

where the canonic user-observation matrices $Y_{k,n}^{u,f}$ from finger $f$ are obtained by Equations (3) and (4) with $X(t)$ in Equation (3) replaced, respectively for $k = -1, 0, +1$, by:

---

[1]This matrix is real-valued in the case of a binary modulation.

29

$$X_k^{u,f}(t) = \underline{R}_m \delta(t - \tau_p(t)) \otimes g^{l_u}(t) c^u(t), \tag{37}$$

where $\delta(t)$ denotes the Dirac impulse. Therefore one obtains:

5
$$Y_n = \sum_{u=1}^{U} \sum_{f=1}^{N_f} \sum_{k=-1}^{+1} s_{n+k}^u \zeta_{f,n}^u Y_{k,n}^{u,f} + N_n^{oth}. \tag{38}$$

A coarser decomposition over fingers of the total interference vector before despreading defined in Equation (26) gives:

10
$$\underline{I}_n = \sum_{i=1}^{NI} \underline{Y}_n^i = \sum_{i=1}^{NI} \sum_{f=1}^{N_f} \psi_n^u \zeta_{f,n}^u \underline{Y}_n^{u,f}. \tag{39}$$

After despreading with the spreading sequence of the low-power user $d$, it gives:

$$I_{PCM,n}^d = \sum_{i=1}^{NI} I_{PCM,n}^{d,i} = = \sum_{i=1}^{NI} \sum_{f=1}^{N_f} \psi_n^u \zeta_{f,n}^u I_{PCM,n}^{d,i,f}. \tag{40}$$
15

Embodiments of the invention which use the above decompositions of interference, denoted as ISR-D implementations before and after despreading, will be described later with reference to Figures 16 and 23.

20 *ISR Combining Before Despreading*

As described hereinbefore, the combining step of STAR is implemented without despreading by replacing Equation (9) for the low-power user with:

$$\hat{s}_n^d = Real\{\underline{W}_n^{d^H} \underline{Y}_n\}, \tag{41}$$

where the spatio-temporal beamformer $\underline{W}_n^d$ now implements ISR without despreading
25 to reject $\underline{I}_n$ by complying with the following constraints (see Equation (15)):

$$\begin{cases} \underline{W}_n^{d^H} \underline{Y}_{0,n}^d = 1, \\ \underline{W}_n^{d^H} C_n = 0, \end{cases} \Rightarrow \begin{cases} \underline{W}_n^{d^H} \underline{Y}_{0,n}^d = 1, \\ \underline{W}_n^{d^H} \underline{I}_n = 0, \end{cases} \tag{42}$$

and $C_n$ is the constraint matrix without despreading that spans the interference subspace
30 of the total interference vector $\underline{I}_n$ (*i.e.*, $\underline{I}_n \in Vec\{C_n\}$).

The constraint matrix without despreading, $C_n$, is common to all low-power users. Thus, it characterizes the interference subspace regardless of the low-power user. In contrast, each constraint matrix after despreading $C_{PCM,n}^d$ in Equaiton (15) is obtained

30

by despreading $C_n$ with the spreading sequence of the corresponding low-power user. Therefore ISR combining before despreading, although equivalent to beamforming after despreading, is computationally much more advantageous.

In contrast to the "after despreading" case described earlier, when the data vector 5 is not despread before processing by the ISR combiner (*i.e.*, the constrained spatio-temporal beamformer) $\underline{W}_n^d$ the estimate of the constraint matrix $\hat{C}_n$ is obtained by:

$$Q_n = \left(\hat{C}_n^H \hat{C}_n\right)^{-1}, \tag{43}$$

$$\Pi_n = I_{M \cdot (2L-1)} - \hat{C}_n Q_n \hat{C}_n^H, \tag{44}$$

10

$$\underline{W}_n^d = \frac{\Pi_n \ \hat{\underline{Y}}_{0,n}^d}{\hat{\underline{Y}}_{0,n}^{d^H} \Pi_n \ \hat{\underline{Y}}_{0,n}^d}, \tag{45}$$

where $I_{M \cdot (2L-1)}$ denotes a $M * (2L - 1) \times M * (2L - 1)$ identity matrix. As before, it can be seen from Equations (43) and (44) that the inverse matrix $Q_n$ is not the direct inverse of constraint matrix $\hat{C}_n$ but part of the pseudo-inverse of $\hat{C}_n$. It should also be noted 15 that the above operations are actually implemented in a much simpler way that exploits redundant or straightforward computations in the data projection and the normalization. As before, the projector $\Pi_n$ orthogonal to the constraint matrix $\hat{C}_n$ is formed once for all low-power users. This would have not been possible with ISR after despreading. Second, the estimate of the low-power response vector $\hat{\underline{Y}}_{0,n}^d$ is projected and normalized. 20 The estimate $\hat{\underline{Y}}_{0,n}^d$ is reconstructed by reshaping the following matrix:

$$\hat{Y}_{0,n}^d = \hat{H}_n^d \otimes \underline{g}_n^{l \cdots} c_l^d \tag{46}$$

the fast convolution with the channel being implemented row-wise with the spread sequence. The channel estimates $\underline{\hat{H}}_n^d$ *i.e.* $\hat{H}_n^d$ is provided by STAR as explained earlier and includes the total contribution of the shaping pulse $\phi(t)$ matched with itself [13]. If 25 the channel time-variations are slow, the channel coefficients can be assumed constant over several symbol durations [20], thereby reducing the number of computationally expensive despreading operations required (see Figure 9).

It should be noted that, although these ISR modes have formulations that are analogous whether ISR is implemented with or without first despreading the data vector, 30 ISR combining of the data without it first being despread reduces complexity significantly.

Receivers which implement these different ISR modes will now be described, using the same reference numerals for components which are identical or closely similar

31

to those of the receiver of Figure 5, with a suffix indicating a difference. A generic ISR receiver which does so without despreading of the data will be described first, followed by one which does so after despreading of the data. Thereafter, specific implementations of different ISR modes will be described.

5   Thus, Figure 9 illustrates a receiver according to a first embodiment of the invention which comprises a first set I of "strong user" receiver modules $21^1...21^{NI}$ which are similar to those in the receiver of Figure 5, and, separated by a broken line 34, a second set D of "low-power" user receiver modules which differ from the receiver modules of set I but are identical to each other so, for convenience, only one, receiver

10 module $21A^d$ comprising a STAR module $20A^d$ having a modified beamformer $47A^d$, is shown. The outputs of the decision rule units $29^1,...,29^{NI}$ and of the channel identification units $28^1,...,28^{NI}$ from the set I modules are shown coupled to a constraints-set generator 42A which processes the corresponding symbol estimates and channel parameter estimates to produce a set of $N_c$ constraints $C_n = \{C_n^1,...,C_n^{N_c}\}$. The

15 constraints-set generator 42A may, however, use hypothetical symbol values instead, or a combination of symbol estimates and hypothetical values, as will be described later. Each individual constraint lies in the same observation space as the observation matrix $Y_n$ from preprocessor 18. The constraints-set generator 42A supplies the set of constraints $C_n$ to a constraint matrix generator 43A which uses them to form a constraint

20 matrix $\hat{C}_n$ and an inverse matrix $Q_n$ which supplies it to the beamformer $47^d$ and each of the corresponding beamformers in the other receiver modules of set D. The actual content of set of constraints $C_n$ and the constraint matrix $\hat{C}_n$ will depend upon the particular ISR mode being implemented, as will be described later.

   The receiver of Figure 9 also comprises a vector reshaper 44 which reshapes the

25 observation matrix $Y_n$ from the preprocessing unit 18 to form an observation vector $\underline{Y}_n$ having dimension $M(2L-1)$ and supplies it to the beamformer $47A^d$ and to each of the other beamformers in the other receiver modules in set D.

   The STAR unit $40A^d$ of receiver module $41A^d$ comprises a channel identification unit $28A^d$, a decision rule unit $27A^d$ and a power estimation unit $30A^d$ which are similar

30 to those of the STAR units $20^1...20^U$ described hereinbefore. In addition to the STAR unit $40A^d$, the receiver module $41A^d$ comprises a despreader $19^d$. The despreader $19^d$ despreads the observation matrix $Y_n$ using the spreading code for user $d$ and supplies the resulting post-correlation observation vector $\underline{Z}_n$ to the channel identification unit $28A^d$

only. The decision rule unit $27A^d$ and power estimation unit $30A^d$ produce output symbol estimates $\hat{b}_n^d$ and power estimates $(\hat{\psi}_n^d)^2$, respectively. The ISR beamformer $47A^d$ of STAR unit $40A^d$ produces corresponding signal component estimates $\hat{s}_n^d$ but differs from the MRC beamformers $27^l...27^{Nl}$ because it operates upon the observation

5 vector $\underline{Y}_n$, which has not been despread. In a manner similar to that described with respect to Figure 5, the channel identification unit $28A^d$ receives the post-correlation observation vector $\underline{Z}_n^d$ and the signal component estimate $\hat{s}_n^d$ and uses them to derive the spread channel estimates $\hat{\underline{Y}}_{0,n}^d$, which it uses to update the weighting coefficients $W_n^d$ of the beamformer $47A^d$ in succeeding symbol periods. The symbol

10 period corresponds to the spread data frame of $M(2L-1)$ elements. The coefficients of the ISR beamformer $47A^d$ also are updated in response to the constraint matrix $\hat{C}_n$ and its inverse $Q_n$, as will be described later. As shown in Figure 9, the same matrices $\hat{C}_n$ and $Q_n$ are supplied to all of the receiver modules in set D, specifically to their beamformers.

15      As shown in Figure 10, the constraint matrix generator means 43A comprises a bank of vector reshapers $48A^1$, ..., $48A^{N_c}$ and a matrix inverter 49A. Each of the vector reshapers $48A^1$, ..., $48A^{N_c}$ reshapes the corresponding one of the set of constraints-set matrices $C_n^1,...,C_n^{N_c}$ to form one column of the constraint matrix $\hat{C}_n$, which is processed by matrix inverter 49A to form inverse matrix $Q_n$. For

20 simplicity of description, it is implicitly assumed that each of the columns of $\hat{C}_n$ is normalized to unity when collecting it from the set of constraints $C_n$.

     As also illustrated in Figure 10, beamformer $47A^d$ can be considered to comprise a coefficient tuning unit $50A^d$ and a set of $M(2L-1)$ multipliers $51_1^d...51_{M(2L-1)}^d$. The coefficient tuning unit $50A^d$ uses the constraint matrix $\hat{C}_n$, the inverse matrix $Q_n$ and the

25 channel parameter estimates $\hat{\underline{Y}}_{0,n}^d$ to adjust weighting coefficients $W_{1,n}^{d*}...W_{M(2L-1),n}^{d*}$ according to Equation 45 *supra*. The multipliers $51_1^d...51_{M(2L-1)}^d$ use the coefficients to weight the individual elements $\underline{Y}_{1,n}...\underline{Y}_{M(2L-1),n}$, respectively, of the observation vector $\underline{Y}_n$. The weighted elements are summed by an adder $52^d$ to form the raw filtered symbol estimate $\hat{s}_n^d$ for output from the beamformer $47A^d$.

30      An alternative configuration of receiver in which the low-power STAR units of set D implement ISR beamforming *after* despreading of the observation matrix $Y_n$ from preprocessor 18 will now be described with reference to Figures 11 and 12, which correspond to Figures 9 and 10. The receiver shown in Figure 11 is similar to that

shown in Figure 9 in that it comprises a preprocessing unit 18 which supplies the observation matrix $Y_n$ to the set I receiver modules $21^1...21^{NI}$, a constraints-set generator 42B and a constraint matrix generator means 43B. It does not, however, include the vector reshaper 44 of Figure 9 and each of the low-power user STAR modules in set D

5 has a modified beamformer. Thus, modified beamformer $47B^d$ operates upon the post-correlation observation vector $\underline{Z}_n^d$ from the output of the despreader $19^d$ which is supplied to both the channel identification unit $28B^d$ and the beamformer $47B^d$. The channel identification unit $28B^d$ generates channel estimates $\hat{H}_n^d$ and supplies them to the beamformer $47B^d$ which updates its coefficients in dependence upon both them and a

10 user-specific constraint matrix $\hat{C}_{PCM,n}^d$ and user-specific inverse matrix $Q_{PCM,n}^d$. It should be noted that the constraint matrix generator means 43B supplies user-specific constraint and inverse matrices to the other receiver modules in set D.

Referring now to Figure 12, the common constraint matrix generator means 43B comprises a bank of user-specific constraint matrix generators, one for each of the

15 receiver modules of set D, and each using a respective one of the spreading codes of the users of set D. Since the only difference between the user-specific constraint matrix generators is that they use different spreading codes, only user-specific constraint matrix $43B^d$ is shown in Figure 12, with the associated beamformer $47A^d$. Thus, user-specific constraint matrix generator $43B^d$ comprises a bank of

20 despreaders $55B^{d,1}, ..., 55B^{d,N_c}$ and a matrix inverter $46B^d$. The despreaders $55B^{d,1}, ..., 55B^{d,N_c}$ despread respective ones of the $N_c$ matrices in the set of constraints $C_n$ to form one column of the individual constraint matrix $\hat{C}_{PCM,n}^d$ implicitly normalized to unity. The matrix inverter $46B^d$ processes individual constraint matrix $\hat{C}_{PCM,n}^d$ to form inverse matrix $Q_{PCM,n}^d$. The user-specific

25 constraint matrix generator $43B^d$ supplies the constraint matrix $\hat{C}_{PCM,n}^d$ and inverse matrix $Q_{PCM,n}^d$ to the coefficient tuning unit $50B^d$ of beamformer $47B^d$. As shown in Figure 12, the beamformer $47B^d$ has $ML$ multipliers $51_1^d...51_{ML}^d$ which multiply weighting coefficients $\underline{W}_{1,n}^{d*}...\underline{W}_{ML,n}^{d*}$ by elements $Z_{1,n}^d...Z_{ML,n}^d$ of the post-correlation observation vector $\underline{Z}_n^d$. As before, adder $52^d$ sums the weighted elements to form the

30 signal component estimate $\hat{s}_n^d$. The beamformer coefficeints are timed according to Equation (18).

Either of these alternative approaches, $i.e.$ with and without despreading of the data vector supplied to the beamformer, may be used with each of several different ways

of implementing the ISR beamforming, *i.e.* ISR modes. It should be noted that all cases use a constraint matrix which tunes the ISR beamformer to unity response to the desired channel and null response to the interference sub-space. In each case, however, the actual composition of the constraint matrix will differ.

5        Specific embodiments of the invention implementing the different ISR modes without despreading of the data will now be described with reference to Figure 13 to 20, following which embodiments implementing the same ISR modes after despreading will be described with reference to Figures 21 to 26.

10 *Interference Subspace Rejection over Total Realisation (ISR-TR)*

The receiver unit shown in Figure 13 is similar to that shown in Figure 9 in that it comprises a set I of receiver modules $21^1...21^{NI}$ for processing signals of $NI$ strongly interfering mobile stations and a set D of receiver modules for signals of other, "low-power", users. The receiver modules of set D are identical so only receiver module

15 $21C^d$, for channel $d$, is shown in Figure 13. As in the receiver of Figure 9, the observation matrix $Y_n$ from preprocessor 18 is supplied directly to each of the despreaders $19^1...19^{NI}$ of the set $I$ receiver modules. Before application to each of the receiver modules of set $D$, however, it is delayed by one symbol period by a delay element 45 and reshaped by vector reshaper 44. The resulting observation vector $Y_{n-1}$

20 is supplied to the beamformer $46C^d$ and to each of the other beamformers in the set D receiver modules (not shown). In addition to beamformer $47C^d$, receiver module $21C^d$ comprises despreader $19^d$ and a STAR receiver unit $20C^d$ comprising channel identification unit $28C^d$, decision rule unit $27C^d$ and power estimation unit $30C^d$ which are similar to those shown in Figure 9. The set of channel parameter

25 estimates $\mathcal{H}_n^1,...,\mathcal{H}_n^{NI}$, which are supplied to the constraints-set generator 42C comprise the channel estimates $\hat{\underline{H}}_n^1,...,\hat{\underline{H}}_n^{NI}$ and the power estimates $\psi_n^1,...,\psi_n^{NI}$.

The constraints-set generator 42C comprises a bank of respreaders $57C^1...57C^{NI}$ each having its output connected to the input of a respective one of a corresponding bank of channel replication units $59C^1...59C^{NI}$ by a corresponding one of a bank of multipliers

30 $58C^1...58C^{NI}$. The respreaders $57C^1...57C^{NI}$ are similar so only one, respreader $57C^u$, is illustrated in Figure 14. Respreader $57C^u$ is similar to the corresponding spreader $13^u$ (Figure 3) in that it spreads the symbol $b_n^u$ from the corresponding decision rule unit $29C^u$ using a periodic personal code sequence $c_l^u$ at a rate $1/T_c$, where $T_c$ is the chip

pulse duration. It differs, however, in that it does not include a shaping-pulse filter. The effects of filtering both at transmission with the shaping-pulse (see Figures 2 and 3) and at reception with the matched shaping-pulse (see Figures 5 and 6) are included baseband in the channel estimate $\hat{H}_n^u$ or $\hat{H}_n^u$, as disclosed in reference [13].

5    Referring again to Figure 13 and, as an example, receiver module 21C[1], replication of the propagation characteristics of channel 14[1] is accomplished by digital filtering in the discrete time domain, $i.e.$ by convolution at the chip rate of the channel estimate $\hat{H}_n^1$ with the respread data $b_n^1 c_l^1$. This filtering operation immediately provides decomposed estimates of the signal contribution of user station 10[1] to the observation

10  matrix $Y_n$. Thus, respreader 57C[1] respreads the symbol $b_n^1$ from decision rule unit 29C[1], multiplier 58C[1] scales it by the total amplitude estimate $\psi_n^1$ and channel replication filter 59C[1] filters the resulting respread symbol using the channel estimate $\hat{H}_n^1$ from channel identification unit 28C[1]. The symbol estimates from the other STAR units in set I are processed in a similar manner.

15  It should be noted that the respreaders 57C[1]...57C[NI], multipliers 58C[1]...58C[NI] and channel filters 59C[1]...50C[NI] correspond to the elements 13[1], 15[1] and 14[1] in the interfering user channel of Figure 2. The coefficients of the channel replication filter units 59C[1]...59C[NI] are updated in successive symbol periods by the channel identification units 28C[1]...28C[NI] using the same coefficients $\hat{H}_n^1...\hat{H}_n^{NI}$, corresponding to the transmission

20  channels 14[1]...14[NI], respectively, used to update their respective MRC beamformers 27C[1]...27C[NI]. It will be appreciated that the re-spread signals $\hat{Y}_{n-1}^1 ... \hat{Y}_{n-1}^{NI}$ from the channel replication filter units 59C[1]...59C[NI], respectively, include information derived from both the sign and the amplitude of each symbol, and channel characteristics information, and so are the equivalents of the set I strong interferer's spread signals as

25  received by the base station antenna elements 12[1]...12[M].

The constraint-set generator 42C also comprises an adder 60 coupled to the outputs of the channel replication units 59C[1]...59C[NI]. The adder 60 sums the estimates $\hat{Y}_{n-1}^1 ... \hat{Y}_{n-1}^{NI}$ of the individual contributions from the different interferers to form the estimate $\hat{I}_{n-1}$ of the total interference from the $NI$ interferers in the received

30  observation matrix $Y_n$. The sum can be called total realization $(TR)$ of the interference. In this embodiment, the constraint matrix generator simply comprises a vector reshaper 43CB which reshapes the total realization matrix $\hat{I}_{n-1}$ to form the vector $\hat{I}_{n-1}$ which, in this embodiment, constitutes the constraint matrix $C_n$. It should be noted that, because

the constraint matrix really is a vector, the inverse matrix $Q_n$ reduces to a scalar and, assuming implicit normalization, is equal to 1. Hence, no matrix inverter is needed.

The reshaped vector $\underline{\hat{I}}_{n-1}$ is supplied to the ISR beamformer 47C$^d$ of receiver module 21C$^d$ and to the beamformers of the other receiver modules in set D. The

5 beamformer 47C$^d$ uses the reshaped vector $\underline{\hat{I}}_{n-1}$ and the channel estimates $\underline{\hat{Y}}^d_{0,n-1}$ to update its coefficients, according to Equation (45), for weighting of the elements of observation vector $\underline{Y}_{n-1}$.

The beamformer 47C$^d$ adjusts its coefficients so that, over a period of time, it will nullify the corresponding interference components in the observation vector $\underline{Y}_{n-1}$ from

10 the vector reshaper 44 and, at the same time, tune for a unity response to the spread channel vector estimate so as to extract the raw signal component estimate $\hat{s}^d_{n-1}$ substantially without distortion.

ISR-TR constitutes the simplest way to characterize the interference subspace, yet the most difficult to achieve accurately; namely by a complete estimation of the

15 instantaneous realization of the total interference vector $\underline{\hat{I}}_n$ in a deterministic-like approach. The constraint matrix is therefore defined by a single null-constraint (i.e., $N_c = 1$) as:

$$\hat{C}_n = \left[ \frac{\underline{\hat{I}}_n}{\|\underline{\hat{I}}_n\|} \right] = \left[ \frac{\sum_{i=1}^{NI} \underline{\hat{Y}}^i_n}{\left\| \sum_{i=1}^{NI} \underline{\hat{Y}}^i_n \right\|} \right] \qquad (47)$$

20

where each estimate $\underline{\hat{Y}}^i_n$ is reconstructed by reshaping the following matrix:

$$\hat{Y}^i_n = \hat{\psi}^i_n \hat{H}^i_n \otimes \hat{b}^i_n c^i. \qquad (48)$$

For each interfering user assigned the index $i = 1, ..., NI$, this mode uses

25 estimates of its received power $(\hat{\psi}^i_n)^2$ and its channel $\underline{\hat{H}}^i_n$, both assumed constant over the adjacent symbols and made available by STAR. This mode also requires a bit-triplet estimate $\left[ \hat{b}^i_{n-1}, \hat{b}^i_n, \hat{b}^i_{n+1} \right]$ of each interfering user (see Equation (23)). To obtain estimates of the signs of the interferer bits for both the current and next iterations (i.e., $\hat{b}^i_n$ and $\hat{b}^i_{n+1}$), the ISR-TR mode requires that the processing of all the

30 low-power users be further delayed by one bit duration and one processing cycle (pc), respectively. The one-bit delay is provided by the delay 45 in Figure 13.

In the ISR-TR mode and in the alternative ISR modes to be described hereafter, the interference (due to the strongest users) is first estimated, then eliminated. It should

be noted that, although this scheme bears some similarity to prior interference cancellation methods which estimate then subtract the interference, the subtraction makes these prior techniques sensitive to estimation errors. ISR on the other hand rejects interference by beamforming which is robust to estimation errors over the power of the

5 interferers. As one example, ISR-TR would still implement a perfect null-constraint if the power estimates were all biased by an identical multiplicative factor while interference cancellers would subtract the wrong amount of interference. The next mode renders ISR even more robust to power estimation errors.

The receiver illustrated in Figure 13 may be modified to reduce the information

10 used to generate the interfering signal estimates $\hat{Y}_{n-1}^1 \dots \hat{Y}_{n-1}^{NI}$, specifically by omitting the amplitude of the user signal estimates, and adapting the ISR beamformer $47C^d$ to provide more *(NI)* null constraints. Such a modified receiver will now be described with reference to Figure 15.

15 *Interference Subspace Rejection over Realisations (ISR-R)*

In the receiver of Figure 15, the receiver modules in set I are identical to those of Figure 13. Receiver module $21D^d$ has the same set of components as that shown in Figure 13 but its beamformer $47D^d$ differs because the constraint matrix differs. The constraints-set generator 42D differs from that shown in Figure 13 in that it omits the

20 multipliers $58C^1 \dots 58C^{NI}$ and the adder 60. The outputs from the power estimation units $30^1 \dots 30^{NI}$ are not used to scale the re-spread signals from the respreaders $57C^1 \dots 57C^{NI}$, respectively. Hence, in the receiver of Figure 15, the signals $\hat{b}_n^1 \dots \hat{b}_n^{NI}$ from the STAR units $20^1 \dots 20^{NI}$, respectively, are re-spread and then filtered by channel replication filter units $59C^1 \dots 59C^{NI}$, respectively, to produce user specific observation matrices

25 $\hat{Y}_{n-1}^1 \dots \hat{Y}_{n-1}^{NI}$, respectively, as the constraints-set $C_n$. In contrast to the receiver of Figure 13, however, these respread matrices are not summed but rather are processed individually by the constraint matrix generator 43D, which comprises a bank of vector reshapers $48D^1 \dots 48D^{NI}$ and a matrix inverter 49D (not shown but similar to those in Figure 10). The resulting constraint matrix $\hat{C}_n$, comprising the column

30 vectors $\hat{Y}_{n-1}^1, \dots, \hat{Y}_{n-1}^{NI}$ is supplied, together with the corresponding inverse matrix $Q_n$, to each of the receiver modules in set D. Again, only receiver module $21D^d$ is shown, and corresponds to that in the embodiment of Figure 13. Each of the vectors $\hat{Y}_{n-1}^1 \dots \hat{Y}_{n-1}^{NI}$, represents an estimate of the interference caused by the

38

corresponding one of the strong interference signals from set I and has the same dimension as the reshaped observation vector $\underline{Y}_{n-1}$.

In this ISR-R mode, the interference subspace is characterized by normalized estimates of the interference vectors $\underline{\hat{Y}}_n^i$. Consequently, it spans their individual realizations with all possible values of the total received powers $(\psi_n^i)^2$. The constraint matrix is defined by $NI$ null-constraints (i.e., $N_c = NI$) as:

$$\hat{C}_n = \left[ \frac{\underline{\hat{Y}}_n^1}{\|\underline{\hat{Y}}_n^1\|}, \dots, \frac{\underline{\hat{Y}}_n^{NI}}{\|\underline{\hat{Y}}_n^{NI}\|} \right], \tag{49}$$

where each estimate $\underline{\hat{Y}}_n^i$ is reconstructed by reshaping the following matrix:

$$\hat{Y}_n^i = \hat{H}_n^i \otimes \hat{b}_n^i c_i^i \tag{50}$$

It should be noted that, in the reconstruction of $\hat{Y}_n^i$, the total amplitude of the $i$-th interferer $\psi_n^i$ (see Figure 15) has been omitted intentionally; hence the higher robustness expected to near-far situations as well as the enlarged margin for power control relaxation.

## Interference Subspace Rejection over Diversity (ISR-D)

The ISR-D receiver shown in Figure 16 is predicated upon the fact that the signal from a particular user will be received by each antenna element via a plurality of sub-paths. Applying the concepts and terminology of so-called RAKE receivers, each sub-path is termed a "finger". In the embodiments of Figures 9, 11, 13 and 15, the channel identification units estimate the parameters for each finger as an intermediate step to estimating the parameters of the whole channel. In the ISR-D receiver shown in Figure 16, the channel identification units $28E^1 \dots 28E^{NI}$ supply the whole channel estimates $\underline{\hat{H}}_n^1 \dots \underline{\hat{H}}_n^{NI}$ respectively, to the beamformers $27^1 \dots 27^{NI}$, respectively, as before. In addition, they supply the sets of channel parameter estimates $\mathcal{H}_n^1 \dots \mathcal{H}_n^{NI}$ of each individual sub-channel or finger to the constraints-set generator 42E. The set of channel parameter estimates $\mathcal{H}_n^i$ comprises the sub-channel estimates $\underline{H}_n^{i,1}, \dots, \underline{H}_n^{i,N_f}$. The constraints-set generator 42E is similar to that shown in Figure 15 in that it comprises a bank of respreaders $57^1 \dots 57^{NI}$ but differs in that the channel replication units $59D^1 \dots 59D^{NI}$ are replaced by sub-channel replication units $59E^1 \dots 59E^{NI}$, respectively. The sub-channel replication units $59E^1 \dots 59E^{NI}$ convolve the respread symbols with the sub-channel estimates $\hat{H}_n^{1,1} \dots \hat{H}_n^{1,N_f}; \dots; \hat{H}_n^{NI,1}, \dots, \hat{H}_n^{NI,N_f}$ respectively, to produce

normalized estimates $\hat{Y}_{n-1}^{1,1} \cdots \hat{Y}_{n-1}^{1,N_f}, \cdots \hat{Y}_{n-1}^{NI,1}, \cdots \hat{Y}_{n-1}^{NI,N_f}$ of the sub-channel-specific observation matrices decomposed over fingers. Hence, the matrices span the space of their realizations with all possible values of the total received powers $(\psi_n^i)^2$ and complex channel coefficients $\zeta_{f,n}^i$. The estimates are supplied to a constraint matrix generator 43E which generally is as shown in Figure 10 and produces the constraint matrix accordingly.

The constraint matrix $\hat{C}_n$ is simply defined by $N_f NI$ null-constraints (i.e., $N_c = Nf \times NI = M \times P \times NI$) as:

$$\hat{C}_n = \left[ \frac{\hat{Y}_n^{1,1}}{\left\|\hat{Y}_n^{1,1}\right\|}, \cdots, \frac{\hat{Y}_n^{1,N_f}}{\left\|\hat{Y}_n^{1,N_f}\right\|}, \cdots, \frac{\hat{Y}_n^{NI,1}}{\left\|\hat{Y}_n^{NI,1}\right\|}, \cdots, \frac{\hat{Y}_n^{NI,N_f}}{\left\|\hat{Y}_n^{NI,N_f}\right\|} \right], \tag{51}$$

Each estimate $\hat{\underline{Y}}_n^{i,f}$ is reconstructed by reshaping the following matrix:

$$\hat{Y}_n^{i,f} = \hat{H}_n^{i,f} \otimes \underline{b}_n^i c_i^i. \tag{52}$$

It should be noted that, in the reconstruction of $\hat{Y}_n^{i,f}$, the total amplitude of the $i$-th interferer $\psi_n^i$ as well as the channel coefficients $\zeta_{f,n}^i$ (see Figure 1) are intentionally omitted; hence the relative robustness of ISR-D to power mismatch, like ISR-R. Unlike other modes, it additionally gains robustness to channel identification errors and remains sensitive only to the estimated channel parameters remaining, namely the multipath time-delays, and to symbol estimation errors.

It should be noted that, in the receivers of Figures 13, 15 and 16, estimation errors of the interference bit signs may introduce differences between the estimated constraints and the theoretical ones. Hence, although ISR-D, ISR-R and ISR-TR modes are satisfactory in most situations, it is possible that the realisation could be erroneous, which would affect the validity of the interference cancellation. Additionally, estimation of the signs of the interference bits for reconstruction in the ISR-D mode, as in the ISR-R and ISR-TR modes, requires that the processing of all of the low-power users be further delayed by one bit duration, i.e., by delay 45, and one processing cycle (pc). To avoid these drawbacks, alternative ISR approaches to implementation of the constraints of Equation (42) are envisaged and will now be described, beginning with ISR-H which avoids processing delays and is completely robust to data estimation errors.

## *Interference Subspace Rejection over Hypotheses (ISR-H)*

It is possible to use a set of signals which represent all possible or hypothetical values for the data of the interfering signal. Each of the interfering signals constitutes a vector in a particular domain. It is possible to predict all possible occurrences for the

5 vectors and process all of them in the ISR beamformer and, therefore, virtually guarantee that the real or actual vector will have been nullified. As mentioned, the strong interferers are relatively few, so it is possible, in a practical system, to determine all of the likely positions of the interference vector and compensate or nullify all of them. Such an alternative embodiment, termed Interference Subspace Rejection over

10 Hypotheses (ISR-H) because it uses all possibilities for the realisations, is illustrated in Figure 17.

The components of the "interferer" receiver modules of set I, namely the despreaders $19^1...19^{NI}$ and STAR units $20^1...20^{NI}$, are basically the same as those in the receiver of Figure 15 and so have the same reference numbers. In the embodiment of

15 Figure 17, however, the constraints-set generator 42F differs because the symbol estimates $\hat{b}_n^1 ... \hat{b}_n^{NI}$ from the outputs of the decision rule units $29^1...29^{NI}$ are not supplied to the respreaders $57F^1...57F^{NI}$, respectively, but are merely outputted to other circuitry in the receiver (not shown).

Instead, bit sequence generators $63F^1...63F^{NI}$ each generate the three

20 possibilities $g_n^1, g_n^2, g_n^3$, which cover all possible estimated values of the previous, current and next bits of the estimated data sequences $\hat{b}_n^1...\hat{b}_n^{NI}$, including the realisation itself (as explained later), and supply them to the respreaders $57F^1...57F^{NI}$, respectively, which each spread each set of three values again by the corresponding one of the spreading codes. The resulting re-spread estimates are filtered by the channel replication filters

25 $59F^1...59F^{NI}$, respectively, to produce, as the constraint set, the matrix estimates $\hat{Y}_{0,n}^1, \hat{Y}_{-1,n}^1, \hat{Y}_{+1,n}^1; ... ; \hat{Y}_{0,n}^{NI}, \hat{Y}_{-1,n}^{NI}, \hat{Y}_{+1,n}^{NI}$. The bit sequence generators could, of course, be replaced by storage units.

The constraint matrix generator 43F is generally as shown in Figure 10 and processes the set of estimate matrices to form the column vectors

30 $\hat{Y}_{0,n}^1, \hat{Y}_{-1,n}^1, \hat{Y}_{+1,n}^1; ... ; \hat{Y}_{0,n}^{NI}, \hat{Y}_{-1,n}^{NI}, \hat{Y}_{+1,n}^{NI}$ of constraint matrix $\hat{C}_n$, which it supplies with corresponding inverse matrix $Q_n$, in common to the beamformer $47F^d$ and the beamformers of the other set D receiver modules.

41

Receiver module $21F^d$ comprises similar components to those of the receiver module $21E^d$ shown in Figure 16. It should be noted, however, that, because the "next" bit is being hypothesized, it need not be known, so the delay 45 is omitted.

As mentioned above, the two bits adjacent to the processed bit of the $i$-th 5 interferer contribute in each bit frame to the corresponding interference vector (symbol) to be rejected. As shown in Figure 18, enumeration of all possible sequences of the processed and adjacent bits gives $2^3 = 8$ triplets, each of three bits. Only one of these triplets could occur at any one time at each bit iteration as one possible realization that generates the user-specific observation matrix $\hat{Y}_n^i$. These eight triplets can be identified 10 within a sign ambiguity with one of the four triplets identified as *(a)...(d)* in the left-hand part of Figure 18, since the four triplets *(e)...(h)* are their opposites.

It should be appreciated that the bit sequence generators $63^1...63^{NI}$ (Figure 17) each supply only three values, $g_n^1$, $g_n^2$, $g_n^3$ because the dimension of the generated signal subspace is 3. It should be noted that frames of duration $3T$, taken from these sequences 15 at any bit rate instant, reproduce the eight possible realisations of the bit triplets of Figure 18. Therefore, at any bit iteration, the bit sequence $b_n^i$ of the interfering mobile station can be locally identified as the summation of the generating sequences $g_n^k$, $k = 1,..., 3$ weighted by the bit signs $b_{n-1}^i, b_n^i$ and $b_{n+1}^i$. Replacing the estimate $\hat{b}_n^i$ in Equation (50) by $g_n^k$, $k = 1,..., 3$, , yields canonic observation matrices that 20 span all possible realisations of the received signal vector from the $i$-th interfering mobile within a sign ambiguity.

In the ISR-H embodiment of Figure 17, the interference subspace is characterized by normalized estimates of the canonic interference vectors $\underline{\hat{Y}}_{k,n}^i$. Accordingly, it spans their individual realizations with all possible values of the total received 25 powers $(\psi_n^1)^2$ and bit triplets $\left[b_{n-1}^i, b_n^i, b_{n+1}^i\right]$. The constraint matrix is defined by $3NI$ null-constraints (i.e., $N_c = 3NI$) as:

$$\hat{C}_n = \left[ \frac{\underline{\hat{Y}}_{0,n}^1}{\left\|\underline{\hat{Y}}_{0,n}^1\right\|}, \frac{\underline{\hat{Y}}_{-1,n}^1}{\left\|\underline{\hat{Y}}_{-1,n}^1\right\|}, \frac{\underline{\hat{Y}}_{+1,n}^1}{\left\|\underline{\hat{Y}}_{+1,n}^1\right\|},..., \frac{\underline{\hat{Y}}_{0,n}^{NI}}{\left\|\underline{\hat{Y}}_{0,n}^{NI}\right\|}, \frac{\underline{\hat{Y}}_{-1,n}^{NI}}{\left\|\underline{\hat{Y}}_{-1,n}^{NI}\right\|}, \frac{\underline{\hat{Y}}_{+1,n}^{NI}}{\left\|\underline{\hat{Y}}_{+1,n}^{NI}\right\|} \right], \qquad (53)$$

30 where each estimate $\underline{\hat{Y}}_{k,n}^i$ is reconstructed, respectively, for $k = -1, 0, +1$ by reshaping the following matrix:

$$\hat{Y}_{k,n}^i = \hat{H}_n^i \otimes g_n^{i,k} c_i^i. \qquad (54)$$

It should also be noted that, in the reconstruction above, only the channel estimates (assumed stationary over the adjacent symbols) are needed for complete interference rejection regardless of any *2D* modulation employed (see Figure 19); hence the extreme robustness expected to power control and bit/symbol errors of interferers.

5 The ISR-H combiner coefficients are symbol-independent and can be computed less frequently when the channel time-variations are slow.

Merging of the D mode with the H mode along the decomposition of Equation (38) yields ISR-HD (hypothesized diversities) with a very close form to the decorrelator. This ISR-HD mode requires a relatively huge number of constraints *(i.e., $3N_f NI$)*.

10 Consequently, the ISR-HD mode is not considered to be practical at this time.

In fact, it would be desirable to reduce the number of constraints required by the ISR-H receiver described above. This can be done using an intermediate mode which is illustrated in Figure 20 and in which the receiver modules of both sets I and D are similar to those of Figure 15; most of their components are identical and have the same

15 reference numbers. In essence, the constraint-set generator 42G of the receiver in Figure 20 combines the constraint-set generators of Figures 15 and 17 in that it uses estimated symbols and hypothetical values. Thus, it comprises a bank of respreaders $57G^1...57G^{NI}$, a corresponding bank of channel replication units $59G^1...59G^{NI}$ and a bank of bit symbol generators $63G^1...63G^{NI}$. In this case, however, each of the bit symbol generators

20 $63G^1...6GE^{NI}$ supplies only one bit symbol to the corresponding one of the respreaders $57G^1...57G^{NI}$, which receive actual bit symbol estimates $\hat{b}_n^1 ... \hat{b}_n^{NI}$, respectively, from the decision rule units $29^1,...,29^{NI}$, respectively. It should be appreciated that, although the bit symbol generators $63G^1,...,63G^{NI}$ each supply only one bit symbol for every actual symbol or realization from the corresponding one of the decision rule units

25 $29^1,...,29^{NI}$, that is sufficient to generate two hypothetical values of "future" symbols $b_{n+1}^1,...,b_{n+1}^{NI}$ for every one of the symbol estimates $\hat{b}_{n+1}^1 ... \hat{b}_{n+1}^{NI}$ since only two hypothetical values of the symbols, namely 1 and -1, are required. The respreaders $57G^1,...,57G^{NI}$ supply the spread triplets to the channel replication units $59G^1...59G^{NI}$ which filter them, using the channel parameter estimates $\hat{H}_n^1 ... \hat{H}_n^{NI}$, respectively, to

30 produce pairs of matrices $\hat{Y}_{r,n}^1, \hat{Y}_{+1,n}^1; ... \hat{Y}_{r,n}^{NI}, \hat{Y}_{+1,n}^{NI}$ and supply them to the constraint matrix generator 43G which is configured generally as shown in Figure 9. The constraint matrix generator 43G reshapes the matrices $\hat{Y}_{r,n}^1, \hat{Y}_{+1,n}^1; ... \hat{Y}_{r,n}^{NI}, \hat{Y}_{+1,n}^{NI}$ to form vectors $\hat{Y}_{r,n}^1, \hat{Y}_{+1,n}^1; ... \hat{Y}_{r,n}^{NI}, \hat{Y}_{+1,n}^{NI}$ which then are used as the column vectors of the constraint

43

matrix $\hat{C}_n$. The constraint matrix generator 43G supplies the constraint matrix $\hat{C}_n$ and the corresponding inverse matrix $\mathcal{Q}_n$ in common to the beamformer 47G$^d$ and the beamformers of other receiver modules in set D.

Hence, the beamformer 47G$^d$ uses the past symbol estimate $\hat{b}_{n-1}^i$ of the
5 interference data as well as the present one $\hat{b}_n^i$ (delayed by one processing cycle, *i.e.* the time taken to derive the interference estimates), and the unknown sign of $b_{n+1}^i$ reduces the number of possible bit triplets and the corresponding realisations for each interference vector to 2.

The receiver of Figure 20, using what is conveniently referred to as ISR-RH
10 mode for reduced hypotheses over the next interference bits, rejects reduced possibilities of the interference vector realisations. Compared to the receiver of Figure 17 which uses the ISR-H mode, it is more sensitive to data estimation errors over $\hat{b}_{n-1}^i$ and $\hat{b}_n^i$ and requires only 2 constraints per interferer instead of 3.

Using the previous and current bit estimates of interferers, uncertainty over the
15 interference subspace can be reduced and it can be characterized by the following matrix of 2NI null-constraints (i.e., $N_c = 2NI$):

where:
$$\hat{C}_n = \left[ \frac{\hat{Y}_{r,n}^1}{\left\| \hat{Y}_{r,n}^1 \right\|}, \frac{\hat{Y}_{+1,n}^1}{\left\| \hat{Y}_{+1,n}^1 \right\|}, \cdots, \frac{\hat{Y}_{r,n}^{NI}}{\left\| \hat{Y}_{r,n}^{NI} \right\|}, \frac{\hat{Y}_{+1,n}^{NI}}{\left\| \hat{Y}_{+1,n}^{NI} \right\|} \right],$$ (55)

20

$$\hat{Y}_{r,n}^i = \hat{b}_n^i \hat{Y}_{0,n}^i + \hat{b}_{n-1}^i \hat{Y}_{-1,n}^i,$$ (56)

and where each estimate $\hat{Y}_{k,n}^i$ is reconstructed by reshaping the matrices in Equation (38), respectively for $k = -1, 0, +1$. It should be noted that this mode requires a delay
25 of one processing cycle for the estimation of the current interference bits.

The ISR-RH mode has the advantage of reducing the number of null-constraints as compared to the ISR-H mode. A larger number of null-constraints indeed increases complexity, particularly when performing the matrix inversion in Equation (43), and may also result in severe noise enhancement, especially when the processing gain $L$ is low.
30 As the number of strong interferes NI increases in a heavily loaded system, the number of null-constraints *(2NI* and *3NI)* approaches the observation dimension $M \times (2L - 1)$ and the constraint-matrix may become degenerate. To reduce complexity, guarantee stability in the matrix inversion of Equation (43), and minimize noise enhancement, the constraint

44

matrix $\hat{C}_n$ in Equations. (43) and (44) is replaced by the orthonormal interference subspace of rank $K$ that spans its column vectors as follows:

$$\hat{V}_n = Vec\{\hat{C}_n\} = \{\underline{\hat{V}}_{n,1}, ..., \underline{\hat{V}}_{n,k}, ..., \underline{\hat{V}}_{n,K}\}. \tag{57}$$

In practice, $\hat{V}_n$ can hardly reflect the real rank of $\hat{C}_n$. It corresponds to the

5  subspace of reduced rank $\hat{K}$ with the highest interference energy to cancel. To further minimize noise enhancement, one can also increase the observation dimension $M \times (2L - 1)$, as will be described later as "X option", and so on.

It should be noted that each of the receivers of Figures 13, 15, 16, 17 and 20 could be modified to perform ISR "after despreading" of the observation vector $Y_n$, in

10  effect in much the same way that the generic "after despreading" receiver of Figure 11 differs from the generic "without despreading" receiver of Figure 9. Such modified receivers will now be described with reference to Figures 21 to 26.

Thus, in the ISR-TR receiver shown in Figure 21, which corresponds to that shown in Figure 13, the delay 45 delays the observation matrix $Y_n$ from the

15  preprocessing unit 18 by 1 bit period and supplies the resulting delayed observation matrix $Y_{n-1}$, in common, to each of the low-power user receiver modules in set D. Only one of these receiver modules, $21H^d$, is shown in Figure 21, since all are identical. The observation matrix $Y_{n-1}$ is despread by despreader $19^d$ and the resulting post-correlation observation vector $Z^d_{n-1}$ is supplied to both the channel identification unit $28H^d$ and the

20  beamformer $47H^d$. The receiver modules of set I and the constraints-set generator 42C are identical to those in the receiver shown in Figure 13, and supply the matrices $\hat{Y}^1_{n-1}$ ... $\hat{Y}^{NI}_{n-1}$ to an adder 60 which adds them to form the total interference matrix $\hat{I}_{n-1}$ which it supplies to each of the receiver modules in set D.

Receiver module $21H^d$ is similar to that shown in Figure 13 but has a second

25  despreader $43H^d$ which uses the spreading code for user d to despread the total interference matrix $\hat{I}_{n-1}$ to form the user-specific constraint matrix as a single column vector $\hat{I}^d_{PCM,n-1}$. This despreader $43H^d$, in effect, constitutes a user-specific constraint matrix generator because the constraint matrix is a vector and an inverse matrix is not needed. Also, in this case, the channel identification unit $28H^d$ supplies the channel

30  estimate $\hat{H}^d_{n-1}$ to the beamformer $47H^d$.

It should be noted that the despread data vector $Z^d_{n-1}$ is equal to $H^d_n s^d_n + I^d_{PCM,n}, + N^d_n$, where $H^d_n$ is the channel response for user station $10^d$, $s^d_n$ is the signal transmitted by the mobile station $10^d$ of user $d$, and $I^d_{PCM,n}$ is the interference

component present in the signal $Z_n^d$ as a result of interference from the signals from the other user stations $10^i$ in set I, where $\underline{I}_{PCM,n}^d$ is as defined in Equation (14). The value $\underline{N}_{PCM,n}^d$ is additional noise which might comprise, for example, the summation of the interference from all of the other users on the system at that time, as well as thermal

5 noise. "Other users" means other than those covered by the channels in set I.

As before, the coefficients of the beamformer $47H^d$ are tuned according to Equations (16) to (18) and the constraint matrix is defined by a single null-constraint (i.e., $N_c = 1$) as:

$$\hat{C}_{PCM,n}^d = \left[ \frac{\hat{\underline{I}}_{PCM,n}^d}{\left\| \hat{\underline{I}}_{PCM,n}^d \right\|} \right] = \left[ \frac{\sum_{i=1}^{NI} \hat{\underline{I}}_{PCM,n}^{d,i}}{\left\| \sum_{i=1}^{NI} \hat{\underline{I}}_{PCM,n}^{d,i} \right\|} \right] \tag{58}$$

where the estimate $\hat{\underline{I}}_{PCM,n}^d$ is obtained by despreading the matrix $\hat{I}_n$ (See Equations (47) and (48)) with the spreading sequence of the desired low-power user.

15 Figure 22 shows a similar modification to the low-power (set D) receiver modules of the "without despreading" ISR-R receiver of Figure 15. In this case, the output of the constraint-set generator 42D, as before, comprises the matrices $\hat{Y}_{n-1}^1 \dots \hat{Y}_{n-1}^{NI}$. As before, only receiver module $21J^d$ is shown in Figure 22 and is identical to that shown in Figure 21 except that the second despreader $43H^d$ is replaced by a user-specific

20 constraint matrix generator $43J^d$ of the kind shown in Figure 12. The channel identification unit $28J^d$ again supplies the vector $\underline{\hat{H}}_{n-1}^d$ to the beamformer $47J^d$. The bank of despreaders in the user-specific constraint matrix generator $43J^d$ despread the respective ones of the matrices $\hat{Y}_{n-1}^1 \dots \hat{Y}_{n-1}^{NI}$ to form the vectors $\hat{\underline{I}}_{PCM,n-1}^{d,1}, \dots, \hat{\underline{I}}_{PCM,n-1}^{d,NI}$ which constitute the columns of the user-specific constraint

25 matrix $\hat{C}_{PCM,n-1}^d$ and the matrix generator $46G^d$ produces the corresponding inverse matrix $Q_{PCM,n-1}^d$. Both of these matrices are supplied to the associated beamformer $47J^d$ which uses them and the channel estimate $\underline{\hat{H}}_{n-1}^d$ to adjust its coefficients that are used to weight the elements of the post-correlation observation vector $\underline{Z}_{n-1}^d$. As before, the coefficients are adjusted according to Equations (16) to (18) and the constraint matrix is

30 defined by $NI$ null-constraints (i.e., $N_c = NI$) as:

$$\hat{C}_{PCM,n}^d = \left[ \frac{\hat{\underline{I}}_{PCM,n}^{d,1}}{\left\| \hat{\underline{I}}_{PCM,n}^{d,1} \right\|}, \dots, \frac{\hat{\underline{I}}_{PCM,n}^{d,NI}}{\left\| \hat{\underline{I}}_{PCM,n}^{d,NI} \right\|} \right], \tag{59}$$

46

where each estimate $\hat{\underline{I}}^{d,i}_{PCM,n}$ is obtained by despreading the matrix $\hat{Y}^i_n$ of Equation (50) with the spreading sequence of the desired low-power user.

Figure 23 illustrates the modification applied to the low-power user receiver module of the ISR-D receiver of Figure 16. Hence, there is no common matrix inverter. Instead, in the receiver of Figure 23, each of the receiver modules of set D has a user-specific constraint matrix generator 43K which recevies the constraints from the constraints-set generator 42E. As illustrated, user-specific constraint matrix generator 43K$^d$ processes the sets of matrices $\hat{Y}^{1,1}_{n-1} ... \hat{Y}^{1,N_f}_{n-1}, ...; \hat{Y}^{NI,1}_{n-1}, ..., \hat{Y}^{NI,N_f}_{n-1}$ to form the set of vectors $\hat{\underline{I}}^{d,1,1}_{PCM,n-1} ... \hat{\underline{I}}^{d,1,N_f}_{PCM,n-1}; ...; \hat{\underline{I}}^{d,NI,1}_{PCM,n-1} ... \hat{\underline{I}}^{d,NI,N_f}_{PCM,n-1}$, which constitute the columns of user-specific constraint matrix $\hat{C}^d_{PCM,n-1}$, and the corresponding inverse matrix $Q^d_{PCM,n-1}$ which it supplies to the beamformer 47K$^d$. As before, the beamformer 47K$^d$ tunes its coefficients according to equations (16) and (18). The constraint matrix is defined by $N_fNI$ null-constraints $(i.e., N_c = N_f \times NI = M \times P \times NI)$ as:

$$\hat{C}^d_{PCM,n} = \left[ \frac{\hat{\underline{I}}^{d,1,1}_{PCM,n}}{\left\| \hat{\underline{I}}^{d,1,1}_{PCM,n} \right\|},...,\frac{\hat{\underline{I}}^{d,1,N_f}_{PCM,n}}{\left\| \hat{\underline{I}}^{d,1,N_f}_{PCM,n} \right\|},...,\frac{\hat{\underline{I}}^{d,NI,1}_{PCM,n}}{\left\| \hat{\underline{I}}^{d,NI,1}_{PCM,n} \right\|},...,\frac{\hat{\underline{I}}^{d,NI,N_f}_{PCM,n}}{\left\| \hat{\underline{I}}^{d,NI,N_f}_{PCM,n} \right\|} \right], \qquad (60)$$

where each estimate $\hat{\underline{I}}^{d,i,f}_{PCM,n}$ is obtained by despreading $\hat{\underline{Y}}^{i,f}_n$ of Equation (52) with the spreading sequence of the desired low-power user.

Figure 24 illustrates application of the modification to the ISR-H receiver of Figure 17. Again, the common constraint matrix generator (43F) is replaced by a user-specific constraint matrix generator 43L$^d$ in receiver module 21L$^d$ and similarly in the other receiver modules of set D. The constraints-set generator 42L' differs from constraints-set generator 42F of Figure 17 because its bit sequence generators 63L',...,63L$^{NI}$ use different generating sequences. The sets of matrices $\hat{Y}^1_{1,n}, \hat{Y}^1_{2,n}, \hat{Y}^1_{3,n}; ...; \hat{Y}^{NI}_{1,n}, \hat{Y}^{NI}_{2,n}, \hat{Y}^{NI}_{3,n}$ from the constraints-set generator 42F' are processed by the user-specific constraint matrix generator 43L$^d$ to form the vectors $\hat{\underline{I}}^{d,1}_{1,n}, \hat{\underline{I}}^{d,1}_{2,n}, \hat{\underline{I}}^{d,1}_{3,n}; ... ; \hat{\underline{I}}^{d,NI}_{1,n}, \hat{\underline{I}}^{d,NI}_{2,n}, \hat{\underline{I}}^{d,NI}_{3,n}$ which constitute the columns of the user-specific constraint matrix $\hat{C}^d_{PCM,n}$, and the matrix inverter (not shown) produces the corresponding inverse matrix $Q^d_{PCM,n}$. The constraint matrix $\hat{C}^d_{PCM,n}$ and the inverse matrix $Q^d_{PCM,n}$ are used by the beamformer 47L$^d$, together with the channel estimate $\hat{H}^d_n$, to adjust its coefficients that are used to weight the elements of the post-correlation observation vector $\underline{Z}^d_n$ received from despreader 19$^d$. As before, the

47

coefficients are adjusted according to Equations (16) and (18) and the constraint matrix is defined by *3NI* null-constraints *(i.e., $N_c = 3NI$)* as:

$$\hat{C}^d_{PCM,n} = \left[ \frac{\hat{I}^{d,1,1}_{PCM,n}}{\left\|\hat{I}^{d,1,1}_{PCM,n}\right\|}, \frac{\hat{I}^{d,1,2}_{PCM,n}}{\left\|\hat{I}^{d,1,2}_{PCM,n}\right\|}, \frac{\hat{I}^{d,1,3}_{PCM,n}}{\left\|\hat{I}^{d,1,3}_{PCM,n}\right\|}, \cdots, \frac{\hat{I}^{d,NI,1}_{PCM,n}}{\left\|\hat{I}^{d,NI,1}_{PCM,n}\right\|}, \frac{\hat{I}^{d,NI,2}_{PCM,n}}{\left\|\hat{I}^{d,NI,2}_{PCM,n}\right\|}, \frac{\hat{I}^{d,NI,3}_{PCM,n}}{\left\|\hat{I}^{d,NI,3}_{PCM,n}\right\|} \right], \quad (61)$$

where each estimate $\hat{I}^{d,i,k}_{PCM,n}$ is obtained by despreading the matrix $\hat{Y}^i_{k,n}$ with the spreading sequence of the desired low-power user.

In this case, each of the bit sequence generators 63L',...,63L$^{NI}$ uses four generating bit sequences $\bar{g}^1(t)$, $\bar{g}^2(t)$, $\bar{g}^3(t)$ and $\bar{g}^4(t)$ as shown in Figure 25.

It should be noted that, in any frame of duration *3T* in Figure 25, a bit triplet of any of the four generating sequences is a linear combination of the others. Therefore, any one of the four possible realisations of each interference vector is a linear combination of the others and the corresponding null-constraint is implicitly implemented by the three remaining null-constraints. The four null-constraints are restricted arbitrarily to the first three possible realisations.

Figure 26 illustrates application of the modification to the ISR-RH receiver of Figure 20. Again, the common constraint matrix generator 43G of Figure 20 is replaced by a set of user-specific constraint matrix generators, 43M$^d$ in receiver module 21M$^d$ and similarly in the other receiver modules of set D. The constraints-set generator 42M shown in Figure 26 differs slightly from that (42G) shown in Figure 20 because each of the bit sequence generators 63M$^1$,...63M$^{NI}$ in the receiver of Figure 26 generate the bit sequence $g^{i,1,n}_n$.

The user-specific constraint generator 43M$^d$ processes the pairs of constraint-set matrices $\hat{Y}^1_{k_1,n}, \hat{Y}^1_{k_2,n}; ...; \hat{Y}^{NI}_{k_1,n}, \hat{Y}^{NI}_{k_2,n}$ from the channel identification units 59M$^1$,...,59M$^{NI}$, respectively, by to produce the corresponding set of vectors $\hat{I}^{d,1,k_1}_{PCM,n}, \hat{I}^{d,1,k_2}_{PCM,n}; ...; \hat{I}^{d,NI,k_1}_{PCM,n}, \hat{I}^{d,NI,k_2}_{PCM,n}$ which constitute the columns of the user-specific constraint matrix $\hat{C}^d_{PCM,n}$, and to produce the corresponding inverse matrix $Q^d_{PCM,n}$.

The constraint matrix $\hat{C}^d_{PCM,n}$ and the inverse matrix $Q^d_{PCM,n}$ are used by the beamformer 47M$^d$, together with the channel estimate $\hat{H}^d_n$, to adjust its coefficients that are used to weight the elements of the post-correlation observation vector $Z^d_n$ received from despreader 19$^d$. As before, the coefficients are adjusted according to Equations

48

(16) to (18) and the constraint matrix is defined by *2NI* null-constraints *(i.e., $N_c = 2NI$)* as follows:

$$\hat{C}^d_{PCM,n} = \left[ \frac{\hat{I}^{d,1,k_1}_{-PCM,n}}{\left\| \hat{I}^{d,1,k_1}_{-PCM,n} \right\|}, \frac{\hat{I}^{d,1,k_1}_{-PCM,n}}{\left\| \hat{I}^{d,1,k_1}_{-PCM,n} \right\|}, ..., \frac{\hat{I}^{d,NI,k_1}_{-PCM,n}}{\left\| \hat{I}^{d,NI,k_1}_{-PCM,n} \right\|}, \frac{\hat{I}^{d,NI,k_1}_{-PCM,n}}{\left\| \hat{I}^{d,NI,k_1}_{-PCM,n} \right\|} \right],$$
(62)

where each pair of estimates $\hat{I}^{d,i,k_1}_{-PCM,n}$ and $\hat{I}^{d,i,k_1}_{-PCM,n}$ is obtained by despreading the matrices $\hat{Y}^i_{k_1,n}$ and $\hat{Y}^i_{k_1,n}$, respectively, with the spreading sequence of the desired low-power user.

## Inter-Symbol Interference (ISI) Rejection

In any of the above-described embodiments of the invention it may be desirable to reduce inter-symbol interference in the receiver modules in set D, especially when low processing rates are involved. As noted in the PCM model where despreading reduces ISI to a negligible amount, for a large processing gain, $\underline{Y}^{d^H}_{0,n}\underline{Y}^d_{-1,n} \simeq 0$ and $\underline{Y}^{d^H}_{0,n}\underline{Y}^d_{+1,n} \simeq 0$. Hence, the before despreading spatio-temporal beamformer $\underline{W}^d_n$ approximately implements the following additional constraints:

$$\begin{cases} \underline{W}^{d^H}_n \hat{\underline{Y}}^d_{-1,n} \simeq 0, \\ \underline{W}^{d^H}_n \hat{\underline{Y}}^d_{+1,n} \simeq 0. \end{cases}$$
(63)

Accordingly, it rejects interference and significantly reduces ISI. Complete ISI rejection can be effected by modifying the receiver to make the set of the channel parameter estimators $\mathcal{H}^d_n$ available to the constraints-sets generator 42 for processing in parallel with those of the set I receiver modules. The resulting additional constraint matrix and inverse matrix would also be supplied to the beamformer $47^d$ and taken into account when processing the data.

In such a case, the following matrix can be formed:

$$\hat{C}^d_{ISI,n} = \left[ \frac{\Pi_n \hat{\underline{Y}}^d_{-1,n}}{\left\| \Pi_n \hat{\underline{Y}}^d_{-1,n} \right\|}, \frac{\Pi_n \hat{\underline{Y}}^d_{+1,n}}{\left\| \Pi_n \hat{\underline{Y}}^d_{+1,n} \right\|} \right],$$
(64)

and the following 2 × 2 matrix

49

$$Q_{ISI,n}^d = \left( \hat{C}_{ISI,n}^{d*} \ \hat{C}_{ISI,n}^d \right)^{-1},$$ (65)

inverted to obtain the constrained spatio-temporal beamformer $\underline{W}_n^d$ before despreading by:

$$\Pi_{ISI,n}^d = I_{M \cdot (2L-1)} - \hat{C}_{ISI,n}^d Q_{ISI,n}^d \hat{C}_{ISI,n}^{d*},$$ (66)

$$\Pi_n^d = \Pi_{ISI,n}^d \ \Pi_n,$$ (67)

$$\underline{W}_n^d = \frac{\Pi_n^d \hat{\underline{Y}}_{0,n}^d}{\hat{\underline{Y}}_{0,n}^{d*} \Pi_n^d \hat{\underline{Y}}_{0,n}^d}.$$ (68)

The projector $\Pi_n$ is produced in the manner described earlier according to Equations (43) and (44). The projector $\Pi_n^d$ orthogonal to both $\hat{C}_{ISI,n}^d$ and $\hat{C}_n$, is formed and then the low-power response vector $\hat{\underline{Y}}_{0,n}^d$ projected and normalized to form the beamformer which fully rejects ISI from the processed user $d$ and interference from the $NI$ users in set I.

It should be noted that, if the suppression of strong interferers is not needed, ISI can still be rejected by the following beamformer:

$$\underline{W}_n^{d \cdot} = \frac{\Pi_{ISI,n}^d \hat{\underline{Y}}_{0,n}^d}{\hat{\underline{Y}}_{0,n}^{d*} \Pi_{ISI,n}^d \hat{\underline{Y}}_{0,n}^d}.$$ (69)

where projector $\Pi_n$ in equations 47 - 49 would be set to identity and hence would have no effect. This is the same as setting the matrix $\hat{C}_n$ to null matrix. If the projector $\Pi_{ISI,n}^d$ in the above equation is replaced by an identity matrix, (equivalent to setting matrix $\hat{C}_{ISI,n}^d$ to null matrix) then a simple MRC beamformer is implemented before despreading. A receiver module using such an MRC beamformer is illustrated in Figure 27 and could be used to replace any of the "contributor" only receiver modules, such as receiver modules $21^1$, ..., $21^{NI}$ in Figure 9 et seq. The receiver module shown in Figure 27 is similar to receiver module $21A^d$ of Figure 9 except that the ISR beamformer $47A^d$ is replaced by an MRC beamformer $27N^d$ which implements the equation

$$\underline{W}_n^d = \frac{\hat{\underline{Y}}_{0,n}^d}{| \hat{\underline{Y}}_{0,n}^d |^2}.$$ (70)

50

It is also envisaged that the receiver module of Figure 27 using the MRC beamformer denoted $\underline{W}^d_{MRC,n}$ in the following, could be incorporated into a STAR which did not use ISR, for example the STAR described in reference [13].

5 *Joint ISR Detection*

In the foregoing embodiments of the invention, ISR was applied to a selected set D of users, typically users with a low data-rate, who would implement ISR in respect of a selected set I of high-rate users. Although this approach is appropriate in most cases, particularly when the number of high-rate users is very low, there may be cases 10 where the mutual interference caused by other high-rate users is significant, in which case mutual ISR among high-rate users may be desired as well. Such a situation is represented by user sets M1 and M2 of Figure 8. Hence, whereas in the foregoing embodiments of the invention, the receiver modules of set I do not perform ISR but merely supply constraints sets for use by the receiver modules of set D, it is envisaged 15 that some or all of the receiver modules in set M1 and M2 also could have beamformers employing ISR. Such a Joint ISR (J-ISR) embodiment will now be described with reference to Figure 28, which shows only one receiver module, $21^i$, as an example. In any symbol period, each such receiver module $21^i$ (i) receives a constraint matrix $\hat{C}_{n-1}$ and an inverse matrix $Q_{n-1}$ and uses them in suppressing interference, 20 including its own interference component, and (ii) contributes constraints to the constraint matrix $\hat{C}_n$ and inverse matrix $Q_n$ which will be used in the next symbol period. In the case of ISR-H mode receivers, which use hypothetical symbols, it is merely a matter of replacing the receiver modules in set I with receiver modules $21^d$ having ISR beamformers, since the constraints sets are generated by the hypothetical 25 symbols from the bit sequence generators $63^1,...,63^{N1}$. Contrary to other ISR modes which require decision-feedback, in the ISR-H mode receiver module, no processing delay is required for one user to cancel another. Hence, ISR-H can be implemented to cancel strong interferers without successive interference cancellation or multi-stage processing, which will be described later.

30      Using $\hat{C}_n$ and $Q_n$ already computed, the ISR combiner for each interferer can be obtained readily by:

$$\underline{W}^i_n = \hat{C}_n Q_n \underline{R}_{3 \cdot (i-1)+1},$$      (71)

51

where $\underline{R}_k = [0, ..., 0, 1, 0, ..., 0]^T$ is a *(3NI)*-dimensional vector with null components except for the *k*-th one. This implementation has the advantage of implicitly rejecting ISI among strong interferers with a single *3NI × 3NI*-matrix inversion.

For the ISR-TR, ISR-R and ISR-D modes, each receiver module, in effect, combines a receiver module of set I with a receiver module of set D, some components being omitted as redundant. Referring again to Figure 28, which shows such a combined receiver module, the preprocessor 18 supplies the observation matrix $Y_n$ to a 1-bit delay 45 and a first vector reshaper 44/1, which reshapes the observation matrix $Y_n$ to form the observation vector $\underline{Y}_n$. A second vector reshaper 44/2 reshapes the delayed observation matrix $Y_{n-1}$ to form delayed observation vector $\underline{Y}_{n-1}$. These matrices and vectors are supplied to the receiver module 21P$^i$ and to others of the receiver modules, together with the constraint matrix $\hat{C}_{n-1}$ and the inverse matrix $Q_{n-1}$ from a common constraint matrix generator 43P, which generates the constraint matrix $C_{n-1}$ and the inverse matrix $Q_{n-1}$ from the constraints-set $C_{n-1}$ produced by constraint set generator 42P.

The receiver module 21P$^i$ comprises a despreader 19$^i$, a channel identification unit 28P$^i$, a power estimation unit 30P$^i$, and a decision rule unit 29P$^i$, all similar to those of the above-described receiver modules. In this case, however, the receiver module 21P$^i$ comprises two beamformers, one an ISR beamformer 47P$^i$ and the other an MRC beamformer 27P$^i$, and an additional decision rule unit 29P/2$^i$ which is connected to the output of MRC beamformer 27P$^i$. The ISR beamformer 47P$^i$ processes the delayed observation vector $\underline{Y}_{n-1}$ to form the estimated signal component estimate $\hat{s}^i_{n-1}$ and supplies it to the first decision rule unit 29P$^i$, the power estimation unit 30P$^i$, and the channel identification unit 28P$^i$, in the usual way. The decision rule unit 29P$^i$ and the power estimation unit 30P$^i$ operate upon the signal component estimate $\hat{s}^i_{n-1}$ to derive the corresponding symbol estimate $\hat{b}^i_{n-1}$ and the power estimate $\psi^i_{n-1}$ and supply them to other parts of the receiver in the usual way.

The despreader 19$^i$ despreads the delayed observation matrix $Y_{n-1}$ to form the post-correlation observation vector $Z^i_{n-1}$ and supplies it to only the channel identification unit 28P$^i$, which uses the post-correlation observation vector $Z^i_{n-1}$ and the signal component estimate to produce both a spread channel estimate $\hat{Y}^i_{0,n-1}$ and a set of channel parameter estimates $\mathcal{H}^i_{n-1}$. At the beginning of the processing cycle, the channel identification unit 28P$^i$ supplies the spread channel estimate $\hat{Y}^i_{0,n-1}$ to both the ISR beamformer 47P$^i$ and

the MRC beamformer 27P$^i$ for use in updating their coefficients, and supplies the set of channel parameter estimates $\mathcal{H}_{n-1}^i$ to the constraints-set generator 42P.

The MRC beamformer 27P$^i$ processes the current observation vector $\underline{Y}_n$ to produce a "future" signal component estimate $\hat{s}_{MRC,n}^i$ for use by the second decision rule

5   unit 29P/2$^i$ to produce the "future" symbol estimate $\hat{b}_{MRC,n}^i$, which it supplies to the constraints-set generator 42P at the beginning of the processing cycle. The constraints-set generator 42P also receives the symbol estimate $\hat{b}_{n-1}^i$ from the decision rule unit 29$^i$, but at the end of the processing cycle. The constraints-set generator 42P buffers the symbol $\hat{b}_{MRC,n}^i$ from the decision rule unit 29P/2$^i$ and the symbol estimate $\hat{b}_{n-1}^i$ from

10  the decision rule unit 29P$^i$ at the end of the processing cycle. Consequently, in a particular symbol period $n-1$, when the constraints-set generator 42P is computing the constraints-set $C_{n-1}$ it has available the set of channel parameter estimates $\mathcal{H}_{n-1}$, the "future" symbol estimate $\hat{b}_{MRC,n}^i$, the "present" symbol estimate $\hat{b}_{MRC,n-1}^i$ and the "past" symbol estimate $\hat{b}_{n-2}^i$, the latter two from its buffer.

15  Each of the other receiver modules in the "joint ISR" set supplies its equivalents of these signals to the constraints-set generator 42P. The constraints-set generator 42P processes them all to form the constraints set $C_{n-1}$ and supplies the same to the constraint matrix generator 42P, which generates the constraint matrix $\hat{C}_n$ and the inverse matrix $Q_n$ and supplies them to the various receiver modules.

20  The constraints-set generator 42P and the constraint matrix generator 43P will be constructed and operate generally in the same manner as the constraints-set generator 43 and constraint matrix generator 42 of the embodiments of the invention described hereinbefore with reference to Figures 9 to 27. Hence, they will differ according to the ISR mode being implemented.

25  When the constraints-set generator 42P of the receiver of Figure 28 is configured for the ISR-D mode, $i.e.$ like the constraints-set generator shown in Figure 16, the constraint matrix $\hat{C}_n$ supplied to the ISR beamformer 47P$^i$ contains enough information for the beamformer 47P$^i$ to estimate the channel parameters itself. Hence, it forwards these estimates to the channel identification unit 28P$^i$ for use in improving the channel

30  parameter estimation and the set of channel estimates produced thereby.

An ISR-RH receiver module will use a similar structure, except that the one-bit delay 45 will be omitted and the constraints-set generator 42P will use the previous symbol, estimate $\hat{b}_{n-1}^i$, the current MRC symbol estimate $\hat{b}_{MRC,n}^i$ and the two

53

hypothetical values for "future" symbol $b_{n+1}^i$ to produce current symbol estimate $\hat{b}_n^i$. Modification of the receiver module shown in Figure 28 to implement such a "ISR-RH mode" will be straightforward for a skilled person and so will not be described hereafter.

In order to implement J-ISR, a more general formulation of the constraint matrix

5   is required. The general ISR constraint matrix counting $N_c$ constraints, is as follows:

$$\hat{C}_n = \left[ \frac{\hat{C}_{n,1}}{\|\hat{C}_{n,1}\|}, \cdots, \frac{\hat{C}_{n,j}}{\|\hat{C}_{n,j}\|}, \cdots, \frac{\hat{C}_{n,N_c}}{\|\hat{C}_{n,N_c}\|} \right] \qquad (72)$$

where the $j$-th constraint $\hat{\underline{C}}_{n,j}$ is given by:

10

$$\hat{\underline{C}}_{n,j} \triangleq \sum_{(u,f,k)\in S_j} \hat{\underline{Y}}_{k,n}^{u,f} \qquad (73)$$

where $S_j$ defines a subset of diversities which form the $j$-th constraint when summed. As shown in Table 2, the sets $S_j$, $j = 1, \cdots, N_c$ are assumed to satisfy the following

15   restrictions:

$$S = S_1 \bigcup S_2 \bigcup \cdots \bigcup S_{N_c} = \{(u,f,k) \mid u=1,\cdots,NI; f=1,\cdots,N_f; k=-1,0,+1\},$$

and

$$S_1 \bigcap S_2 \bigcap \cdots \bigcap S_{N_c} = \varnothing,$$

20

$\varnothing$ being the empty set. Table 1 defines the sets $S_j$, $j=1, \cdots, N_c$ for all presented ISR modes of operation.

The objective signal belongs to the total interference subspace as defined by the span of the common constraint matrix $\hat{C}_n$. Therefore, to avoid signal cancellation of

25   the desired user $d$ by the projection:

$$\Pi_n^d = I_{M \cdot (2L-1)} - \hat{C}_n^d \underline{Q}_n \hat{C}_n^H, \qquad (74)$$

the desired-signal blocking matrix $\hat{C}_n^d$ is introduced, as given by:

30

$$\hat{C}_n^d = \left[ \frac{\hat{C}_{n,1}^d}{\|\hat{C}_{n,1}^d\|}, \cdots, \frac{\hat{C}_{n,j}^d}{\|\hat{C}_{n,j}^d\|}, \cdots, \frac{\hat{C}_{n,N_c}^d}{\|\hat{C}_{n,N_c}^d\|} \right], \qquad (75)$$

where:

$$\hat{\underline{C}}_{n,j}^d \triangleq \sum_{(u,f,k)\in S_j \backslash S^d} \hat{\underline{Y}}_{k,n}^{u,f}, \qquad (76)$$

54

with $S^d = \{(u,f,k)\,|\,u = d;\, f = 1,\, ...,\, N_f;\, k = 0\}$. Normally $S^d$ is a small subset of $S$ and $\hat{C}_n^d$ is very close to $\hat{C}_n$.

## *Joint multi-user data estimation and channel gain estimation in ISR-D*

Neglecting the signal contributions from the weak-power low-rate users, and limiting to the signals of the $NI$ interferers, $\underline{Y}_n$, can be formulated as:

$$\underline{Y}_n = \sum_{i=1}^{NI} \sum_{f=1}^{N_f} \psi_n^i \, \zeta_{f,n}^i \underline{Y}_n^{i,f} + \underline{N}_n^{pth} \tag{77}$$

$$= C_n \left[\psi_n^i \zeta_{1,n}^1, ..., \psi_n^1 \zeta_{N_f,n}^1, ... \psi_n^{NI} \zeta_{1,n}^{NI}, ... \psi_n^{NI} \zeta_{N_f,n}^{NI}\right]^T + \underline{N}_n^{pth} \tag{78}$$

$$= C_n \underline{\Gamma}_n + \underline{N}_n^{pth}, \tag{79}$$

where $\underline{\Gamma}_n$ is a $N_f NI \times 1$ vector which aligns channel coefficients from all fingers over all users. Estimation of $\underline{\Gamma}_n$, may be regarded as a multi-source problem:

$$\underline{\hat{\Gamma}}_n = Q_n \hat{C}_n^H \underline{Y}_n. \tag{80}$$

This constitutes one step of ISR-D operations and allows joint multi-user channel identification.

Multi-stage processing may be used in combination with those of the above-described embodiments which use the above-described joint ISR, *i.e.* all except the receivers implementing ISR-H mode. It should be appreciated that, in each of the receivers which use decision-feedback modes of ISR (TR,R,D,RH), coarse MRC symbol estimates are used in order to reconstruct signals for the ISR operation. Because they are based upon signals which include the interference to be suppressed, the MRC estimates are less reliable than ISR estimates, causing worse reconstruction errors. Better results can be obtained by using multi-stage processing and, in successive stages other than the first, using improved ISR estimates to reconstruct and perform the ISR operation again.

55

Operation of a multi-stage processing receiver module which would perform several iterations to generate a particular symbol estimate is illustrated in Figure 29, which depicts the same components, namely constraint-sets generator 42P, constraint matrix generator 43P, ISR beamformer $47P^i$ and decision rule unit $29P/1^i$, MRC

5 beamformer $27P^i$ and decision rule unit $29P/2^i$, in several successive symbol periods, representing iterations 1, 2,...,$N_s$ of frame $n$ which targets the symbol estimate $\hat{b}^i_{n-1}$ for user station $10^i$. Iteration 1, if alone, would represent the operation of the receiver module $21^i$ of Figure 28 in which the constraints-set generator 42P uses the coarse symbol estimates $\hat{b}^i_{MRC,n-1}$ previously received from the second decision rule unit $29P/2^i$

10 (and others as applicable) and buffered. In each iteration within the frame, the other variables used by the constraints-set generator 42P remain the same. These variables comprise, from at least each "contributor" receiver module in the same joint processing set, the previous symbol estimate $\hat{b}^i_{n-2}$, the set of channel parameters $\mathcal{H}^i_{n-1}$ and the current MRC symbol estimate $\hat{b}^i_{MRC,n}$. Likewise, the spread channel estimate $\hat{Y}^i_{0,n-1}$ and

15 the delayed observation vector $\underline{Y}_{n-1}$ used by the ISR beamformer $47P^i$ will remain the same.

In iteration 1, the constraint matrix generator 42P generates constraint matrix $\hat{C}_{n-1}(1)$ and the inverse matrix $Q_{n-1}(1)$ and supplies them to the beamformer $47P^i$ which uses them, and the spread channel estimate $\hat{Y}^i_{0,n-1}$ to tune its coefficients for

20 weighting each element of the delayed observation vector $\underline{Y}_{n-1}$, as previously described, to produce a signal component estimate which the decision rule unit $29P/1^i$ processes to produce the symbol estimate $\hat{b}^i_{n-1}(1)$ at iteration 1, which would be the same as that generated by the receiver of Figure 28. This symbol estimate $\hat{b}^i_{n-1}(1)$ is more accurate than the initial coarse MRC estimate $\hat{b}^i_{MRC,n-1}(0)$ so it is used in iteration 2 as the input

25 to the constraints-set generator $42P^i$, i.e., instead of the estimate coarse MRC

56

beamformer 27P$^i$ estimate. As a result, in iteration 2, the constraint matrix generator 42P produces a more accurate constraint matrix $\hat{C}_{n-1}(2)$ and inverse matrix $Q_{n-1}(2)$. Using these improved matrices, the ISR beamformer 47P$^i$ is tuned more accurately, and so produces a more accurate symbol estimate $\hat{b}^i_{n-1}(2)$ in iteration 2. This improved symbol estimate is used in iteration 3, and this iterative process is repeated for a total of $N_s$ iterations. Iteration $N_s$ will use the symbol estimate $\hat{b}^i_{n-1}(N_s-1)$ produced by the preceding iteration and will itself produce a symbol estimate $\hat{b}^i_{n-1}(N_s)$ which is the target symbol estimate of frame $n$ and hence is outputted as symbol estimate $\hat{b}^i_{n-1}$.

This symbol estimate $\hat{b}^i_{n-1}$ will be buffered and used by the constraints-set generator 42P in every iteration of the next frame $(n+1)$ instead of symbol estimate $\hat{b}^i_{n-2}$. Other variables will be incremented appropriately and, in iteration 1 of frame $n+1$, a new coarse MRC beamformer 27P$^i$ symbol estimate $\hat{b}^i_{MRC,n+1}$ will be used by the constraints-set generator 42P. The iterative process will then be repeated, upgrading the symbol estimate in each interation, as before.

It should be noted that, in Figure 29, the inputs to the channel identification unit 28P$^i$ use subscripts which reflect the fact that they are produced by a previous iteration. These subscripts were not used in Figure 28 because it was not appropriate to show the transition between two cycles. The transition was clear, however, from the theoretical discussion.

One stage ISR operation can be generalized as follows:

$$\hat{s}^d_n(1) = \hat{s}^d_{MRC,n} - \underline{W}^{d*}_{MRC,n} \hat{C}^d_n(1)\underline{v}_n(1), \quad \underline{v}_n(1) = Q_n(1)\hat{C}_n(1)^H \underline{Y}_n, \tag{81}$$

where $\hat{s}^d_n(1)$ is the ISR estimate from first ISR stage, $\hat{s}^u_{MRC,n}$ is the MRC signal estimate, and the constraint matrices $\hat{C}_n(1)$, $\hat{C}^d_n(1)$, and $Q_n(1)$ are formed from MRC estimates at the first stage. Generalizing notation, the signal estimate at stage $N_s$ may be derived after the following iterations:

57

$$\hat{s}_n^d(2) = \hat{s}_{MRC,n}^d - \underline{W}_{MRC,n}^{d*}\hat{C}_n^d(2)\underline{v}_n(2), \quad \underline{v}_n(2) = Q_n(2)\hat{C}_n(2)^H\underline{Y}_n,$$

$$\vdots \tag{82}$$

$$\hat{s}_n^d(N_s) = \hat{s}_{MRC,n}^d - \underline{W}_{MRC,n}^{d*}\hat{C}_n^d(N_s)\underline{v}_n(N_s). \quad \underline{v}_n(N_s) = Q_n(N_s)\hat{C}_n(N_s)^H\underline{Y}_n,$$

5   The multistage approach has a complexity cost; however, complexity can be reduced because many computations from one stage to the next are redundant. For instance, the costly computation $\underline{v}(j)$ could instead be tracked because $\underline{v}(j) \approx \underline{v}(j-1)$ if the number of symbol estimation errors does not change much from stage to stage, which can be expected in most situations.

10   In practice, the receiver of Figure 28 could be combined with one of the earlier embodiments to create a receiver for a "hierarchical" situation, *i.e.*, as described hereinbefore with reference to Figure 8, in which a first group of receiver modules, for the weakest signals, like those in set D of Figure 8, for example, are "recipients" only, *i.e.*, they do not contribute to the constraint matrix at all; a second group of receiver

15   modules, for the strongest signals, like the receiver modules of set I in Figure 8, do not need to cancel interference and so are "contributors" only, *i.e.*, they only contribute constraints-sets to the constraint matrix used by other receiver modules; and a third set of receiver modules, for intermediate strength signals, like the receiver modules of sets M2 of Figure 8, are both "recipients" and "contributors", *i.e.* they both use the

20   constraint matrix from the set I receiver modules to cancel interference from the strongest signals and contribute to the constraint matrix that is used by the set D receiver modules. Generally, this approach is referred to as "Group ISR" (G-ISR) and the equations for the constraint matrices and inverse matrices comprising the set $K_n = \left\{\hat{C}_{Outset,n}, Q_{Outset,n}, \hat{C}_{Inset,n}, Q_{Inset,n}\right\}$ used by the ISR beamformers in the different

25   receivers are as follows:

58

$$Q_{Outset,n} = \left( \hat{C}_{Outset,n}^{H} \hat{C}_{Outset,n} \right)^{-1}, \tag{83}$$

$$\Pi_{Outset,n} = I_{M \cdot (2L-1)} - \hat{C}_{Outset,n} Q_{Outset,n} \hat{C}_{Outset,n}^{H}, \tag{84}$$

$$\hat{C}_{Inset,n} = \Pi_{Outset,n} \hat{C}_{Inset,n}, \tag{85}$$

$$Q_{Inset,n} = \left( \hat{C}_{Inset,n}^{d_H} \hat{C}_{Inset,n} \right)^{-1}, \tag{86}$$

$$\Pi_{Inset,n}^{d} = I_{M \cdot (2L-1)} - \hat{C}_{Inset,n}^{d} Q_{Inset,n} \hat{C}_{Inset,n}^{H}, \tag{87}$$

$$\Pi_{n}^{d} = \Pi_{Inset,n}^{d} \Pi_{Outset,n}, \tag{88}$$

$$\underline{W}_{n}^{d} = \frac{\Pi_{n}^{d} \hat{\underline{Y}}_{0,n}^{d}}{\hat{\underline{Y}}_{0,n}^{d} \Pi_{n}^{d} \hat{\underline{Y}}_{0,n}^{d}} = \Pi_{n}^{d} \times \frac{\hat{\underline{Y}}_{0,n}^{d}}{\underline{Y}_{0,n}^{d} \Pi_{n}^{d} \hat{\underline{Y}}_{0,n}^{d}}. \tag{89}$$

It should be noted that normalization of the columns of $\hat{C}_{Inset,n}$ and $\hat{C}_{Outset,n}$ is implicit.

A receiver module for set D will set $\Pi_{Inset}$ in Equation (88) to identity which means that only "outset" interference will be cancelled. Otherwise, the processing will be as described for other receivers of set D.

A receiver in set M1 does not need to cancel "outset" interference, but does need to cancel "inset" interference. Consequently, it will set $\Pi_{Outset}$ in Equation (88) to identity so that only inset interference will be cancelled. This corresponds to the joint ISR embodiment described with reference to Figure 28.

Finally, a receiver in set I does not need to cancel any interference. Consequently, it will set both $\Pi_{Inset}$ and $\Pi_{Outset}$ to identity, which means that nothing will be cancelled. This corresponds to the group I receiver modules $21^{1}...21^{NI}$ described with reference to Figures 9, 11, 13, 15-17, 20-24 and 26.

_Successive versus Parallel Detection_

Although the embodiments of ISR receivers described hereinbefore use a parallel implementation, ISR may also be implemented in a successive manner, denoted S-ISR,

59

as illustrated in Figure 30. Assuming implementation of successive ISR among $NI$

interferers, $U$ users, and assuming without loss of generality that are sorted in order of

decreasing strength such that user 1 is the strongest and user $NI$ is the weakest user,

when processing user $i$ in S-ISR, the ISR estimate can be computed as:

$$\hat{s}_n^i = \hat{s}_{MRC,n}^i - \underline{W}_{MRC,n}^{i^H} \hat{C}_{i,n}^i \underline{v}_n(i), \quad \underline{v}_n(i) = \underline{Q}_n^i \hat{C}_{i,n}^H \underline{Y}_n, \tag{90}$$

where $\hat{C}_{i,n}$ spans only the subspace of users $1, \cdots, i\text{-}1^2$, $\underline{Q}_n^i$ is the corresponding inverse

and where $\hat{C}_{i,n}^i$ is the user specific constraint matrix. Clearly, $\hat{C}_{i,n}^i$ is no longer

common for all users, which entails expensive matrix inversion for each user. However,

with ISR-TR this inversion is avoided, since $\hat{C}_{i,n}^{i^H}\hat{C}_{i,n}^i$ is a scalar, and S-ISR-TR is a good

alternative to its parallel counterpart, ISR-TR. Other ISR modes may take advantage of

the common elements of $\hat{C}_{i,n}$ from one processing cycle to the next using matrix

inversion by partitioning.

It should also be appreciated that the different ISR modes may be mixed,

conveniently chosen according to the characteristics of their signals or transmission

channels, or data rates, resulting hybrid ISR implementations (H-ISR). For example,

referring to Figure 8, the sets I, M1 and M2 might use the different modes ISR-H, ISR-

D and ISR-TR, respectively, and the receiver modules in set D would use the different

modes to cancel the "outset" interference from those three sets. Of course, alternatively

or additionally, different modes might be used within any one of the sets.

In all of the above-described embodiments of the invention, the channel

identification units $28^d$ in the ISR receiver modules use the post-correlation observation

vector $\underline{Z}_n^i$ to generate the spread channel estimate $\hat{Y}_{0,n}^d$ (by spreading $\underline{\hat{H}}_n^d$ ).

Unfortunately, the interference present in the observation matrix $Y_n$ is still present in the

---

[2] And also user $i$ if ISR rejection is desired.

post-correlation observation vector $\underline{Z}_n^i$ (see Equation (14)) and, even though it is reduced in power by despreading, it detracts from the accuracy of the spread channel estimate $\hat{\underline{Y}}_{0,n}^d$. As has been discussed hereinbefore, specifically with reference to Equations (83) to (89), the ISR beamformer $47^d$ effectively constitutes a

5   projector $\Pi_n^d$ and a tuning and combining portion

$$\frac{\hat{\underline{Y}}_{0,n}^d}{\hat{\underline{Y}}_{0,n}^{d\ H}\ \Pi_n^d\ \hat{\underline{Y}}_{0,n}^d}$$

10   which, in effect, comprises a residual MRC beamformer $\underline{W}_n^d = \dfrac{\hat{\underline{Y}}_{0,n}^{\Pi,d}}{|\hat{\underline{Y}}_{0,n}^{\Pi,d}|^2}$.

Figure 31 illustrates a modification, applicable to all embodiments of the invention described herein including those described hereafter, which exploits this relationship to improve the spread channel estimate $\hat{\underline{Y}}_{0,n}^d$ (or unspread channel estimate $\underline{\hat{H}}_n^d$) by using

15   the projector $\Pi_n^d$ to suppress the interference component from the observation vector $\underline{Y}_n$. In the receiver module of Figure 31, the ISR beamformer $47Q^d$ is shown as comprising a projector $100^d$ and a residual MRC beamformer portion $27Q^d$. The projector $100^d$ multiplies the projection $\Pi_n^d$ by the observation vector $\underline{Y}_n$ to produce the "cleaned" observation vector $\underline{Y}_n^{\Pi,d}$ and supplies it to the residual MRC beamformer $27Q^d$, which

20   effectively comprises a tuner and combiner to process the "cleaned" observation vector $\underline{Y}_n^{\Pi,d}$ and produce the signal component estimate $\hat{s}_n^d$ from which decision rule unit $29Q^d$ derives the symbol estimate $\hat{b}_n^d$ in the usual way.

The "cleaned" observation vector $\underline{Y}_n^{\Pi,d}$ is reshaped by matrix reshaper $102Q^d$ to form "cleaned" observation matrix $\underline{Y}_n^{\Pi,d}$ which despreader $19^d$ despreads to form the

61

"cleaned" post-correlation observation vector $\underline{Z}_n^{\Pi,d}$ for application to the channel

identification unit 28Q$^d$ for use in deriving the spread channel estimate $\underline{\hat{Y}}_{0,n}^d$.

The new "cleaned" vector resulting from the projection of the observation

vector $\underline{Y}_n$ by $\Pi_n^d$ is defined as follows:

5
$$\underline{Y}_n^{\Pi,d} = \Pi_n^d \underline{Y}_n = \Pi_n^d \left\{ \sum_{u \in \{1,...,N\} \cup \{d\}} \underline{Y}_n^u + \underline{N}_n \right\} \simeq (\Pi_n^d \underline{Y}_{0,n}^d) s_n^d + (\Pi_n^d \underline{N}_n) = \underline{Y}_{0,n}^{\Pi,d} s_n^d + \underline{N}_n^{\Pi,d}. \quad (91)$$

The new observation vector is free from the interferers and ISI and contains a

projected version of the channel vector $\underline{Y}_{0,n}^{\Pi,d}$. Without being a condition, it is reasonable

to assume that the projector $\Pi_n^d$ is almost orthogonal to the channel vector, especially

in high processing gain situations and/or in the presence of few interferers, and therefore

10 consider that $\underline{Y}_{0,n}^{\Pi,d} \simeq \underline{Y}_{0,n}^d$. When despreader 19$^d$ despreads $\underline{y}_n^{\Pi,d}$ with the spreading

sequence of the desired user $d$, it produces an interference-free projected post-correlation

observation vector $\underline{Z}_n^{\Pi,n}$ which the channel identification unit 28Q$^d$ uses to create the

channel estimate $\underline{\hat{Y}}_{0,n}^d$ to use in updating the coefficients of the residual MRC

beamformer portion 27Q$^d$.

15      With respect to the new observation vectors $\underline{y}_n^{\Pi,d}$ and $\underline{Z}_n^{\Pi,n}$, before and after

despreading, respectively, the ISR and DFI steps in STAR are modified as follows:

$$\underline{W}_n^d = \frac{\underline{\hat{Y}}_{0,n}^{\Pi,d}}{\|\underline{\hat{Y}}_{0,n}^{\Pi,d}\|^2} \equiv \frac{\underline{\hat{Y}}_{0,n}^d}{\underline{\hat{Y}}_{0,n}^{d^H} \Pi_n^d \underline{\hat{Y}}_{0,n}^d}, \quad (92)$$

$$\hat{s}_n^d = Real\{\underline{W}_n^{d^H} \underline{Y}_n^{\Pi,d}\}, \quad (93)$$

20

$$\underline{\hat{H}}_{n+1}^d = \underline{\hat{H}}_n^d + \mu (\underline{Z}_n^{\Pi,d} - \underline{\hat{H}}_n^d \hat{s}_n^d) \hat{s}_n^d. \quad (94)$$

The equivalence between the two expressions of the beamformer coefficients in

Equation (92) due to the nilpotent property of projections should be noted. In more

adverse near-far situations, the modification illustrated in Figure 31 allows more reliable

25 channel identification than simple DFI and hence increases near-far resistance. If

62

necessary, this new DFI version will be termed Π-DFI. It is expected to be suitable for

situations where the interferers are moderately strong and when the null constraints cover

them all. For simplicity of discussion, projection of the observation will become implicit

without reference to $\underline{Y}^d_{\Pi,n}$, $\underline{Z}^d_{\Pi,n}$ or to the corresponding modifications in STAR-ISR

5  operations.


## *Expanding Dimensionality (X-option)*

When the number of users becomes high compared to the processing gain, the

dimension of the interference subspace becomes comparable to the total dimension *(M(2L*

10  *-1))*. The penalty paid is an often devastating enhancement of the white noise. Unlike

ISR-TR, which always requires a single constraint, other DF modes, namely ISR-R and

ISR-D, may suffer a large degradation because the number of constraints these modes

require easily becomes comparable to the total dimension available. However, the

dimension may be increased by using additional data in the observation. This option also

15  allows for complete asynchronous transmission and for the application of ISR to Mixed

Spreading Factor (MSF) systems.

The matched-filtering observation vector $\underline{Y}_n$ is generated to include additional past

spread data which has already been processed. If the model is expanded to include past

processed $N_X$ symbols and arrive at a total temporal dimension $N_T = (N_X+1)L-1$, the

20  observation becomes:

$$\underline{\underline{Y}}_n = \begin{bmatrix} \underline{Y}_{n-N_X+1} \\ \vdots \\ \underline{Y}_n \end{bmatrix} = \sum_{u=1}^{U} \sum_{f=1}^{N_f} \begin{bmatrix} \underline{Y}^{u,f}_{n-N_X+1} \\ \vdots \\ \underline{Y}^{u,f}_n \end{bmatrix} + \begin{bmatrix} \underline{N}^{pth}_{n-N_X+1} \\ \vdots \\ \underline{N}^{pth}_n \end{bmatrix} = \sum_{u=1}^{U} \sum_{f=1}^{N_f} \underline{\underline{Y}}^{u,f}_n + \underline{\underline{N}}^{pth}_n \qquad (95)$$

where double underlining stresses the extended model. It should be noted that $\underline{\underline{y}}^{u,j}_j$ is

overlapping temporally $\underline{\underline{y}}^{u,j}_{j\pm 1}$ and only the first $ML$ samples of the past frames $n-1$, $n-2$,

.. etc. are used; however the same syntax is used for simplicity of notation.

As an example, application of the X option to ISR-D, referred to as ISR-DX,

5  requires the following constraint matrix:

$$
\hat{C}_n = \left[ \frac{\hat{\underline{\underline{Y}}}^{1,1}_n}{\left\| \hat{\underline{\underline{Y}}}^{1,1}_n \right\|}, \dots, \frac{\hat{\underline{\underline{Y}}}^{1,N_f}_n}{\left\| \hat{\underline{\underline{Y}}}^{1,N_f}_n \right\|}, \dots, \frac{\hat{\underline{\underline{Y}}}^{N_I,1}_n}{\left\| \hat{\underline{\underline{Y}}}^{N_I,1}_n \right\|}, \dots, \frac{\hat{\underline{\underline{Y}}}^{N_I,N_f}_n}{\left\| \hat{\underline{\underline{Y}}}^{N_I,N_f}_n \right\|} \right] . \tag{96}
$$

10  The extended vectors in Equation (96) have been treated in the same way as those in

Equation (95), i.e., by concatenating reconstructed vectors from consecutive symbols in

the extended frame and by implicitly discarding overlapping dimensions in the

concatenated vectors. Clearly, extension of the observation space leaves additional

degrees of freedom and results in less white noise enhancement. However, it may exact

15  a penalty in the presence of reconstruction errors.

Although the X-option was illustrated in the case of ISR-D, its application to the

remaining DF modes is straightforward. It should also be noted that the X-option allows

for processing of more than one symbol at each frame while still requiring one matrix

inversion only. The duration of the frame, however, should be small compared to the

20  variations of the channel.

In the above-described embodiments, ISR was applied to a quasi-synchronous

system where all temporal delays were limited to $0 < \tau < L$. Although this model

reflects well the large processing gain situation, where the limit $(L \to \infty)$, allows for

placing a frame of duration $2L - 1$ chips which fully cover one bit of all users, including

25  delay spreads. With realistic processing gains, and in particular in the low processing

64

gain situation, this model tends to approach a synchronous scenario. Using the X-option serves as a method supporting complete asynchronous transmission.

Referring to Figure 32, assuming that the users of the system have processing gain $L$ as usual, the transmitted signal of any user is cyclo-stationary and a possible time-

5   delay of the primary path $\tau_1$ is therefore $0 < \tau_1 < L$ where possible time delays of remaining paths are $\tau_1 < \tau_2 < ... < L + \Delta\tau$ where $\Delta\tau$ is the largest possible delay spread considered. To ensure that the frame covers at least one bit of all users, the frame must at least span $L + \Delta\tau$ in the despread domain and therefore $2L + \Delta\tau$ in the spread domain. The observation should be extended slightly beyond that to ease

10  interpolation near the edges of the frame.

Multi-Modulation (MM), Multi-Code (MC), and Mixed Spreading Factor (MSF) are technologies that potentially can offer mixed-rate traffic in wideband CDMA. MSF, which has become very timely, was shown to outperform MC in terms of performance and complexity and is also proposed by UMTS 3 third generation mobile system as the

15  mixed-rate scenario. Application of ISR to MSF as the mixed rate scenario considered herein will now be discussed.

In MSF, mixed rate traffic is obtained by assigning different processing gains while using the same carrier and chip-rate. In a system counting two groups of users, a low-rate (LR) and a high rate (HR) group, this means that every time a LR rate user

20  transmits 1 symbol, a HR user transmits $2r + 1$ HR symbols, $r = L_l/L_h$ being the ratio of the LR processing gain to HR processing gain. This is illustrated in Figure 33 with $r = 2$.

Therefore, fitting the ISR frame subject to LR users or in general the lowest-rate users ensures that also at least $r$ HR symbols are covered when HR and LR have the

25  same delay spread. The ISR generalizes readily to this scenario regarding every HR user

65

as $r$ LR users. In Figure 33, the grey shaded HR/LR bits symbolize the current bits to be estimated; whereas, former bits have already been estimated (ISR-bits) and future bits are unexplored. It should be noted that current HR bits should be chosen to lie at the end of the frame.

5

### Multicode

It is envisaged that a user station could use multiple codes, $N_m$ in number, each to transmit a different stream of symbols. Figure 34 illustrates this modification as applied to a "without despreading" receiver module $21R^d$ for receiving such a multicode

10 signal and using ISR cancellation to cancel interference from other users. The receiver module shown in Figure 34 is similar to that shown in Figure 9 except that, instead of a single ISR beamformer $47^d$; the receiver module of Figure 34 has a bank of ISR beamformers $47R^{d,1},...,47R^{d,N_m}$ for extracting signal component estimates $\hat{s}_n^{d,1},...,\hat{s}_n^{d,N_m}$, respectively, and supplying them to a bank of decision rule units $29R^{d,1},...,29R^{d,N_m}$,

15 respectively which produce a corresponding plurality of symbol estimates $\hat{b}_n^{d,1},...,\hat{b}_n^{d,N_m}$. Likewise, the receiver module $21R^d$ has a bank of despreaders $19^{d,1},...,19^{d,N_m}$ each of which uses a respective one of the multiple spreading codes of the corresponding user $d$ to despread the observation matrix $Y_n$ from the preprocessing unit 18 to produce a corresponding one of a multiplicity of post-correlation observation

20 vectors $Z_n^{d,1},...,Z_n^{d,N_m}$ which are supplied to a common channel identification unit $28R^d$. It should be appreciated that the post-correlation observation vectors share the same channel characteristics, i.e., of the channel $14^d$ between user station $10^d$ and the base station antenna array. Consequently, only one channel identification unit $28R^d$ is required, which essentially processes the plural signal component

25 estimates $\hat{s}_n^{d,1},...,\hat{s}_n^{d,N_m}$ and the post-correlation observation vectors and, in essence,

66

averages the results to produce a single channel estimate $\hat{H}_n^d$ representing the physical channel $14^d$. The channel identification unit $28R^d$ has a bank of spreaders (not shown) which spread the channel estimate $\hat{H}_n^d$ using the multiple spreading codes to create a set of spread channel estimates $\underline{Y}_{0,n}^{d,1}, ..., \underline{Y}_{0,n}^{d,N_m}$, which it supplies to the ISR

5 beamformers $47R^{d,1}, ..., 47R^{d,N_m}$, respectively. Likewise, the power estimation unit $30R^d$ is adapted to receive plural signal component estimates $\hat{s}_n^{d,1}, ..., \hat{s}_n^{d,N_m}$ and essentially average their powers to produce the power estimate $\psi_n^d$.

While using all of the multiple codes advantageously gives a more accurate channel estimate, it requires many expensive despreading operations. In order to reduce

10 the cost and complexity, the receiver module $21M^d$ may use only a subset of the spreading codes.

It can be demonstrated that the multiple spreading codes can be replaced by a single spreading code formed by multiplying each of the multiple spreading codes by the corresponding one of the symbol estimates $\hat{b}_n^{d,1}, ..., \hat{b}_n^{d,N_m}$ and combining the results.

15 Figure 35 illustrates a receiver module which implements this variation. Thus, the receiver module $21R^d$ shown in Figure 35 differs from that shown in Figure 34 in that the bank of despreaders $19^{d,1}, ..., 19^{d,N_m}$ are replaced by a single despreader $19^{d,b}$ which receives the symbol estimates $\hat{b}_n^{d,1}, ..., \hat{b}_n^{d,N_m}$ and multiplies them by the multiple spreading codes to form a compound spreading code, which it then uses to despread the

20 observation matrix $Y_n$ and form a single post-correlation observation vector $\underline{Z}_n^{d,b}$. The channel identification unit $28R^d$ does not receive the signal component estimates but instead receives the total amplitude $\psi_n^d$ from the power estimation unit $30R^d$. This serves as a compound signal component estimate because the use of the compound code is equivalent to modulating a constant "1" or a constant "-1" with that code, as will be

25 formulated by equation later. The channel identification unit $28R^d$ processes the single

67

post-correlation observation vector $Z_n^{d,\delta}$ to produce a single channel estimate $\hat{H}_n^d$ and spreads it, as before, using the multiple spreading codes to form the multiple spread channel estimates $\hat{Y}_{0,n}^{d,1},...,\hat{Y}_{0,n}^{d,N_m}$ for use by the beamformers $47R^{d,1},...,47R^{d,N_m}$ as before.

The theory of such multicode operation will now be developed. Assuming for simplicity that each user assigned the index $u$ transmits $N_m$ streams of DBPSK data $b^{u,1}(t),...,b^{u,N_m}(t)$, using $N_m$ spreading codes $c^{u,1}(t),...,c^{u,N_m}(t)$, each spread stream can be seen as a separate user among a total of $U \times N_m$ access channels, assigned the couple-index $(u,l)$. The data model can then be written as follows:

$$Y_n = \sum_{u=1}^{U} \sum_{l=1}^{N_m} \sum_{k=-1}^{+1} \psi_n^u b_{n+k}^{u,l} Y_{k,n}^{u,l} + N_n^{pth} = \sum_{u=1}^{U} \sum_{l=1}^{N_m} \sum_{f=1}^{N_f} \sum_{k=-1}^{+1} \psi_n^u b_{n+k}^{u,l} \varsigma_{f,n}^u Y_{k,n}^{u,l,f} + N_n^{pth}, \quad (97)$$

where the canonic $u$-th user $l$-th code observation matrices $Y_{k,n}^{u,l,f}$ from finger $f$ are obtained by Equations (3) and (4) of with $X(t)$ in Equaiton (3) replaced, respectively for $k = -1,0,+1$,

by:

$$X_k^{u,l,f}(t) = \underline{R}_m \delta(t - \tau_p(t)) \otimes g^{l,u}(t) c^{u,l}(t). \quad (98)$$

In the equation above, $\underline{R}_m = [0, ...., 0, 1, 0, ..., 0]^T$ is an $M$-dimensional vector with null components except for the $m$-th one and $\delta(t)$ denotes the Dirac impulse. Reshaping matrices into vectors yields:

$$\underline{Y}_n = \sum_{u=1}^{U} \sum_{l=1}^{N_m} \sum_{k=-1}^{+1} \psi_n^u b_{n+k}^{u,l} \underline{Y}_{k,n}^{u,l} + N_n^{pth} = \sum_{u=1}^{U} \sum_{l=1}^{N_m} \sum_{f=1}^{N_f} \sum_{k=-1}^{+1} \psi_n^u b_{n+k}^{u,l} \varsigma_{f,n}^u \underline{Y}_{k,n}^{u,l,f} + N_n^{pth}, \quad (99)$$

The particularity of the above multi-code model, where $N_m$ codes of each user share the same physical channel $\underline{H}_n^u$ and the same total received power $(\psi_n^u)^2$ should be noted. Exploitation of these common features will be discussed hereinafter in relation to adapting of the power-control and the channel-identification procedures to the multi-code configuration. The ISR combining step will now be explained.

Considering first joint ISR combining among the group of $N$ interferers, the regular ISR modes, namely TR, R, D, H and RH easily generalize to the new multi-code

68

configuration of $N_m NI$ users instead of $NI$, as shown in Table 3. ISR combining operations are carried out as usual using the constraint and blocking matrices $\hat{C}_n$ and $\hat{C}_n^{i',l'}$, respectively. It should be noted, however, that a further dimension of interference decomposition and rejection arises over the codes of each user,

5  yielding two additional ISR modes. The new modes depicted in Table 3 and referred to as MCR and MCD (multi-code R and D) characterize interference from the entire set of codes of each user by its total realization or by the decomposition of this total realization over diversities, respectively. They combine the R and D modes, respectively, with the TR mode by summing the corresponding constraints over all the multi-codes of each

10 user.

Although these modes partly implement TR over codes, they are still robust to power estimation errors. Indeed, the fact that the received power of a given user is a common parameter shared between all codes enables its elimination from the columns of the constrain matrices (see Table 3). The MCR and MCD modes inherit the

15 advantages of the R and D modes, respectively. They relatively increase their sensitivity to data estimation errors compared to the original modes, since they accumulate symbol errors over codes. However, they reduce the number of constraints by $N_m$.

For a desired user assigned the index d, the constraint matrix $\hat{C}_n$ is used to form the projector $\Pi_n$. The receiver of the data stream from a user-code assigned the couple-

20 index $(d,l)$ can simply reject the $NI$ interfering multi-code users by steering a unit response to $\hat{Y}_{0,n}^{d,l}$ and a null response to the constraint matrix $\hat{C}_n$ with the projector $\Pi_n$. It can further reject ISI by steering nulls to $\hat{Y}_{-1,n}^{d,l}$ and $\hat{Y}_{+1,n}^{d,l}$. However, the signals received from other multi-codes contribute to self-ISI. This interference, referred to here as MC-ISI, is implicity suppressed when receiving an interfering user.

25 It can be suppressed too when receiving the desired low-power user by joint ISR among

the codes of each mobile with any of the ISR modes. The multi-code constraint and

blocking matrices $\hat{C}_{MC,n}^{d}$ and $\hat{C}_{MC,n}^{d,l}$, respectively, as shown in Table 4 are formed, and

derive the ISR beamformer coefficients for user-code $(d,l)$ derived, as follows:

$$Q_{MC,n}^{d} = \left(\hat{C}_{MC,n}^{d^{H}}\hat{C}_{MC,n}^{d}\right)^{-1},\qquad(100)$$

$$\Pi_{MC,n}^{d,l} = I_{M \cdot (2L-1)} - \hat{C}_{MC,n}^{d,l}Q_{MC,n}^{d}\hat{C}_{MC,n}^{d^{H}},\qquad(101)$$

$$\Pi_{n}^{d,l} = \Pi_{MC,n}^{d,l}\Pi_{n},\qquad(102)$$

$$\underline{W}_{n}^{d,l} = \frac{\Pi_{n}^{d,l}\hat{\underline{Y}}_{0,n}^{d,l}}{\hat{\underline{Y}}_{0,n}^{d,l^{H}}\Pi_{n}^{d,l}\hat{\underline{Y}}_{0,n}^{d,l}}.\qquad(103)$$

The projector $\Pi_{n}^{d,l}$ that is orthogonal to both MC-ISI and to the *NI* interferers is formed

and then its response normalized to have a unity response to $\hat{\underline{Y}}_{0,n}^{d,l}$.

The above processing organization of ISR among the high-power or low-power

user-codes themselves or between both subsets is a particular example that illustrates G-

ISR well. The fact that joint ISR among the high-power users and joint ISR among the

codes of a particular low-power user may each implement a different mode is another

example that illustrates H-ISR well. In the more general case, ISR can implement a

composite mode that reduces to a different mode with respect to each user. For instance,

within the group of *NI* interferers, each user-code assigned the index *(i,l)* can form its

own multi-code constraint and blocking matrices $\hat{C}_{MC,n}^{i}$ and $\hat{C}_{MC,n}^{i,l}$ along a user-specific

mode ($\Pi_{n}$ should be set to identity in Table 4). The constraint and blocking matrices

then can be reconstructed for joint ISR processing by aligning the individual constraint

and blocking matrices row-wise into larger matrices as follows:

$$\hat{C}_{n}^{i} = \left[\hat{C}_{MC,n}^{1},...,\hat{C}_{MC,n}^{NI}\right],\qquad(104)$$

$$\hat{C}_{n}^{i,l} = \left[\hat{C}_{MC,n}^{1},...,\hat{C}_{MC,n}^{i-1},\hat{C}_{MC,n}^{i,l},\hat{C}_{MC,n}^{i+1},...,\hat{C}_{MC,n}^{NI}\right].\qquad(105)$$

70

This example illustrates the potential flexibility of ISR in designing an optimal interference suppression strategy that would allocate the null constraints among users in the most efficient way to achieve the best performance/complexity tradeoff. It should be noted that, in the particular case where the TR mode is implemented, the matrices in

5   Equations (104) and (105) are in fact vectors which sum the individual multi-code constraint vectors $\hat{C}^l_{MC,n}$ and $\hat{C}^{i,1}_{MC,n}$, respectively.

After deriving the beamformer coefficients, each MC user assigned the index $u$ estimates its $N_m$ streams of data for $l = 1, ..., N_m$ as follows (see Figure 34):

$$\hat{s}^{u,l}_n = Real\left\{\underline{W}^{u,l}_n{}^H \underline{Y}_n\right\}, \tag{106}$$

10

$$\hat{b}^{u,l}_n = Sign\left\{\hat{s}^{u,l}_n\right\}, \tag{107}$$

and exploits the fact that its $N_m$ access channels share the same power, and hence smooths the instantaneous signal power of each data stream over all its codes as follows:

15

$$(\hat{\psi}^u_n)^2 = (1-\alpha)(\hat{\psi}^u_{n-1})^2 + \alpha\frac{\sum_{l=1}^{N_m}|\hat{s}^{u,l}_n|^2}{N_m}. \tag{108}$$

It should be noted that the multi-code data-streams can be estimated using MRC, simply by setting the constraint matrices to null matrices. This option will be referred to as MC-MRC.

After despreading of the post-correlation observation vector $\underline{Y}_n$ by the $N_m$

20   spreading codes of a user assigned the index $u$, the following post-correlation observation vectors for $l = 1, ..., N_m$ are obtained as follows:

$$\underline{Z}^{u,l}_n = \underline{H}^u_n \psi^u_n b^{u,l}_n + \underline{N}^{u,l}_{PCM,n} = \underline{H}^u s^{u,l}_n + \underline{N}^{u,l}_{PCM,n}. \tag{109}$$

The fact that all user-codes propagate through the same channel is exploited in the following cooperative channel identification scheme (see Figure 34):

25

$$\underline{\hat{H}}^u_{n+1} = \underline{\hat{H}}^u_n + \frac{\mu}{N_m}\sum_{l=1}^{N_m}\left(\underline{Z}^{u,l}_n - \underline{\hat{H}}^u_n\hat{s}^{u,l}_n\right)\hat{s}^{u,l}_n, \tag{110}$$

71

which implements a modified DFI scheme, referred to as multi-code cooperative DFI (MC-CDFI). MC-CDFI amounts to having the user-codes cooperate in channel identification by estimating their propagation vectors separately, then averaging them over all codes to provide a better channel estimate. It should be noted that implicit

5 incorporation of the II-DFI version in the above MC-CDFI scheme further enhances channel identification.

Since the STAR exploits a data channel as a pilot, it can take advantage of a maximum of $N_m$ expensive despreading operations. To limit their number in practice, MC-CDFI can be restricted to a smaller subset of 1 to $N_m$ user-codes. A compromise

10 can be found between channel estimation enhancement and complexity increase.

Another solution that reduces the number of despreading operations reconstructs the following data-modulated cumulative-code after ISR combining and symbol estimation i Equations (106) and (107):

$$c_k^{u,\delta} = \frac{1}{N_m} \sum_{l=1}^{N_m} \hat{b}_n^{u,l} c_k^{u,l}. \tag{111}$$

15

A single despreading operation with this code yields:

$$\underline{Z}_n^{u,\delta} = \psi_n^u \underline{H}_n^u \left( \frac{\sum_{l=1}^{N_m} \hat{b}_n^{u,l} b_n^{u,l}}{N_m} \right) + \left( \frac{\sum_{l=1}^{N_m} \underline{N}_{PCM,n}^{u,l}}{N_m} \right) \simeq \psi_n^u \underline{H}_n^u + \underline{N}_{PCM,n}^{u,\delta}. \tag{112}$$

20 It has the advantage of further reducing the noise level by $N_m$ after despreading, while keeping the signal power practically at the same level[3]. The data-modulated cumulative-code can be used to implement channel identification as follows:

$$a = sign\left\{ Re\left\{ \hat{\underline{H}}_n^{u\,H} \underline{Z}_n^{u,\delta} \right\} \right\},$$

---

[3] There is a small power loss due symbol estimation errors (very low in practice).

72

$$\underline{\tilde{H}}^u_{n+1} = \underline{\hat{H}}^u_n + \mu\left(\underline{Z}^{u,\delta}_n - \underline{\hat{H}}^u_n a\psi^u_n\right)a\psi^u_n.$$ (113)

This CDFI version is referred to as δ-CDFI (see Figure 35).

Whereas multicode operation involves user stations transmitting using multiple spreading codes, but usually the same data rate, it is also envisaged that different users 5 within the same system may transmit at different data rates. It can be demonstrated that the receiver modules shown in Figures 34 and 35 need only minor modifications in order to handle multirate transmissions since, as will now be explained, multicode and multirate are essentially interchangeable.

10 *Multi-Code Approach to Multi-Rate*

Reconsidering now the conventional MR-CDMA, in this context, STAR-ISR operations previously were implemented at the rate $1/T$ where $T$ is the symbol duration. As described earlier, with reference to Figure 32, the "X option" extensions, enables reduction of noise enhancement by increasing the dimension of the observation space and 15 provides larger margin for time-delay tracking in asynchronous transmissions. A complementary approach that decomposes the observation frame into blocks rather than extends it using past reconstructed data will now be described.

This block-processing version of STAR-ISR will still operate at the rate $1/T$ on data frames barely larger than the processing period $T$. However, it will decompose 20 each data stream within that frame into data blocks of duration $T_r$ where $T_r$ is a power-of-2 fraction of $T$. The resolution rate $1/T_r$ can be selected in the interval $[1, T, 1/T_c]$. Hence, a receiver module that processes data frames at a processing rate $1/T$ with a resolution rate $1/T_r$ can only extract or suppress data transmissions at rates slower than or equal to $1/T_r$. Also, the channel parameters of the processed transmissions must be 25 almost constant in the interval $T$, the processing period. This period should be chosen

73

to be much larger than the delay spread $\Delta\tau$ for asynchronous transmissions, but short enough not to exceed the coherence time of the channel.

In one processing period, STAR-ISR can simultaneously extract or suppress a maximum $N_m = T/T_r$ blocks ($N_m$ is a power of 2). In the $n$-th processing period of

5 duration $T$, a stream of data $b^u(t)$ yields $N_m$ samples $b_n^{u,1},...,b_n^{u,N_m}$ sampled at the resolution rate. Over this processing period, therefore, the spread data can be developed as follows:

$$c^u(t)b^u(t) = \sum_{l=1}^{N_m} b_n^{u,l} \sqcup_{T_r}^l(t - nT)c^u(t), \qquad (114)$$

where $\sqcup_{T_r}^l(t)$ is the indicator function of the interval $[(l - 1)T_r, lT_r)$. This equation can

10 be rewritten as follows:

$$c^u(t)b^u(t) = \sum_{l=1}^{N_m} b^{u,l}(t)c^{u,l}(t), \qquad (115)$$

where $b^{u,1}(t),...,b^{u,N_m}(t)$ represent $N_m$ data-streams at rate $1/T$ spread by $N_m$ virtual orthogonal codes $c^{u,1}(t),...,c^{u,N_m}(t)$ (see Figure (36).

With the above virtual decomposition, one arrives at a MC-CDMA model where

15 each of the processed users can be seen as a mobile that code-multiplexes $N_m$ data-streams over $N_m$ access channels. This model establishes an equivalence between MC-CDMA and MR-CDMA and provides a unifying framework for processing both interfaces simultaneously. In this unifying context, codes can be continuous or bursty. Use of bursty codes establishes another link with hybrid time-multiplexing CDMA (T-

20 CDMA); only the codes there are of an elementary duration $T_r$ that inserts either symbols or fractions of symbols. A larger framework that incorporates MR-CDMA, MC-CDM, and hybrid T-CDMA can be envisaged to support HDR transmissions for third generation wireless systems.

74

Exploiting this MC approach to MR-CDMA, the data model of MR-CDMA will be developed to reflect a MC-CDMA structure, then a block-processing version of STAR-ISR derived that implements estimation of a symbol fraction or sequence.

The multi-code model of Equation (97) applies immediately to MR-CDMA. However, due to the fact that codes are bursty with duration $T_r < T$, the self-ISI vectors $\hat{\underline{Y}}^{u,l}_{-1,n}$ and $\hat{\underline{Y}}^{u,l}_{+1,n}$ and the spread propagation vector $\underline{Y}^{u,l}_{0,n}$ of a given user-code do not overlap with each other. If $\overline{\Delta\tau}$ denotes an arbitrarily enlarged delay-spread (reference [20]) to leave an increased uncertainty margin for the tracking of time-varying multipath-delays *(i.e.,* $\Delta\tau < \overline{\Delta\tau} < T$), and if $N_r = \lceil \overline{\Delta\tau}/T_r \rceil$ denotes the maximum delay-spread in $T_r$ units, then only the last $N_r$ symbols $b^{u,N_m-N_r+1}_{n-1}, ..., b^{u,N_m}_{n-1}$ among the past-symbols in the previous frame may contribute to self-ISI in the current processed frame (see Figure 37):

$$Y_n = \sum_{u=1}^{U} \left\{ \sum_{l=N_m-N_r+1}^{N_m} \psi^u_n b^{u,l}_{n-1} Y^{u,l}_{-1,n} + \sum_{l=1}^{N_m} \psi^u_n b^{u,l}_n Y^{u,l}_{0,n} + \sum_{l=1}^{N_m} \psi^u_n b^{u,l}_{n+1} Y^{u,l}_{+1,n} \right\} + N^{pth}_n. \quad (116)$$

In this frame of duration $2T - T_c$, the desired signals' contribution from the $N_m$ current symbols is contained in the first interval of duration $T + \overline{\Delta\tau}$, whereas the remaining interval of the frame contains non-overlapping interference from the last $N_m - N_r$ future symbols in the next frame, namely $b^{u,N_r+1}_{n+1}, ..., b^{u,N_m}_{n+1}$ (see Figure 37). The remaining part of the frame can be skipped without any signal contribution loss from the current bits. Hence, the duration of the processed frame can be reduced to $T + \overline{\Delta\tau} - T_c$ as follows:

$$Y_n = \left[ Y_{n,0}, Y_{n,1}, ..., Y_{n,L \cdot L_a - 2} \right], \quad (117)$$

where $L_\Delta = \lceil \overline{\Delta \tau} / T_c \rceil$ is the maximum length of the enlarged delay-spread in chip samples. With the data block-size reduced to $M \times (L + L_\Delta - 1)$, the matched-filtering observation matrix reduces to:

$$Y_n = \sum_{u=1}^{U} \left\{ \sum_{l=N_m-N_r+1}^{N_m} \psi_n^u b_{n-1}^{u,l} Y_{-1,n}^{u,l} + \sum_{l=1}^{N_m} \psi_n^u b_n^{u,l} Y_{0,n}^{u,l} + \sum_{l=1}^{N_r} \psi_n^u b_{n+1}^{u,l} Y_{+1,n}^{u,l} \right\} + N_n^{pth}, \quad (118)$$

where $N_n^{pth}$ is the noise matrix reduced to the same dimension. This data model equation can be rewritten in the following compact vector form:

$$\underline{Y}_n = \sum_{u=1}^{U} \sum_{l=1}^{N_m} \sum_{k=-1}^{+1} \psi_n^u b_{n+k}^{u,l} \underline{Y}_{k,n}^{u,l} \lambda_k^l + \underline{N}_n^{pth}, \quad (119)$$

where $\lambda_{k_l} = 0$ if $k = -1$ and $l \in \{1,...,N_r\}$ or if $k = +1$ and $l \in \{N_m - N_r + 1,..., N_m\}$, and 1 otherwise.

The constraint matrices can be formed in an MC approach to implement joint or user-specific ISR processing in any of the modes described in Tables 3 or 4, respectively. In contrast to the conventional MC-CDMA, the factor $\lambda_k^l$ discards all non-overlapping interference vectors in the processed frame and somehow unbalances ISI contribution among the virtual multi-code streams. In the DF modes, only the central streams of each user *(i.e., l = N_r + 1, ..., N_m - N_r)* sum symbol contributions from the previous, current and future symbols; whereas the remaining streams sum signal contributions from either the current and the previous or the current and the future symbols. Indeed, the $2(N_m - N_r)$ ISI terms discarded from summation contribute with null vectors to the processed frame. In the ISR-H mode, the columns previously allocated to individually suppress these vectors are eliminated from the constraint matrices, thereby reducing the number of its columns to $N_H = N_m + 2N_r$ constraints per

76

user[4] (see Tables 3 and 4). ISR-H hence approaches ISR-R in computational complexity when $N_r$ is small compared to $N_m$.

After derivation of the beamformer coefficients of each virtual user-code assigned the couple-index $(u,l)$, its signal component $s_n^{u,l}$ is estimated using Equation (106). In
5 this process, each ISR combiner rejects the processed interferers regardless of their exact data rates, which only need to be higher than the resolution rate. This feature finds its best use when implementing ISR at the mobile station on the downlink where data rates of suppressed interferers are not necessarily known to the desired mobile-station. For instance, orthogonal variable spreading factor (OVSF) allocation of Walsh spreading
10 codes is no longer necessary. On the uplink, each transmission rate is known to the base station. However, one can still gain from this feature by allowing joint and well integrated processing of mixed data traffic at a common resolution rate.

Indeed, the estimation of the signal components provides sequences oversampled to the resolution rate $1/T_r$. Hence, after a given data stream is decomposed at this
15 common rate, its signal component estimate must be restored to its original rate in an "analysis/synthesis" scheme. To do so, the data rate $1/T_u \leq 1/T_r$ of user $u$ is defined and it is assumed temporarily that it is faster than the processing rate $(i.e., 1/T_u \geq 1/T)$. Hence, one can extract from each frame $F_u = T/T_u \leq N_m$ signal component estimates out of $N_m$ by averaging the oversampled sequence $s_n^{u,l}$ over consecutive blocks of size
20 $B_u = N_m/F_u = T_u/T_r$ for $n' = 0,..., F_u - 1$ as follows:

$$\hat{s}_{nF_u+n'} = \frac{\sum_{l=n'B_u+1}^{(n'+1)B_u} \hat{s}_n^{u,l}}{B_u}, \tag{120}$$

[4]ISR may be equally reformulated with $N_m + 2N_r$ generating sequences that process all the contributing symbols as if they were independent streams without MC-ISI. Only
25 the $N_m$ current symbols are estimated then; the $2N_r$ remaining symbols being corrupted by the edge effect.

77

$$\hat{b}^{u}_{nF_u+n'} = Sign\{\hat{s}^{u}_{nF_u+n'}\}, \qquad (121)$$

$$(\hat{\psi}^{u}_{n})^{2} = (1 - \alpha)(\hat{\psi}^{u}_{n-1})^{2} + \alpha \frac{\displaystyle\sum_{n'=0}^{F_u-1} |\hat{s}^{u}_{nF_u+n'}|^{2}}{F_u}. \qquad (122)$$

In the particular case where the data rate is equal to the processing rate *(i.e., $1/T_u = 1/T$)*, the equations above have simpler expressions with $F_u = 1$ and $B_u = N_m$:

$$\hat{s}^{u}_{n} = \frac{\displaystyle\sum_{l=1}^{N_m} \hat{s}^{u,l}_{n}}{N_m}, \qquad (123)$$

$$\hat{b}^{u}_{n} = Sign\{\hat{s}^{u}_{n}\}, \qquad (124)$$

$$(\hat{\psi}^{u}_{n})^{2} = (1 - \alpha)(\hat{\psi}^{u}_{n-1})^{2} + \alpha \; |\hat{s}^{u}_{n}|^{2}. \qquad (125)$$

If the data rate is slower than the processing rate, the signal component estimate $\hat{s}^{u}_{n}$ of Equation (123) is further averaged over consecutive blocks of size $F'_u = T_u/T$ to yield the following subsampled sequence:

$$\hat{s}^{u}_{\lfloor n/F'_u \rfloor} = \frac{\displaystyle\sum_{n'=0}^{F'_u-1} \hat{s}^{u}_{\lfloor n/F'_u \rfloor F'_u+n'}}{F'_u}. \qquad (126)$$

Symbol and power estimations in Equations (124) and (125) are on the other hand modified as follows:

$$\hat{b}^{u}_{\lfloor n/F'_u \rfloor} = Sign\{\hat{s}^{u}_{\lfloor n/F'_u \rfloor}\}, \qquad (127)$$

78

$$\left(\hat{\varphi}^{u}_{\lfloor n/F_{c}\rfloor}\right)^{2} = (1 - \alpha)\left(\hat{\varphi}^{u}_{\lfloor n/F_{c}\rfloor -1}\right)^{2} + \alpha \ |\hat{s}^{u}_{\lfloor n/F_{c}\rfloor}|^{2}. \tag{128}$$

It should be noted that a higher value is needed for the smoothing factor $\alpha$ to adapt to a slower update rate of power estimation. If the channel power variations are faster than the data rate, then it is preferable to keep the power estimation update at the processing rate in Equation (125). In this case, Equation (126) is modified as follows[5]:

$$\hat{s}_{\lfloor n/F_{c}\rfloor} = \frac{\sum_{n'=0}^{F_{c}-1} \hat{\mathcal{V}}^{u}_{\lfloor n/F_{c}\rfloor F_{c}+n'} \hat{s}^{u}_{\lfloor n/F_{c}\rfloor F_{c}+n'}}{\sum_{n'=0}^{F_{c}-1} \left(\hat{\mathcal{V}}^{u}_{\lfloor n/F_{c}\rfloor F_{c}+n'}\right)^{2}}, \tag{129}$$

to take into account channel power variations within each symbol duration.

It should be noted that the multi-rate data-streams can be estimated using MRC, simply by setting the constraint matrices to null matrices. This option may be referred to as MR-MRC.

It should be also noted that combination of Equations (106) and (120), along with Equation (128) for data rates slower than the processing rate, successively implements the processing gain of each user in fractioned ISR combining steps.

In general, regrouping the symbol-fractions back to their original rate can be exploited in the design of the constraint matrices; first by reducing reconstruction errors from enhanced decision feedback; and secondly by reducing the number of constraints

---

[5] This signal component estimate is not used for power estimation. Only its sign is taken in Equaiton (127) as the estimate of the corresponding bit. Hence, power normalization given here for completeness is skipped in practice.

79

of a given user $u$ from $N_m$ to $F_u$ in the modes implementing decomposition over user-codes (*i.e.*, R, D, and H). For these modes, the common factor $N_mNI$ appearing in the total number of constraints $N_c$ reduces to $\sum_{i=1}^{NI} F_i$, by regrouping the constraint vectors over the user-code indices that restore a complete symbol within the limit of the 5 processing period[6].

Regrouping the constraints of user $u$ to match its original transmission rate amounts to regrouping the codes of this user into a smaller subset that corresponds to a subdivision of its complete code over durations covering its symbol periods instead of the resolution periods. In fact, user $u$ can be characterized by $F_u$ concatenated multi-10 codes instead of $N_m$. Overall, MR-CDMA can be modeled as a mixed MC-CDMA system where each user assigned the index $u$ has its own number $F_u$ of multi-codes (see Figure 38). Therefore, the ISR-combining and channel-identification steps can be carried out in one step along the MC formulation of the previous section, using user-codes simply renumbered from 1 to $F_u$ for simplicity. Hence, as shown in Figure 39, the only 15 change needed to the receiver module of Figure 34 is to the bank of despreaders. In the receiver module shown in Figure 34, the spreading codes used by the despreaders $19^{d,1},...,19^{d,F_d}$ comprise segments of the spreading code of user $d$, *i.e.*, the segments together form the part of the code used in a particular frame. The number of code segments $F_u$ corresponds to the number of symbols $b_n^{u,1},...,b_n^{u,F_u}$ transmitted in the 20 frame. The estimates of these symbols, and the signal component estimates $\hat{s}_n^{u,1},...,\hat{s}_n^{u,F_u}$ map with those of Equations (120), (121), (123) and (124) within a parallel/serial transform.

---

[6] Feedback of symbols with rates slower than the processing rate to the constraints-set generator is feasible.

This illustrates again the flexibility afforded by using ISR in designing optimal interference suppression strategies that suit well with MR-CDMA. It enables simultaneous processing of blocks of symbols or fractions of symbols in an integrated manner at two common resolution and processing rates.

5      To carry out channel identification operations, the $M \times L_\Delta$ reduced-size post-correlation observation matrix of user-code $(u,l)$ is defined as follows:

$$Z_n^{u,l} = \left[ Z_{n,0}^{u,l}, Z_{n,1}^{n,l}, ..., Z_{n,L_\Delta-1}^{u,l} \right],\qquad(130)$$

where the columns of this matrix are given for $j = 0,...,L_\Delta - 1$ by:

$$Z_{n,j}^{u,l} = \frac{1}{L_r}\sum_{j'=0}^{L-1} Y_{n,j+j'} C_{j'}^{u,l} = \frac{1}{L_r} \sum_{j'=(l-1) \cdot L_r}^{l \cdot L_r} Y_{n,j+j'} C_{j'}^{u}.\qquad(131)$$

10

This correlation with the virtual user-code $(u,l)$ amounts to partial despreading by a reduced processing gain $L_r = T_s/T_c = L/N_m$, using the $l$-th block of length $L_r$ of the user's code $c_{j'}^u$. It should be noted that, in contrast to conventional MC-CDMA, the above partial despreading operations are less expensive in terms of complexity per user-

15  code.

The reduced-size post-correlation observation vector $\underline{Z}_n^{u,l}$ resulting from vector-reshaping of $Z_n^{u,l}$ has the same model expression of Equations (109), except that vectors there all have reduced dimension $(ML_\Delta) \times 1$. It should be noted that the post-correlation window length $L_\Delta$ was fixed long enough to contain the delay-spread with an

20  enlarged margin for asynchronous time-delay estimation from the reduced-size propagation vector $\underline{H}_n^u$ (reference [20]). Identification with post-correlation windows shorter than $L$, investigated in [6], reduces complexity and proves to work nearly as well as the original full-window version of STAR $(i.e, L_\Delta = L)$.

Channel identification with the MC-CDFI scheme of Equation (110) can be

25  readily implemented using the user-code post-correlation observation vectors $\underline{Z}_n^{u,l}$.

81

However, this procedure would feed back symbol fractions without taking full advantage

of the complete processing gain. Instead, the vectors $\underline{Z}_n^{u,l}$ are regrouped and averaged

in the same way the signal component estimates are restored to their original rate in

Equations (120, (123) or (126), and $\underline{Z}_{nF_u+n'}^u$, $\underline{Z}_n^u$ or $\underline{Z}_{\lfloor n/F_u \rfloor}^u$, respectively[7] are obtained.

5    Hence, the CDFI channel identification procedure, renamed MR-CDFI, is implemented

as follows:

$$\underline{\hat{H}}_{n+1}^u = \underline{\hat{H}}_n^u + \frac{\mu}{F_u}\sum_{n'=0}^{F_u}\left(\underline{Z}_{nF_u+n'}^u - \underline{\hat{H}}_n^u \hat{s}_{nF_u+n'}^u\right)\hat{s}_{nF_u+n'}^u, \tag{132}$$

when the data-rate is faster than the processing rate[8], or by:

10    $$\underline{\hat{H}}_{n+1}^u = \underline{\hat{H}}_n^u + \mu\left(\underline{Z}_n^u - \underline{\hat{H}}_n^u \hat{s}_n^u\right)\hat{s}_n^u, \tag{133}$$

in the particular case where the data rate is equal to the processing rate, or by:

$$\underline{\hat{H}}_{\lfloor n/F_u \rfloor}^u = \underline{\hat{H}}_{\lfloor n/F_u \rfloor}^u + \mu\left(\underline{Z}_{\lfloor n/F_u \rfloor}^u - \underline{\hat{H}}_{\lfloor n/F_u \rfloor}^u \hat{s}_{\lfloor n/F_u \rfloor}^u\right)\hat{s}_{\lfloor n/F_u \rfloor}^u, \tag{134}$$

when the data-rate is slower than the processing rate. It should be noted that channel

identification at data rates faster than the processing gain in Equation (132) has a

15    structure similar to MC-CDFI. Averaging over $F_u$ despread observations there can be

reduced to a smaller subset to gain in complexity like in MC-CDMA. Use of the $\delta$-

CDFI version described in Equations (111) to (113) instead of, or combination with, the

above scheme are other alternatives that reduce the amount of complexity due to

despreading operations.

20        By regrouping codes to match the original data transmission rates as discussed

earlier (see Figure 38), channel identification can be easily reformulated along a mixed

---

[7] In practice, these vectors are computed directly from $Y_n$ in regular despreading
steps which exploit the entire spreading sequences in one step along a mixed MC-CDMA
scheme.

25    [8]Implementation of $F_u$ channel updates (with time-delay tracking) instead of averaging
is computationally more expensive.

MC-CDMA model where each user is characterized by $F_u$ multi-codes and $F_u$ despread vectors $\underline{Z}_n^{u,1},...,\underline{Z}_n^{u,F_u}$, as shown in Figure 39.

To reduce further the number of expensive despreading operations, slower channel identification (reference [20]) can update channel coefficients less frequently if the channel can still show very weak variations over larger update periods. However, high mobility can prevent the implementation of this scheme and faster channel identification update may even be required. For data rates faster than the processing rate, updating at a rate higher than the processing rate is not necessary. The processing period $T$ is chosen to guarantee that the channel parameters are constant over that time interval. For data rates slower than the processing rate, the channel update rate could be increased above the data rate up to the processing rate using Equation (133) and partial despreading to provide $\underline{Z}_n^u$. In Equation (133), $\hat{s}^u_{\lfloor n/F_u \rfloor}$ from Equation (126) should be fed back instead of $\hat{s}^u_n$ to benefit from the entire processing gain in the decision feedback process.

Although the foregoing embodiments of the invention have been described as receiver modules for a base station, *i.e.*, implementing ISR for the uplink, the invention is equally applicable to the downlink, *i.e.*, to receiver modules of user stations.

## *Downlink ISR*

To implement ISR rejection, the user/mobile station needs to identify the group of users (*i.e.*, interferers) to suppress. Assuming temporarily that suppression is restricted to in-cell users, served by base-station $v$, and that the number of suppressed interferers is limited to $NI$ to reduce the number of receivers needed at the desired base-station to detect each of the suppressed users, in order to identify the best users to suppress, the user station can probe the access channels of base-station $v$, seeking the $NI$

83

strongest transmissions. Another scheme would require that the strongest in-cell interfering mobiles cooperate by accessing the first $NI$ channels $(i.e., u = i \in \{1,...,NI\})$ of base-station $v$.

Once the $NI$ suppression channels have been identified, the desired user-station
5 can operate as a "virtual base-station" receiving from $NI$ mobiles on a "virtual uplink". If the desired user is not among the $NI$ interferers, an additional user station is considered. Similar $NI$ channels may be identified for transmissions from the neighbouring base-stations. Accordingly, consideration will be given to the $NB$ base-stations, assigned the index $v' \in \{1,...,NB\}$, which include the desired base-station with
10 index $v' = v$ without loss of generality. This formulation allows the user-station to apply block-processing STAR-ISR with specific adaptations of ISR combining and channel identification to the downlink.

In essence, each "virtual base station" user station would be equipped with a set of receiver modules similar to the receiver modules $21^1,...,21^u$, one for extracting a
15 symbol estimate using the spreading code of that user station and the others using spreading codes of other users to process actual or hypothesized symbol estimates for the signals of those other users. The receiver would have the usual constraints-set generator and constraint matrix generator and cancel ISR in the manner previously described according to the mode concerned.

20 It should be appreciated, however, that the signals for other users emanating from a base station are similar to multicode or multirate signals. Consequently, it would be preferable for at least some of the user station receiver modules to implement the multicode or multirate embodiments of the invention with reference to Figures 34 and 39. Unlike the base station receiver, the user station's receiver modules usually would
25 not know the data rates of the other users in the system. In some cases, it would be

84

feasible to estimate the data rate from the received signal. Where that was not feasible or desired, however, the multirate or multicode receiver modules described with reference to Figures 34 and 39 could need to be modified to dispense with the need to know the data rate.

5          Referring to Figure 40, the user station receiver comprises a plurality of receiver modules similar to those of Figure 39, one for each of the $NB$ base stations whose $NI$ strongest users' signals are to be cancelled, though only receiver module $21^v$ is shown in Figure 38. Recognizing that one or more of those $NI$ signals could be multirate or multicode, and hence involve not only different spreading codes but also different code

10  segmentations, the number of despreaders equals $\sum_{i=1}^{i=NI} F_i$, $i.e.$ $19^{v,1,1},...,$ $19^{v,1,F_1},...,$ $19^{v,i,1},...,$ $19^{v,i,F_i},...,$ $19^{v,NI,1},...,$ $19^{v,NI,F_{NI}}$. In any given base station, the $NI$ users are power-controlled independently and so are received by the mobile/user station with different powers. Consequently, it is necessary to take into account their power separately, so the power estimates from power estimation means $30T^v$ are supplied to

15  the channel estimation unit $28T^v$. The channel identification unit $28T^v$ processes the data in the same way as previously described, spreading the resulting channel estimate $\underline{H}^v_{0,n}$ to form the spread channel estimates $\underline{Y}^{v,1,1}_{0,n},...,$ $\underline{Y}^{v,NI,F_{NI}}_{0,n}$ and supplying them to the ISR beamformers $47T^{v,1,1},...,$ $47T^{v,NI,F_{NI}}$, respectively, for use in processing the observation vector $Y_n$.

20          The resulting signal component estimates $\hat{s}^{v,1,1}_n,...,$ $\hat{s}^{v,NI,F_{NI}}_n$ are similarly fed back to the channel identification unit $28T^v$ to update the channel parameter estimates and to the decision rule units $30T^{v,1,1}, ...,$ $30T^{v,NI,F_{NI}}$ for production of the corresponding symbol estimates $\hat{b}^{v,1,1}_n,...,$ $\hat{b}^{v,NI,F_{NI}}_n$. In all modes except ISR-H, these symbol estimates are supplied to the constraints-set generator, together with the set of

25  channel parameter estimates $\mathcal{H}^v_n$, from channel identification unit $28T^v$ for use in

85

forming the set of constraints $C_n$. The set of channel parameter estimates includes the power estimates from the power estimation units.

If the desired user is not among the $NI$ strong users of the serving base station $v$, the user station receiver will also include a separate receiver module which could be

5 similar to that shown in Figure 39. However, bearing in mind that the channel estimate derived by the receiver modules for the serving base station's strong users in Figure 40 will be for the same channel, but more accurate than the estimate produced by the channel identification unit of Figure 39, it would be preferable to omit the channel identification unit $(29^{F_i})$ and despreaders $19^{d,1}$,..., $19^{d,F_i}$ (Figure 39), and supply the

10 spread channel estimates from the channel identification unit of the receiver module for serving base station $v$, as shown in Figure 41.

The receiver module shown in Figure 40 is predicated upon the data rates of each set of $NI$ users being known to the instant user station receiver. When that is not the case, the receiver module shown in Figure 40 may be modified as shown in Figure 42,

15 $i.e.$, by changing the despreaders to segment the code and oversample at a fixed rate that is higher than or equal to the highest data rate that is to be suppressed.

It is also possible to reduce the number of despreading operations performed by the receiver module of Figure 42 by using a set of compound segment codes as previously described with reference to Figure 35 to compound over segments. However,

20 as shown in Figure 43, a set of different compound codes could be used to compound over the set of $NI$ interferers. It would also be possible to combine the embodiment of Figure 43 with that of Figure 35 and compound over both the set of interferers and each set of code segments.

A desired user station receiver receiving transmissions on the downlink from its

25 base-station and from the base-stations in the neighbouring cells will now be discussed.

Each base-station communicates with the group of user stations located in its cell. Indices $v$ and $u$ will be used to denote a transmission from base-station $v$ destined for user $u$. For simplicity of notation, the index of the desired user station receiving those transmissions will be omitted, all of the signals being implicity observed and processed by that desired user station.

Considering a base-station assigned the index $v$, its contribution to the matched-filtering observation vector $\underline{Y}_n$ of the desired user station is given by the signal vector of the $v$-th base-station $\underline{Y}_n^v$ defined as:

$$\underline{Y}_{u,n}^v = \sum_{u=1}^{U_v} \underline{Y}_{u,n}^{v,u},$$ (135)

where the vector $\underline{Y}_{u,n}^{v,u}$ denotes the signal contribution from one of the $U_v$ users communicating with base-station $v$ and assigned the index $u$. Using the block-processing approach described in the previous section, the vector $\underline{Y}_{u,n}^{v,u}$ can be decomposed as follows:

$$\underline{Y}_n^{v,u} = \psi_n^{v,u} \sum_{l=k}^{N_n} \sum_{k=-1}^{+1} \psi_n^{v,u,l} b_{n+k}^{v,u,l} \zeta_{f,n}^v \underline{Y}_{k,n}^{v,u,l} \Lambda_k^l.$$ (136)

It should be noted that the channel coefficients $\zeta_{f,n}^v$ just hold the index of the base-station $v$. Indeed, transmissions from base-station $u$ to all its mobiles propagate to the desired user station through a common channel. Base-station signals therefore show a multi-code structure at two levels. One comes from the virtual or real decomposition of each user-stream into multiple codes, and one, inherent to the downlink, comes from summation of code-multiplexed user-streams with different powers. As will be described hereinafter, this multi-code structure will be exploited to enhance cooperative channel identification at both levels.

87

In a first step, the desired user-station estimates the multi-code constraint and blocking matrices of each of the processed in-cell users *(i.e., u ∈ {1,...,NI} ∪ {d})*. Table 4 shows how to build these matrices, renamed here as $\hat{C}^{v,u}_{MC,n}$ and $\hat{C}^{v,u,l}_{MC,n}$ to show the index *v* of the serving base-station. Indexing the symbol and channel parameter estimates with *v* in Table 4 follows from Equation (136). In a second step, the user-station estimates the base-specific constraint and blocking matrices $\hat{C}^{v}_{BS,n}$ and $\hat{C}^{v,u,l}_{BS,n}$ using Table 5. These matrices enable suppression of the in-cell interferers using one of the modes described in Table 5. For the downlink, a new mode BR, for base-realization, replaces the TR mode of Table 3. Suppression of interfering signals from multiple base-

10 stations adds another dimension of interference decomposition and results in TR over the downlink as shown in Table 6. Therefore, in a third step the mobile-station estimates the base-specific constraint and blocking matrices $\hat{C}^{v}_{BS,n}$ and $\hat{C}^{v,u,l}_{BS,n}$ from the interfering base-stations and concatenates them row-wise to form the multi-base constraint and blocking matrices denoted as $\hat{C}_{n}$ and $\hat{C}^{v,u,l}_{n}$, respectively. In the TR mode, the base-

15 specific constraint and blocking vectors in the BR mode now are summed over all interfering base-stations, leaving a single constraint. For the other modes, the number of constraints $N_c$ in Table 3 is multiplied by the number of interfering base-stations *NB*. The receiver module dedicated to extracting the data destined to the desired mobile-station *# d* from the serving base station *# v* is depicted in Figure 38.

20     It should be noted that the multi-rate data-streams can be estimated using MRC on the downlink, simply by setting the constraint matrices to null matrices[9]. This option will be termed D-MRC.

---

[9] In this case, ISR processing is not needed and the desired signal is expected to be strong enough to enable reliable channel identification for its own.

88

If the user-station knows[10] the data rates of the suppressed users, it can estimate

their symbols[11] as long as their symbol rate does not exceed the processing rate. As

mentioned hereinbefore, this block-based implementation of the symbol detection

improves reconstruction of the constraint matrices from reduced decision feedback

5    errors[12]. Otherwise, the user-station can process all interfering channels at the common

resolution rate regardless of their transmission rate. It should be noted that estimation

of the interferers' powers is necessary for reconstruction in both the BR and TR modes,

for channel identification as detailed below, and possibly for interference-channel probing

and selection. It is carried out at the processing rate.

10    Identification of the propagation channels from each of the interfering base-

stations to the desired user station is required to carry out the ISR operations.

Considering the in-cell propagation channel, its identification from the post-correlation

vectors of the desired user is possible as described hereinbefore with reference to Figure

39. It exploits the fact that the multi-codes of the desired user propagate through the

15    same channel. However, the in-cell interfering users share this common channel as well.

Therefore, the MC-CDFI and MR-CDFI approaches apply at this level as well. Indeed,

the user-station has access to data channels which can be viewed as $Nl \times N_m$ virtual

pilot-channels with strong powers. It is preferable to implement cooperative channel

identification over the interfering users whether the desired user is among the in-cell

20    [10]Data-rate detection can be implemented using subspace rank estimation over each
stochastic sequence of $N_m$ symbol fractions.

[11] In the ISR-H mode, only the signal component estimates are needed for power and
channel estimation (see next subsection).

[12] Recovery of the interfering symbols at data rates slower than the processing gain
25    could be exploited in slow channel identification. However, selection of a user as a
strong interferer suggests that its transmission rate should be high.

interferers or not. The same scheme applies to the neighbouring base-stations and therefore enables the identification of the propagation channel from each out-cell interfering base-station using its $NI$ interfering users.

If the data rates are known to the base-station, identification of the propagation

5  channel from a given base-station $v' \in \{1,...,NB\}$ can be carried out individually from each of its $NI$ interfering users, as described in the previous section. To further enhance channel identification, the resulting individual channel estimates are averaged over the interfering users. Both steps combine into one as follows:

$$\underline{\hat{H}}_{n+1}^{v'} = \underline{\hat{H}}_{n}^{v'} + \frac{\mu}{\sum\limits_{i=1}^{NI} \left(\psi_{n}^{v',i}\right)^{2}} \sum\limits_{i=1}^{NI} \frac{1}{F_i} \sum\limits_{n'=0}^{F_i} \left(\underline{Z}_{nF_i+n'}^{v',i} - \underline{\hat{H}}_{n}^{u} \hat{s}_{nF_i+n'}^{v',i}\right) \hat{s}_{nF_i+n'}^{v',i}. \tag{137}$$

10

This downlink version of MR-CDFI, referred to as DMR-CDFI, is illustrated in Figure 40. It should be noted that averaging over the interferers takes into account normalization by their total power. To reduce the number of despreading operations, averaging over interferers can be limited to a smaller set ranging between 1 and $NI$.

15  If the data rates of the interfering users are unknown to the user-station, identification can be then carried out along the steps described with reference to Figure 34 to process interfering signals at the common resolution rate as follows:

$$\underline{\hat{H}}_{n+1}^{v'} = \underline{\hat{H}}_{n}^{v'} + \frac{\mu}{N_m \sum\limits_{i=1}^{NI} \left(\psi_{n}^{v',i}\right)^{2}} \sum\limits_{i=1}^{NI} \sum\limits_{l=1}^{N_n} \left(\underline{Z}_{n}^{v',i,l} - \underline{\hat{H}}_{n}^{v'} \hat{s}_{n}^{v',i,l}\right) \hat{s}_{n}^{v',i,l}. \tag{138}$$

20

This downlink version of MC-CDFI, referred to as DMC-CDFI, is illustrated in Figure 42. To reduce the number of despreading operations, averaging over interferers and user-codes can be limited to smaller subsets ranging between 1 and $NI$ and 1 and $N_m$, respectively.

90

An alternative solution that reduces the number of despreading operations utilizes

the following cumulative multi-codes for $l = 1,\ldots,N_m$:

$$c_k^{v',\Sigma,l} = \frac{1}{\sqrt{NI}}\sum_{i=1}^{NI} c_k^{v',i,l}. \tag{139}$$

5

Despreading with these cumulative codes yields:

$$\underline{Z}_n^{v',\Sigma,l} = \underline{H}_n^{v'}\left[\frac{\sum_{i=1}^{NI} s_n^{v',i,l}}{\sqrt{NI}}\right] + \left[\frac{\sum_{i=1}^{NI} \underline{N}_{PCM,n}^{v',i,l}}{\sqrt{NI}}\right] = \underline{H}_n^{v'} s_n^{v',\Sigma,l} + \underline{N}_{PCM,n}^{v',\Sigma,l}. \tag{140}$$

10 Averaging the user-codes over interferers does not reduce noise further after

despreading. However, the composite signal $s_n^{v',\Sigma,l}$ collects an average power from the

$NI$ interferers and therefore benefits from higher diversity. The cumulative multi-codes

can be used to implement channel identification as follows:

$$\underline{\mathcal{H}}_{n+1}' = \underline{\hat{\mathcal{H}}}_n' + \frac{\mu}{N_m\left(\mathcal{V}_n^{v',\Sigma}\right)^2}\sum_{l=1}^{N_m}\left(\underline{Z}_n^{v',\Sigma,l} - \underline{\hat{\mathcal{H}}}_n' s_n^{v',\Sigma,l}\right)s_n^{v',\Sigma,l}, \tag{141}$$

15

where:

$$s_n^{v',\Sigma,l} = \frac{\sum_{i=1}^{NI} s_n^{v',i,l}}{\sqrt{NI}}, \tag{142}$$

20

$$\left(\mathcal{V}_n^{v',\Sigma}\right)^2 = (1-\alpha)\left(\mathcal{V}_{n-1}^{v',\Sigma}\right)^2 + \alpha\frac{\sum_{l=1}^{N_m}\sum_{i=1}^{NI} |s_n^{v',i,l}|^2}{N_m NI}. \tag{143}$$

This downlink version of MC-CDFI, referred to as DSMC-CDFI, is illustrated in Figure

43. Again, averaging over a smaller set of user-codes reduces the number of

25 despreading operations. Use of the δ-CDFI version described in Equations (111) to

91

(113) instead of, or combination with, the above scheme[13], are other alternatives that reduce the amount of complexity due to despreading operations. Their implementation on the downlink is *ad hoc* and follows from the given descriptions.

---

5    [13] Summing user-codes over resolution periods does not increase diversity. However, use of the $\delta$-CDFI version further reduces noise after despreading.

92

TABLE 1

| - | IC Method | $N_c$ | Delay | Robustness to estimation errors of | | | | |
|---|---|---|---|---|---|---|---|---|
| | | | | Timing | Phase | Power | Symbols | |
| PIC | Subtracts reconstructed interference | - | 1+PC | | | | | |
| SIC | Subtracts reconstructed interference of higher power users | - | 1+$NI$ PC | | | | | |
| ISR-H | Nulls reconstructed bits of interfering users | 3$NI$ | 1PC | | ✓ | ✓ | ✓ | |
| ISR-D | Nulls reconstructed interfering diversities | $MPNI$ | 1+1PC | | ✓ | ✓ | | |
| ISR-R | Nulls reconstructed interfering users | $NI$ | 1+1PC | | (some) | ✓ | | |
| ISR-TR | Nulls total reconstructed interference | 1 | 1+1PC | | | (some) | | |
| ISR-TR-S | Nulls total reconstructed interference of higher power users | 1 | 1+$NI$ PC | | | (some) | | |

93

TABLE 2

| | $S_j$ | $j =$ |
|---|---|---|
| ISR-TR | $S_j = \{(u,f,l) \mid u = 1, ..., N_u; f = 1, ..., N_f; l = -1,0,1\}$ | $1$ |
| ISR-R | $S_j = \{(u,f,l) \mid u = j; f = 1, ..., N_f; l = -1,0,1\}$ | $1, ..., N_u$ |
| ISR-H | $S_j = \left\{(u,f,l) \mid u = \lfloor \frac{j-1}{3} \rfloor; f = 1, ..., N_f; l = j - \lfloor \frac{j-1}{3} \rfloor - 1\right\}$ | $1, ..., 3N_u$ |
| ISR-D | $S_j = \left\{(u,f,l) \mid u = \lfloor \frac{j-1}{N_f} \rfloor; f = j - \lfloor \frac{j-1}{N_f} \rfloor; l = -1,0,1\right\}$ | $1, ..., N_f N_u$ |

TABLE 3

94

| | $\hat{C}_n \rightarrow \left[\dfrac{\hat{C}_{n,J}}{\|\hat{C}_{n,J}\|}\right]^{\cdots} \rightarrow \left[\cdots,\hat{C}_{n,J},\cdots\right]^{=}$ | $\hat{C}_n^{l,l'} \rightarrow \left[\dfrac{\hat{C}_{n,J}^{l,l'}}{\|\hat{C}_{n,J}^{l,l'}\|}\right]^{\cdots} \rightarrow \left[\cdots,\hat{C}_{n,J}^{l,l'},\cdots\right]^{=}$ | |
|---|---|---|---|
| | | | $N_c$ |
| TR | $\left[\displaystyle\sum_{i=1}^{NI}\sum_{n=1}^{N_n}\sum_{f=1}^{N_f}\sum_{k=-1}^{+1}\psi_n^i b_{n+k}^{i,l}\xi_f \hat{y}_{f,n-k,n}^{i,l,l}\lambda_k\right]$ | $\left[\displaystyle\sum_{i=1}^{NI}\sum_{n=1}^{N_n}\sum_{f=1}^{N_f}\sum_{k=-1}^{+1}\psi_n^i b_{n+k}^{i,l}\xi_f \hat{y}_{f,n-k,n}^{i,l',0}\delta_{i,l,k}^{l}\lambda_k\right]$ | 1 |
| MCR | $\left[\cdots,\displaystyle\sum_{n=1}^{N_n}\sum_{k=-1}^{+1}b_{n+k}^{i,l}\xi_f \hat{y}_{f,n-k,n}^{i,l,l}\lambda_k,\cdots\right]$ | $\left[\cdots,\displaystyle\sum_{n=1}^{N_n}\sum_{k=-1}^{+1}b_{n+k}^{i,l}\xi_f \hat{y}_{f,n-k,n}^{i,l',0}\delta_{i,l,k}^{l}\lambda_k,\cdots\right]$ | NI |
| MCD | $\left[\cdots,\displaystyle\sum_{n=1}^{N_n}\sum_{k=-1}^{+1}b_{n+k}^{i,l}\hat{y}_{f,n-k,n}^{i,l,l}\lambda_k,\cdots\right]$ | $\left[\cdots,\displaystyle\sum_{n=1}^{N_n}\sum_{k=-1}^{+1}b_{n+k}^{i,l}\hat{y}_{f,n-k,n}^{i,l',0}\delta_{i,l,k}^{l}\lambda_k,\cdots\right]$ | $N_f NI$ |

5

95

| | | | |
|---|---|---|---|
| R | $\left[\ldots,\ \sum_{j=1}^{N_j}\sum_{k=-1}^{+1} b_{n+k}^{i,l}\,\xi_k^{i,l}\,\varsigma_{f,n-k,n}^{i,l}\,\lambda_k^l,\ \ldots\right]$ | $\left[\ldots,\ \sum_{j=1}^{N_j}\sum_{k=-1}^{+1} b_{n+k}^{i,l}\,\xi_k^{i,l}\,\varsigma_{f,n-k,n}^{i,l}\,\bar{\delta}_{i,l,k}^{i',l',0}\,\lambda_k^l,\ \ldots\right]$ | $N_mNl$ |
| D | $\left[\ldots,\ \sum_{k=-1}^{+1} b_{n+k}^{i,l}\,\varsigma_{f,n-k,n}^{i,l}\,\lambda_k^l,\ \ldots\right]$ | $\left[\ldots,\ \sum_{k=-1}^{+1} b_{n+k}^{i,l}\,\varsigma_{f,n-k,n}^{i,l}\,\bar{\delta}_{i,l,k}^{i',l',0}\,\lambda_k^l,\ \ldots\right]$ | $N_jN_mNl$ |
| H | $\left[\ldots,\ \sum_{j=1}^{N_j}\varsigma_{f,n-k,n}^{i,l}\,\lambda_k^l,\ \ldots\right]$ | $\left[\ldots,\ \sum_{j=1}^{N_j}\varsigma_{f,n-k,n}^{i,l}\,\bar{\delta}_{i,l,k}^{i',l',0}\,\lambda_k^l,\ \ldots\right]$ | $N_HNl$ |

TABLE 3

Table 3 shows common constraint and blocking matrices $\mathcal{C}_n$ and $\mathcal{C}_n^{i',l'}$, respectively, and the corresponding number of constraints or columns $N_c$ for each ISR mode: Generic columns are shown before normalization and $\bar{\delta}_{i,l,k}^{i',l',k'} = 0$ if $(i,l,k) = (i',l',k')$ and 1 otherwise. In the conventional MC case, $\lambda_k^l = 1$ and $N_H = 3N_m$. In the MR case modeled as MC-CDMA, $\lambda_k^l = 0$ if $k = -1$ and $l \in \{1, \ldots, N_r\}$ or if $k = +1$ and $l \in \{N_m - N_r + 1, \ldots, N_m\}$, and 1 otherwise. In the H mode, $2(N_m - N_r)$ columns or more in $\mathcal{C}_n$ are null. These columns and the corresponding ones in $\tilde{\mathcal{C}}_n^{i',l'}$ are removed leaving a maximum of $N_H = N_m + 2N_r$ constraints.

TABLE 4

| | $\mathcal{C}_{MCn}^{\mu}$ | $\mathcal{C}_{MCn}^{\mu,l}$ | |
|---|---|---|---|
| | $\uparrow$ | $\uparrow$ | |
| | $\left[\cdots \dfrac{\Pi_n \hat{\mathcal{C}}_{n,j}}{\|\Pi_n \hat{\mathcal{C}}_{n,j}\|}\right]$ | $\left[\cdots \dfrac{\Pi_n \hat{\mathcal{C}}_{n,j}^{l}}{\|\Pi_n \hat{\mathcal{C}}_{n,j}^{\mu}\|}\right]$ | |
| | $\uparrow$ | $\uparrow$ | |
| | $\left[\cdots \hat{\mathcal{C}}_{n,j}^{\mu} \cdots\right]$ | $\left[\cdots \hat{\mathcal{C}}_{n,j}^{\mu,l} \cdots\right]$ | |
| MCR | $\left[\cdots, \displaystyle\sum_{f=1}^{N_n}\sum_{f=1}^{N_f}\sum_{k=1}^{+1} b_{n+k}^{\mu,l}\, \hat{\zeta}_{f,n-k,n}^{\mu}\, \hat{\gamma}_{k,n}^{\mu,l}\, \lambda_k^{l}\right]$ | $\left[\cdots, \displaystyle\sum_{l=1}^{N_n}\sum_{f=1}^{N_f}\sum_{k=1}^{+1} b_{n+k,n}^{\mu,l}\, \hat{\zeta}_{f,n-k,n}^{\mu}\, \hat{\gamma}_{k,n}^{\mu,l}\, \hat{\sigma}_{l,k}^{l,0}\, \lambda_k^{l}\right]$ | $N_c$ |
| MCD | $\left[\cdots, \displaystyle\sum_{l=1}^{N_n}\sum_{k=1}^{+1} b_{n+k,n}^{\mu,l}\, \hat{\gamma}_{k,n}^{\mu,l}\, \lambda_k^{l}, \cdots\right]$ | $\left[\cdots, \displaystyle\sum_{l=1}^{N_n}\sum_{k=1}^{+1} b_{n+k,n}^{\mu,l}\, \hat{\gamma}_{k,n}^{\mu,l}\, \hat{\sigma}_{l,k}^{l,0}\, \lambda_k^{l}, \cdots\right]$ | 1 |
| | | | $N_f$ |
| R | $\left[\cdots, \displaystyle\sum_{f=1}^{N_f}\sum_{k=1}^{+1} b_{n+k,n}^{\mu,l}\, \hat{\zeta}_{f,n-k,n}^{\mu}\, \hat{\gamma}_{k,n}^{\mu,l}\, \lambda_k^{l}, \cdots\right]$ | $\left[\cdots, \displaystyle\sum_{f=1}^{N_f}\sum_{k=1}^{+1} b_{n+k,n}^{\mu,l}\, \hat{\zeta}_{f,n-k,n}^{\mu}\, \hat{\gamma}_{k,n}^{\mu,l}\, \hat{\sigma}_{l,k}^{l,0}\, \lambda_k^{l}, \cdots\right]$ | $N_m$ |

96

5

97

## TABLE 4

| | $\mathcal{C}_{MC,n}^{u}$ | $\mathcal{C}_{MC,n}^{u,l'}$ | |
|---|---|---|---|
| D | $\left[\cdots, \sum_{k=-1}^{+1} b_{n+k}^{u,l} \Upsilon_{k,n}^{u,l} \lambda_k^l, \cdots\right]$ | $\left[\cdots, \sum_{k=-1}^{+1} b_{n+k}^{u,l} \Upsilon_{k,n}^{u,l} \overline{\delta}_{l,k}^{l',0} \lambda_k^l, \cdots\right]$ | $N_f N_m$ |
| H | $\left[\cdots, \sum_{j=1}^{N_f} \varsigma_{j,n}^{u} \Upsilon_{j,n}^{u,l} \lambda_k^l, \cdots\right]$ | $\left[\cdots, \sum_{j=1}^{N_f} \varsigma_{j,n}^{u} \Upsilon_{j,n}^{u,l} \overline{\delta}_{l,k}^{l',0} \lambda_k^l, \cdots\right]$ | $N_H$ |

Table 4 shows multi-code constraint and blocking matrices $\mathcal{C}_{MC,n}^{u}$ and $\mathcal{C}_{MC,n}^{u,l'}$, respectively, and the corresponding number of constraints or columns $N_c$ for each ISR mode: Generic columns are shown before projection and normalization and $\overline{\delta}_{l,k}^{l',k'} = 0$ if $(l,k) = (l',k')$ and 1 otherwise. In the conventional MC case, $\lambda_k^l = 1$ and $N_H = 3N_m$. In the MR case modeled as MC-CDMA, $\lambda_k^l = 0$ if $k = -1$ and $l \in \{1, ..., N_r\}$ or if $k = +1$ and $l \in \{N_m - N_r + 1, ..., N_m\}$, and 1 otherwise. In the H mode, $2(N_m - N_r)$ columns in $\mathcal{C}_{MC,n}^{u}$ are null. These columns and the corresponding ones in $\mathcal{C}_{MC,n}^{u,l'}$ are removed leaving a maximum of $N_H = N_m + 2N_r$ constraints.

TABLE 5

| | BR |
|---|---|
| 5    $\hat{C}^{v}_{BS,n} \Leftarrow$ | $\left[ \displaystyle\sum_{u=1}^{NI} \psi_n^{v,u} \sum_{l=1}^{N_m} \sum_{f=1}^{N_f} \sum_{k=-1}^{+1} \hat{b}^{v,i,l}_{n+k} \hat{\zeta}^{v}_{f,n} \underline{\hat{Y}}^{v,i,l,f}_{k,n} \lambda^l_k \right]$ |
| $\hat{C}^{v,i',l'}_{BS,n} \Leftarrow$ | $\left[ \displaystyle\sum_{u=1}^{NI} \psi_n^{v,u} \sum_{l=1}^{N_m} \sum_{f=1}^{N_f} \sum_{k=-1}^{+1} \hat{b}^{v,i,l}_{n+k} \hat{\zeta}^{v}_{f,n} \underline{\hat{Y}}^{v,i,l,f}_{k,n} \bar{\delta}^{i',l',0}_{i,l,k} \lambda^l_k \right]$ |
| $N_c$ | 1 |

10                     TABLE 5

Table 5 shows base-specific constraint and blocking matrices $\hat{C}^{v}_{BS,n}$ and $\hat{C}^{v,i',l'}_{BS,n}$ which will apply to the modes shown in Table 3 except for TR, replaced by BR. Indices of remaining modes in Table 3 should be modified to include the index of the base-station $v$ as shown for the TR mode. It should be noted that channel coefficients $\hat{\zeta}^{u}_{f,n}$ hold the

15   index of the base-station $u$ instead of the user $i$. Transmissions to all user-stations from base-station $u$ propagate to the desired user station through a common channel. It should also be noted that summation over users is weighted by the estimate of the total amplitude due to user-independent power control. Definitions of $\bar{\delta}^{i',l',0}_{i,l,k}$ and $\lambda^l_k$ are given in Table 3.

20

TABLE 6

| | TR |
|---|---|
| 25   $\hat{C}_n \Leftarrow$ | $\left[ \displaystyle\sum_{v=1}^{NB} \sum_{U=1}^{NI} \psi_n^{v,u} \sum_{l=1}^{N_m} \sum_{f=1}^{N_f} \sum_{k=-1}^{+1} \hat{b}^{v,i,l}_{n+k} \hat{\zeta}^{v}_{f,n} \underline{\hat{Y}}^{v,i,l,f}_{k,n} \lambda^l_k \right]$ |
| $\hat{C}^{v',i',l'}_n \Leftarrow$ | $\left[ \displaystyle\sum_{v=1}^{NB} \sum_{u=1}^{NI} \psi_n^{v,u} \sum_{l=1}^{N_m} \sum_{f=1}^{N_f} \sum_{k=-1}^{+1} \hat{b}^{v,i,l}_{n+k} \hat{\zeta}^{v}_{f,n} \underline{\hat{Y}}^{v,i,l,f}_{k,n} \bar{\delta}^{v',i',l',0}_{v,i,l,k} \lambda^l_k \right]$ |

99

| $N_c$ | 1 |
|---|---|
|  | BR |
| $\hat{C}_n =$ | $\left[ \dots, \sum_{u=1}^{NI} \psi_n^{v,u} \sum_{l=1}^{N_m} \sum_{f=1}^{N_f} \sum_{k=-1}^{+1} \hat{b}_{n+k}^{v,i,l} \hat{s}_{f,n}^{v} \hat{Y}_{k,n}^{v,i,l,f} \lambda_k^l \right]$ |
| $\hat{C}_n^{v',i',l'} =$ | $\left[ \dots, \sum_{u=1}^{NI} \psi_n^{v,u} \sum_{l=1}^{N_m} \sum_{f=1}^{N_f} \sum_{k=-1}^{+1} \hat{b}_{n+k}^{v,i,l} \hat{s}_{f,n}^{v} \hat{Y}_{k,n}^{v,i,l,f} \overline{\delta}_{v,i,l,k}^{v',i',l',0} \lambda_k^l, \dots \right]$ |
| $N_c$ | NB |

TABLE 6

Table 6 shows multi-base constraint and blocking matrices $\hat{C}_n$ and $\hat{C}_n^{v',i',l'}$ which apply to the modes of Table 3 by row-wise aligning the constraint and blocking matrices $\hat{C}_{BS,n}$ and $\hat{C}_{BS,n}^{v',i',l'}$ from base-stations into larger matrices $\hat{C}_n$ and $\hat{C}_n^{v',i',l'}$ in the way suggested by Equations (104) and (105). The number of constraints in Table 5 is multiplied by $NB$ as shown here for the BR mode. The additional TR mode sums the constraint-vectors of the BR mode over all base-stations. The definition of $\lambda_k^l$ is given in Table 3 and $\overline{\delta}_{v,i,l,k}^{v',i',l',l'} = 0$ if $(v,i,l,k) = (v', i', l', k')$ and 1 otherwise.

It should be appreciated that, when ISR is used for the downlink, it will function where the mobile station has a single antenna.

Embodiments of the invention are not limited to DBPSK but could provide for practical implementation of ISR in mixed-rate traffic with MPSK or MQAM modulations without increased computing complexity. Even orthogonal Walsh signalling can be implemented at the cost of a computational increase corresponding to the number of Walsh sequences.

It should also be noted that, although the above-described embodiments are asynchronous, a skilled person would be able to apply the invention to synchronous systems without undue experimentation.

100

It should be appreciated that the decision rule units do not have to provide a binary output; they could output the symbol and some other signal state.

The invention comprehends various other modifications to the above-described embodiments. For example, long *PN* codes could be used, as could mixed rate or mixed modulations, large delay-spreads and large inter-user delay-spreads. Also, the invention can be used in CDMA systems employing pilot signals.

101

REFERENCES

For further information, the reader is directed to the following documents, the contents of which are incorporated herein by reference.

5   1.   F. Adachi, M.Sawahashi and H. Suda, "Wideband DS-CDMA for next generation mobile communications systems", IEEE communications Magazine, vol. 36, No. 9, pp. 55-69, September 1998.

2.   A. Duell-Hallen, J. Holtzman, and Z. Zvonar, "Multiuser detection for CDMA
10       systems", *IEEE Personal Communications*, pp. 46-58, April 1995.

3.   S. Moshavi, "Multi-user detection for DS-CDMA communications", *IEEE Communications Magazine*, pp. 124-136, October 1996.

15  4.   S. Verdu, "Minimum probability of error for asynchronous Gaussian multiple-access channels", *IEEE Trans. on Information Theory*, vol. 32, no. 1, pp. 85-96, January 1986.

5.   K.S. Schneider, "Optimum detection of code division multiplexed signals", *IEEE*
20       *Trans. on Aerospace and Electronic Systems*, vol. 15, pp. 181-185, January 1979.

6.   R. Kohno, M. Hatori, and H. Imai, "Cancellation techniques of co-channel interference in asynchronous spread spectrum multiple access systems",
25       *Electronics and Communications in Japan*, vol. 66-A, no. 5, pp. 20-29, 1983.

7.   Z. Xie, R.T. Short, and C.K. Rushforth, "A family of suboptimum detectors for coherent multi-user communications", *IEEE Journal on Selected Areas in Communications*, vol. 8, no. 4, pp. 683-690, May 1990.
30

8.   A.J. Viterbi, "Very low rate convolutional codes for maximum theoretical performance of spread-spectrum multiple-access channels", *IEEE Journal of Selected Areas in Communications*, vol. 8, no. 4, pp. 641-649, May 1990.

102

9.    M.K. Varanasi and B. Aazhang, "Multistage detection in asynchronous code-division multiple-access communications", *IEEE Trans. on Communications*, vol. 38, no. 4, pp. 509-519, April 1990.

5   10.   R. Kohno et al, "Combination of an adaptive array antenna and a canceller of interference for direct-sequence spread-spectrum multiple-access system", *IEEE Journal on Selected Areas in Communications*, vol. 8, no. 4, pp. 675-682, May 1990.

10  11.   A. Duell-Hallen, "Decorrelating decision-feedback multi-user detector for synchronous code-division multiple-access channel", *IEEE Trans. on Communications*, vol. 41, no. 2, pp. 285-290, February 1993.

12.   A. Klein, G.K. Kaleh, and P.W. Baier, "Zero forcing and minimum mean-
15    square-error equalization for multi-user detection in code-division multiple-access channels", *IEEE Trans. on Vehicular Technology*, vol. 45, no. 2, pp. 276-287, May 1996.

13.   S. Affes and P. Mermelstein, "A new receiver structure for asynchronous CDMA
20    : STAR - the spatio-temporal array-receiver", *IEEE Journal on Selected Areas in Communications*, vol. 16, no. 8, pp. 1411-1422, October 1998.

14.   S. Affes, S. Gazor, and Y. Grenier, "An algorithm for multisource beamforming and multitarget tracking", *IEEE Trans. on Signal Processing*, vol. 44, no. 6, pp.
25    1512-1522, June 1996.

15.   P. Patel and J. Holtzman, "Analysis of a simple successive interference cancellation scheme in a DS/CDMA system", *IEEE Journal on Selected Areas in Communications*, vol. 12, no. 5, pp. 796-807, June 1994.

30
16.   J. Choi, "Partial decorrelating detection for DS-CDMA systems", *Proceedings of IEEE PIMRC '99*, Osaka, Japan, vol. 1, pp. 60-64, September 12-15, 1999.

103

17.    S. Affes and P. Mermelstein, "Signal Processing Improvements for Smart Antenna Signals in IS-95 CDMA", Proceedings of *IEEE PIMRC '98*, Boston, U.S.A., Vol. II, pp. 967-972, September 8-11, 1998.

5  18.    S. Affes and P. Mermelstein, "Performance of a CDMA beamforming array-receiver in spatially-correlated Rayleigh-fading multipath", *Proc. of IEEE VTC'99*, Houston, USA, May 16-20, 1999.

19.    H. Hansen, S. Affes and P. Mermelstein, "A beamformer for CDMA with
10    enhanced near-far resistance", *Proc. of IEEE ICC'99*, Vancouver, Canada, Vol. 3, pp. 1583-1587, June 6-10, 1999.

20.    K. Cheikhrouhou, S. Affes, and P. Mermelstein, "Impact of synchronization on receiver performance in wideband CDMA networks", *Proc. 34th Asilomar*
15    *Conference on Signals, and Computers*, Pacific Grove, USA, to appear, October 29-November 1, 2000.

21.    S. Affes, A. Louzi, N. Kandil, and P. Mermelstein, "A high capacity CDMA array-receiver requiring reduced pilot power", *Proc. of IEEE GLOBECOM*
20    *'2000*, San Francisco, USA, to appear, November 27-December 1, 2000.

22.    S. Affes, H. Hansen, and P. Mermelstein, "Interference subspace rejection in wideband CDMA - part I: Modes for mixed power operation", *to be submitted.*

25  23.    H. Hansen, S. Affes, and P. Mermelstein, "Interference subspace rejection in wideband CDMA - part II: Modes for high data-rate operation", *to be submitted.*

24.    E.H. Dinan and B. Jabbari, "Spreading codes for direct sequence CDMA and wideband CDMA cellular networks", *IEEE Communications Magazine*, vol. 36,
30    no. 9, pp. 48-54, September 1998.

104

25.  R. Lupas and S. Verdu, "Near-far resistance of multiuser detectors in asynchronous channels", *IEEE Trans. on Communications*, vol 38, no. 4, pp.496-508, April 1990.

26.  A. Duell-Hallen, "A family of multiuser decision-feedback detectors for asynchronous code-division multiple-access channels", *IEEE Trans. on Communications*, vol. 43, no. 5, pp. 796-807, June 1994.

27.  C. Schlegel, P. Alexander, and S. Roy, "Coded asynchronous CDMA and its efficient detection", *IEEE Trans. on Information Theory*, vol. 44, no. 7, pp. 2837-2847, November 1998.

28.  L.K. Rasmussen, T.J. Lim, and A.-L. "A matrix-algebraic approach to successive interference cancellation in CDMA", *IEEE Trans. on Communications*, vol. 48, no. 1, pp. 145-151, January 2000.

29.  M. Latva-aho and M.J. Juntti, "LMMSE detection for DS-CDMA systems in fading channels, *IEEE Trans. on Communications*, vol. 48, no. 2, pp. 194-199, February 2000.

105

CLAIMS:

1.    A receiver suitable for either a base station or a user station of a CDMA communications system comprising at least one base station (11) and a plurality of user stations ($10^1...10^U$) each communicating with said at least one base station via a
5    corresponding one of a plurality of channels, said base station and each user station having a transmitter and a said receiver, the receiver receiving a signal comprising components corresponding to signals from the different transmitters of the base station and/or user stations and comprising processing means (18) for deriving an observation matrix from the received signal, the receiver comprising a plurality of receiver modules
10  (21) each comprising means (19) for deriving from the observation matrix one or both of a corresponding observation vector and post-correlation observation vector and a beamformer for processing one or other of the observation vector and the post-correlation observation vector to provide estimates of symbols transmitted by a corresponding user station, and means (42,43) for providing at least one constraint
15  matrix representing interference subspace of components of the received signal corresponding to selected ones of the user signals of the plurality of receiver modules, at least one ($21^d$) of said plurality of receiver modules having means ($28^d$) responsive to at least the post-correlation observation vector for deriving an estimate of the channel parameters for the channel between the receiver and the corresponding transmitter, and
20  a beamformer ($47^d$) for processing one or other of the observation vector and the post-correlation observation vector to produce estimates of the symbols transmitted by said transmitter, the beamformer having means for adjusting coefficients of the beamformer in dependence upon the constraint matrix and the channel estimate so as to tune the beamformer to provide a substantially unity response for that portion of the received
25  signal from the corresponding transmitter and a substantially null response to that portion of the received signal corresponding to predetermined ones of other user signals and/or base station signals also received by the receiver.

2.    A receiver for either a base station of a CDMA communications system in which
30  a plurality of user stations ($10^1...10^U$) each having an antenna array comprising one or more antennas communicate with a base station (11) having an antenna array (12) comprising one or more reception antennas ($12^1...12^M$), each of the user stations having spreading means ($13^1...13^U$) for using a spreading code ($c^1(t)...c^U(t)$) unique to that

station to spread a corresponding one of a plurality of user signals $(b^1_n...b^U_n)$ and means for transmitting the spread user signals to the base station antenna array (12) via a propagation channel $(14^1...14^U)$ unique to that user station,

the receiver comprising preprocessing means (18) and a plurality of receiver

5     modules $(21^1...21^U)$ having their respective inputs connected in common to an output of the preprocessing means (18) and each corresponding to a respective one of the user stations,

the preprocessing means (18) being arranged to receive from the antenna array an antenna array signal vector $(X(t))$ comprising a plurality of spread data

10     vectors $(X^1(t)...X^U(t))$ corresponding to the signals from the different user stations received by the reception antenna array and having means for filtering, sampling and buffering the antenna array signal vector $(X(t))$ to produce a succession of observation matrices $(Y_n)$, and supplying the observation matrices $(Y_n)$ to each of the receiver modules $(21^1...21^U)$;

15     each of the receiver modules $(21^1...21^U)$ comprising a despreader $(19^u)$, a channel identification means $(28^u)$, a beamformer $(27^u)$ and output means $(29^u, 30^u)$,

the despreader $(19^u)$ being arranged to despread each observation matrix using the spreading code of the corresponding user to form a post-correlation observation vector $(\underline{Z}_n)$ and the channel identification means $(28^u)$ being arranged to derive from the

20     post-correlation observation vector a set of estimated channel parameters $(\underline{\hat{H}}^u_n)$ for the channel whereby the signal from the corresponding user station reached the antenna array,

the beamformer $(27^u)$ having means (51) for weighting each of the elements of each observation vector in turn using weighting coefficients $(W^d_n)$, tuning means (50)

25     for adjusting the weighting coefficients $(W^d_n)$ in dependence upon at least said estimated channel parameters, and means (52) for combining the weighted elements to produce a respective symbol of a corresponding one of a plurality of output signals $(\hat{b}^1_n...\hat{b}^U_n)$ corresponding to the plurality of user signals $(b^1_n...b^U_n)$, respectively,

the receiver further comprising constraints-set generation means (42) responsive

30     to a set of channel parameter estimates and either or both of an actual value of the symbol from at least one of the beamformers and at least one hypothetical symbol value for deriving a constraints-set,      constraint matrix generation means (43) responsive

107

to said constraints-set to form at least one constraint matrix and for generating an inverse matrix by inverting the constraint matrix and conjugating it with itself;

the respective tuning means of at least some of the beamformers being responsive to said at least one constraint matrix to adjust the weighting coefficients $(\mathcal{S}_n^d)$ of their

5 respective beamformers such that, in successive symbol periods, the coefficients of each of said at least some of the beamformers are adjusted so as to tune a substantially unity response for that portion of the antenna array signal vector corresponding to the user signal from the corresponding user station and a substantially null response to that portion of the antenna array signal vector corresponding to the user signals received from

10 those user stations corresponding to the receiver modules which contribute a constraint waveform to the constraint matrix generation means;

the output means of each receiver module being responsive to the output of the corresponding beamformer for providing estimates of the symbols of the corresponding user signal.

15

3. A receiver according to claim 1 or 2, wherein:-

the receiver further comprises means (44) for reshaping each of the observation matrices to form an observation vector;

the ISR beamformer operates upon the observation vectors,

20 the channel estimation unit supplies spread channel parameters to the beamformer for use in updating its coefficients;

the constraint matrix generator supplies user-specific observation matrices to the constraint matrix generator; and

the constraint matrix generator comprises means for reshaping each user-specific

25 observation matrix to form a respective one of a plurality of columns of the constraint matrix and supplies the resulting constraint matrix to each of the desired user stations. (Fig. 9)

4. A receiver according to claim 1 or 2, wherein:

30 the constraints-set generator (42C) comprises a plurality of respreaders (57C etc) each for respreading a respective one of the estimated symbols from the STAR units, means (58C etc) for scaling each of the respread symbol estimates by the amplitude of the corresponding estimated symbol, and a plurality of channel replication means (59C)

108

having coefficients adjustable in dependence upon the channel coefficient estimate for filtering the corresponding respread and scaled symbol estimate to provide a user-specific observation matrix estimate and means for summing the user-specific observation matrices and supplying the observation matrix estimate so obtained to the constraint

5 matrix generator, the constraint matrix generator comprising means (43C) for reshaping the estimated observation matrix to form a single column constraint matrix and supplying the constraint matrix to the beamformer.

(ISR-TR Fig. 13)

10 5.    A receiver according to claim 1 or 2, wherein the

constraints-set generator (42E) comprises respreaders (57D) and channel replicators (59D), the set of observation matrices are supplied to the constraint matrix generator (43D) which reshapes each matrix to form one column of the constraint matrix.

(ISR-R Fig. 15)

15

6.    A receiver according to claim 1 or 2, wherein the channel identification unit generates an estimate of each of a plurality of sub-channels of the propagation channel and the channel replicator produces a set of observation matrices comprising one for each of said sub-channels.

20 (ISR-D Fig. 16)

7.    A receiver according to claim 1 or 2, wherein the constraints-set generator uses hypothetical values of said symbols to produce said set of user-specific observation matrices.

25 (ISR-H Fig. 17)

8.    A receiver according to claim 1 or 2, wherein the constraints-set

uses a combination of estimated symbol values and hypothetical symbol values in producing said set of user-specific observation matrices.

30 (ISR-RH Fig. 20)

109

9.    A receiver according to any one of claims 3 to 8, wherein the beamformer operates upon the post-correlation observation vector and the constraint matrix generator comprises means for despreading each of the user-specific observation matrices. (Figs. 21, 22, 23, 24, 26 - AD)

5

10.    A receiver according to claim 1, wherein the ISR receiver module employs both an MRC beamformer and an ISR beamformer.

11.    A receiver according to claim 1, wherein the receiver module employs group ISR.

10

12.    A receiver according to claim 1, comprising a plurality of receiver modules arranged adapted to perform successive ISR, the receiver modules being arranged in hierarchical order according to signal power and each lower power receiver module using a constraint matrix formed from the constraints supplied by each of the higher power

15  receiver modules.

13.    A receiver according to claim 1, wherein the ISR receiver module is adapted to receive multicode signals and the despreader comprises means for despreading the observation matrix using a plurality of codes corresponding to the multicodes.

20

14.    A receiver according to claim 12, wherein the despreader uses a compound code formed by weighting the multicodes with the corresponding estimated symbols.

15.    A receiver according to claim 1, wherein the receiver module performs multirate

25  ISR.

16.    A receiver according to any one of claims 11 to 15, wherein the receiver is located at a user/mobile station and receives signals from a plurality of base stations.

30

Mobile
station # 1

Mobile
station # d

Mobile
station # u

Mobile
station # i

Mobile
station # U

$10^1$
$10^d$
$10^u$
$10^i$
$10^U$

$14^1$
$14^d$
$14^u$
$14^i$
$14^U$

Channel $\psi_{ch}^u(t)H^u(t)$

path #1
path #p
path #P

path #1
path #p
path #P

$\psi_{ch}^u(t)G_p^u(t)\varepsilon_p^u(t)\delta(t - \tau_p^u(t))$

antenna #1

antenna #M

$12^1$

$12^M$

$11$

Base
station

FIG. 1

FIG. 2

$13^u$

$$b_n^u \xrightarrow{\quad} \bigotimes \xrightarrow{\quad} \boxed{\begin{array}{c} \text{Chip pulse} \\ \phi(t) \end{array}} \xrightarrow{\quad} b^u(t)c^u(t)$$

$c_i^u$

FIG. 3



$13^u$     $\psi_{pc}^u(t)$     $14^u$

$$b_n^u \xrightarrow{\quad} \boxed{\begin{array}{c} \text{Spreader} \\ \# \, u \end{array}} \xrightarrow{\quad 17^u} \bigotimes \xrightarrow{\quad} \boxed{\begin{array}{c} \text{Channel} \\ \psi_{ch}^u(t)H^u(t) \end{array}} \xrightarrow{\quad} X^u(t)$$

$M$

FIG. 4(a)     $\equiv$

$13^u$     $\psi^u(t) = \psi_{pc}^u(t)\psi_{ch}^u(t)$     $14^u$

$$b_n^u \xrightarrow{\quad} \boxed{\begin{array}{c} \text{Spreader} \\ \# \, u \end{array}} \xrightarrow{\quad} \bigotimes \xrightarrow{\quad} \boxed{\begin{array}{c} \text{Channel} \\ H^u(t) \end{array}} \xrightarrow{\quad} X^u(t)$$

$17^u$     $M$

FIG. 4(b)

FIG. 4

FIG. 5   PRIOR ART

$X(t)$
$M \times 1$

22

Matched pulse
$\phi(T_c - t)$

$Y(t)$
$M \times 1$

13

Sampler
rate $1/T_c$

$Y_{n,l}$
$M \times 1$

24

Buffer
$M \times (2L-1)$

$\mathbf{Y}_n$
$M \times (2L-1)$

18

FIG. 6

$\mathbf{Y}_n$
$M \times (2L-1)$

25$^u$

Filter
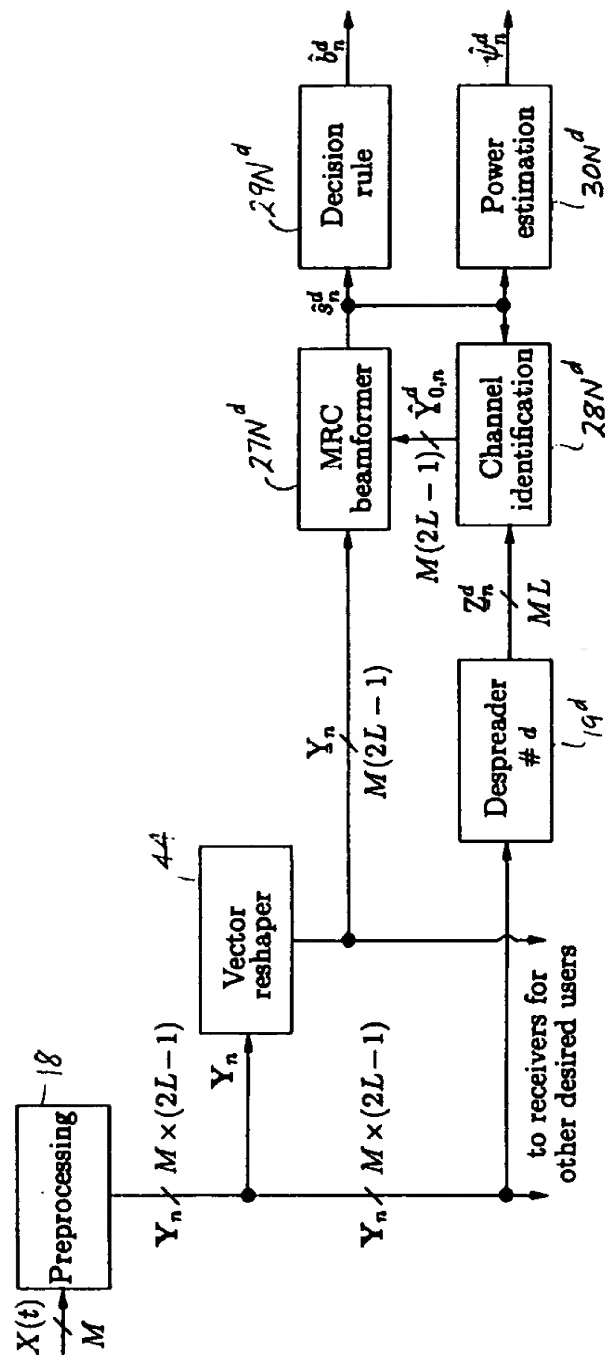$c_{L-l}^u$
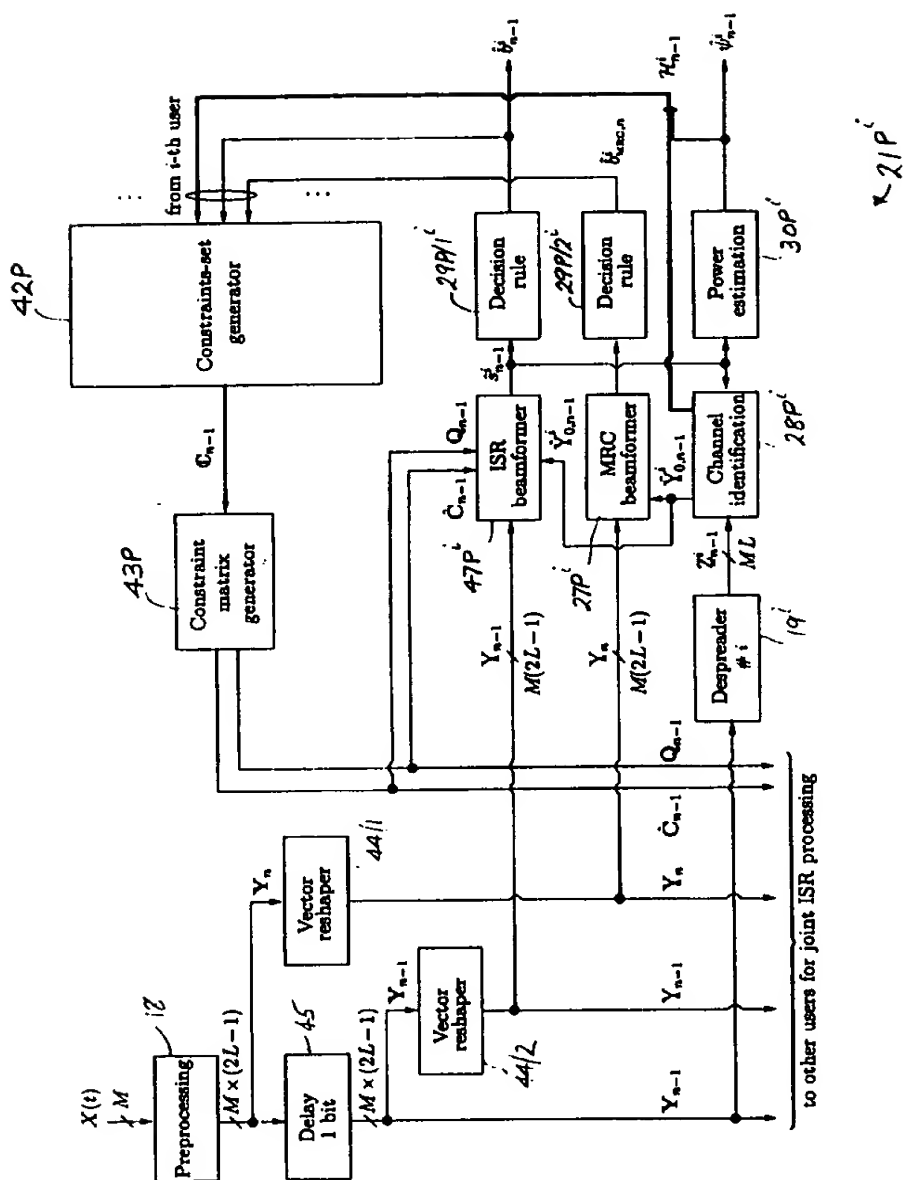
$\mathbf{Z}_n^u$
$M \times L$

26$^u$

Vector
reshaper

$\underline{Z}_n^u$
$ML \times 1$

19$^u$

FIG. 7

FIG. 8

FIG. 9

FIG. 10

FIG. 11

FIG. 12

FIG. 13

$57^u$

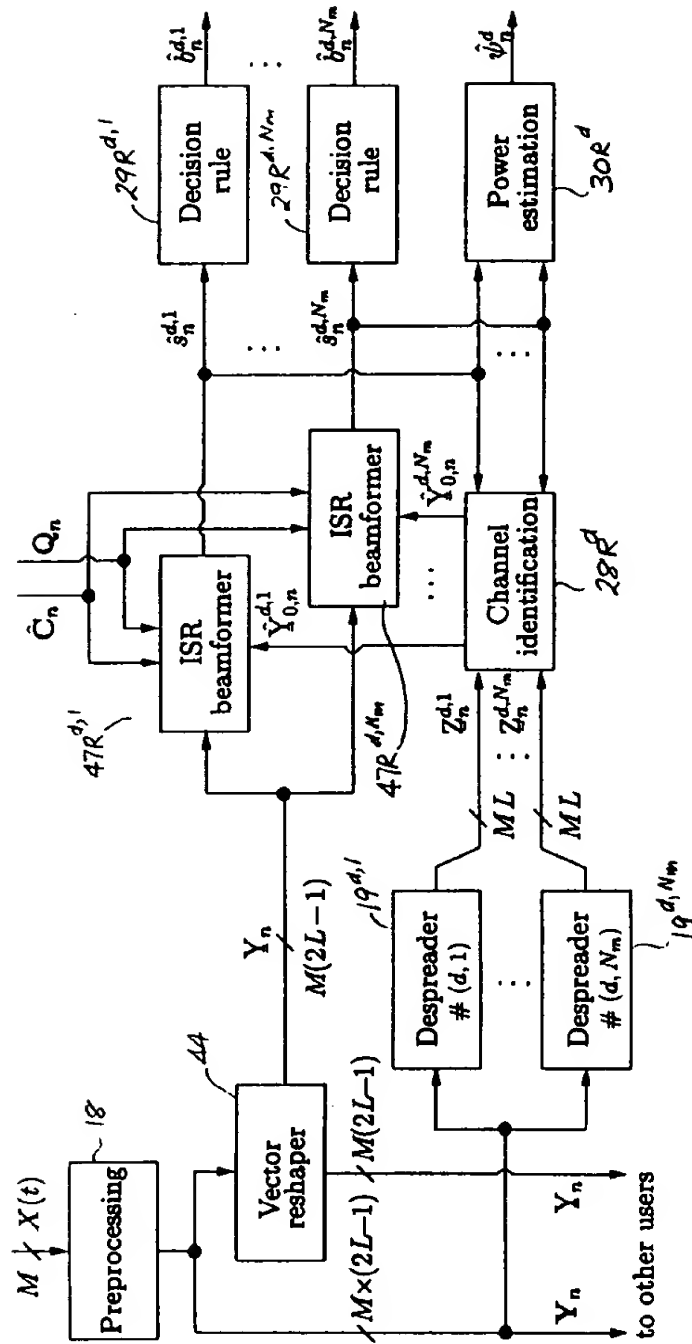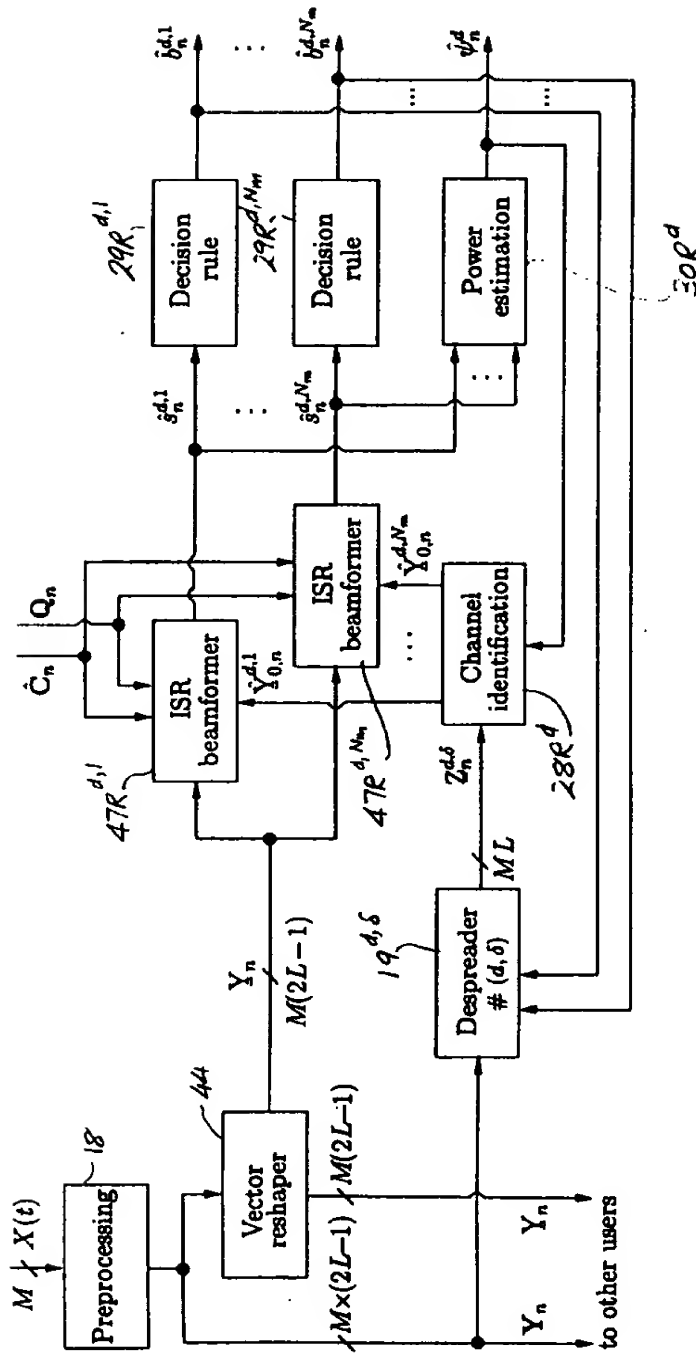$$\hat{b}_n^u \longrightarrow \otimes \xrightarrow{\quad} \hat{b}_n^u c_l^u$$
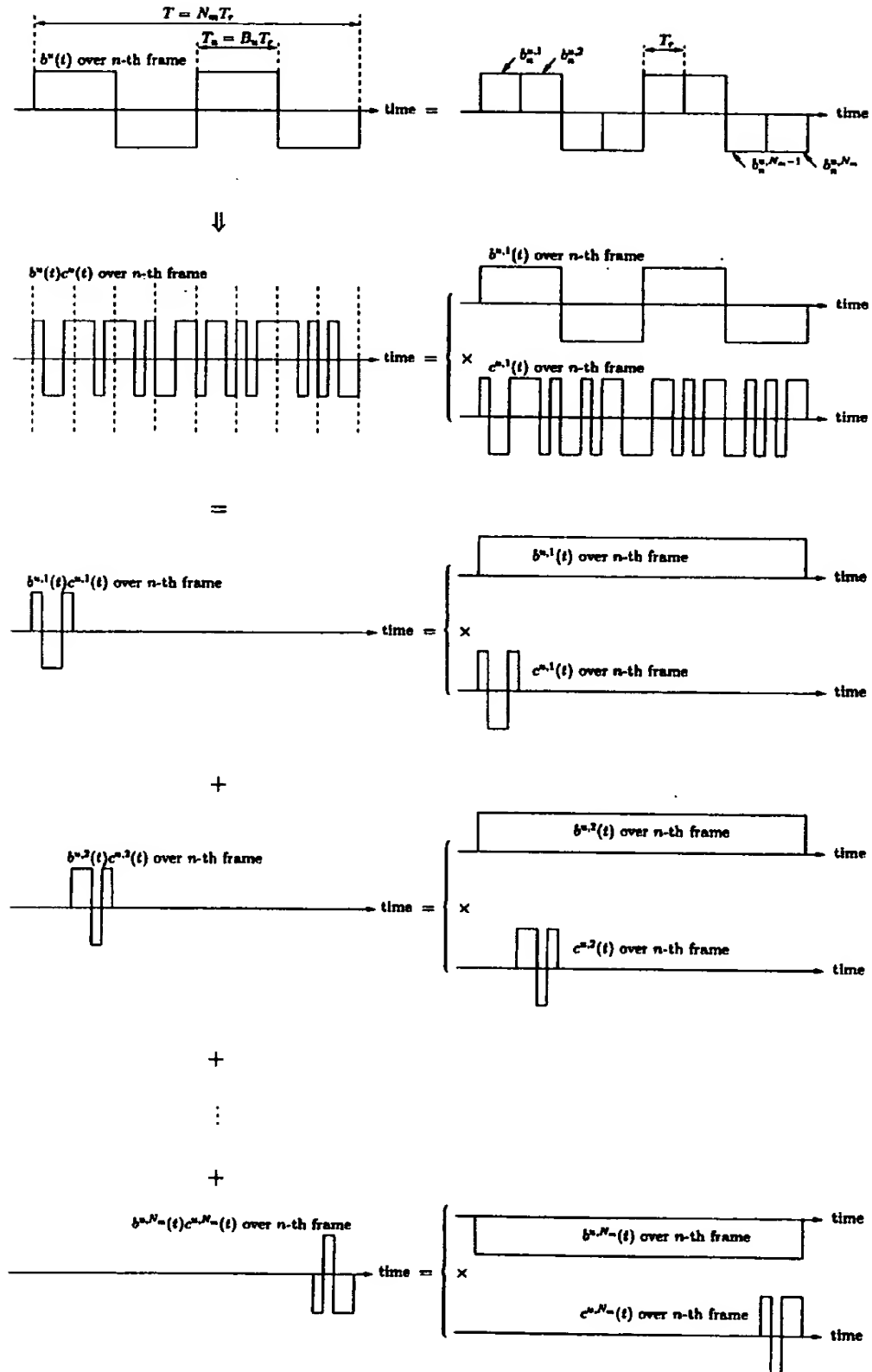
$$\downarrow c_l^u$$

FIG. 14

FIG. 15

FIG. 16

FIG. 17

FIG. 18



FIG. 19

FIG. 20

FIG. 21

FIG. 22

FIG. 23

FIG. 24

FIG. 25

FIG. 26

FIG. 27

FIG. 28

FIG. 29

FIG. 30

FIG. 31

Signal

Proc. frame starts

1. path begins

2. path begins

1. path ends

2. path ends

Proc. frame ends

$\tau_1$

$\tau_2$

$\tau_1 + LT_c$

$\tau_2 + LT_c$

frame size

**FIG. 32**

FIG. 33

**FIG. 34**

FIG. 35

**FIG. 36**

**FIG. 37**

# FIG. 38

FIG. 39

**FIG. 40**

**FIG. 41**

**FIG. 42**

**FIG. 43**

FIG. 1

FIG. 2

FIG. 3



FIG. 4(a)

$\equiv$

FIG. 4(b)

FIG. 4

FIG. 5   PRIOR ART

FIG. 6

FIG. 7

data rate

high

medium

low

Outset(3)

Inset(3)

Inset(2)

Outset(4)

I

M1

M2

D

FIG. 8

FIG. 9

FIG. 10

FIG. 11

FIG. 12

FIG. 13

$57^u$

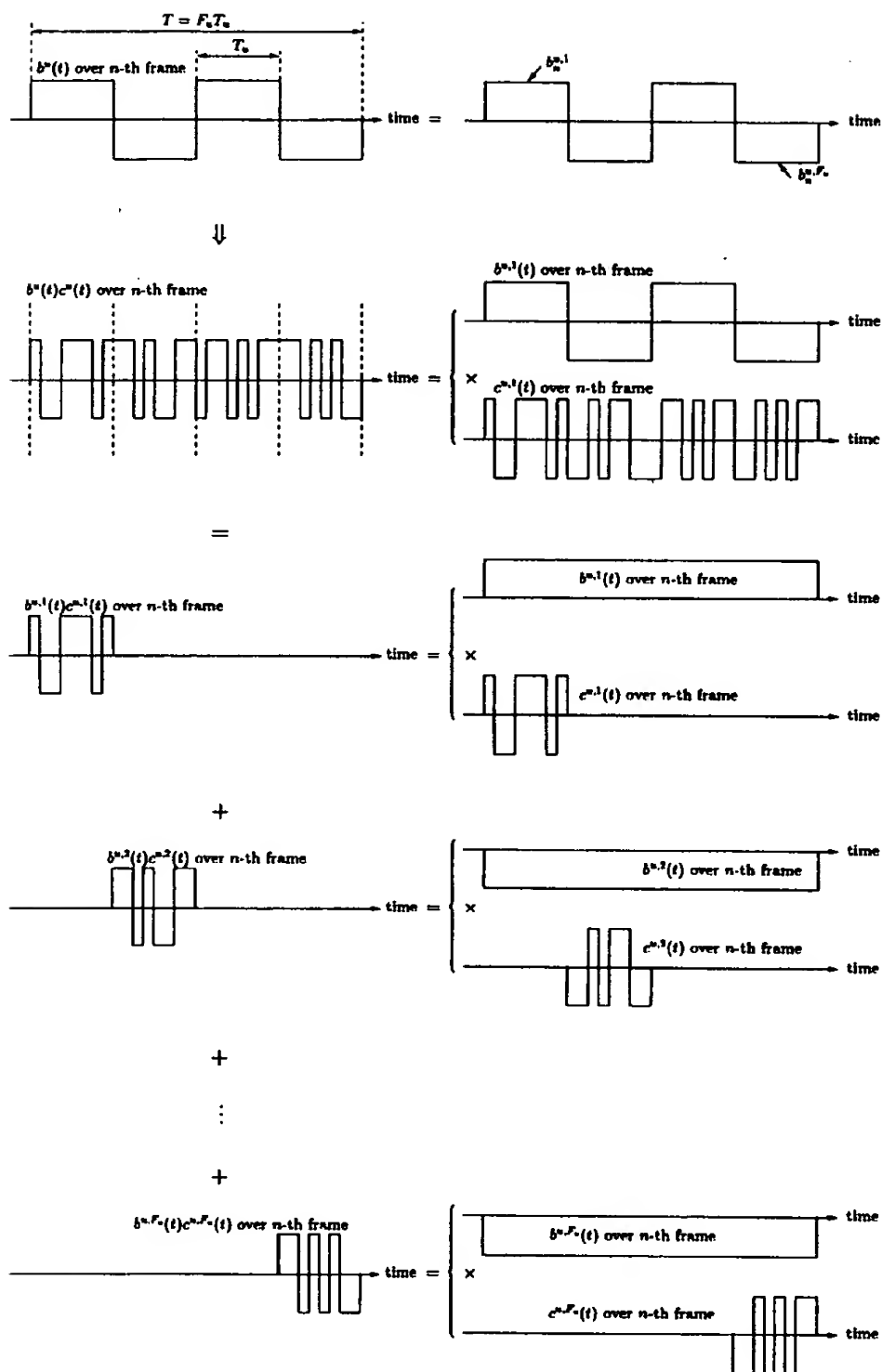$$\hat{b}_n^u \longrightarrow \underset{\downarrow c_l^u}{\times} \longrightarrow \hat{b}_n^u c_l^u$$

FIG. 14

FIG. 15

FIG. 16

FIG. 17

FIG. 18



FIG. 19

FIG. 20

FIG. 21

FIG. 22

FIG. 23

FIG. 24

FIG. 25

FIG. 26

FIG. 27

FIG. 28

FIG. 29

FIG. 30

FIG. 31

FIG. 32

CA 02318658 2000-09-12

Frame $n$

LR

$Y^{1,1}_{n-1}$     $Y^{1,1}_{n}$     $Y^{1,1}_{n+1}$

HR

$Y^{2,1}_{(n-2)r+1}$   $Y^{2,1}_{(n-1)r}$   $Y^{2,1}_{(n-1)r+1}$   $Y^{2,1}_{nr}$   $Y^{2,1}_{nr+1}$   $Y^{2,1}_{(n+1)r}$   $Y^{2,1}_{(n+1)r+1}$

FIG. 33

FIG. 34

**FIG. 35**

**FIG. 36**

**FIG. 37**

FIG. 38

**FIG. 39**

FIG. 40

**FIG. 41**

**FIG. 42**

**FIG. 43**